Anterior synostotic plagiocephaly – A quantitative analysis of craniofacial features using computed tomography

Nivana Mohan

216017401

Submitted in fulfilment of the requirements for the degree

Master of Medical Science

in the School of Laboratory Medicine and Medical Sciences,

University of KwaZulu-Natal

2021

PREFACE

This study is a representation of original work by the author and has not been submitted to other universities in any form. The work is under review in an accredited journal in line with the thesis guidelines of the University of KwaZulu-Natal. Acknowledgement in the text has been made where the work of others was used.

The research described in this project was supervised by Prof L. Lazarus (Discipline of Clinical Anatomy, School of Laboratory Medicine and Medical Sciences, College of Health Sciences, University of KwaZulu-Natal, South Africa), Prof A. Madaree (Department of Plastic and Reconstructive Surgery, University of Kwazulu-Natal, Durban. South Africa) and Dr R. Harrichandparsad (Department of Neurosurgery, University of Kwazulu-Natal, Durban. South Africa) and was conducted in the above-mentioned institution (on Westville campus) and Inkosi Albert Luthuli Central Hospital.

DECLARATION

I, Miss Nivana Mohan, declare as follows:

1) That the work described in this thesis has not been submitted to the University of KwaZulu-Natal or other tertiary institutions for purposes of obtaining an academic qualification, whether by myself or any other party.

2) That my contribution to the project as primary author and principal investigator was as follows:

- collection of data needed for literature review;
- collection, analysis, and interpretation of data; and
- formulation of manuscripts and compilation of the research dissertation.

3) That the contributions of others to the project were as follows:

- Prof L. Lazarus acted as the main supervisor, aiding in the formulation of the research idea and study design, reviewing all work before submission, giving corrections and feedback on work done.
- Prof A. Madaree acted as co-supervisor, aiding in the formulation of the research idea and study design, reviewing all work before submission, giving corrections and feedback on work done.
- Prof R. Harrichandparsad acted as co-supervisor, aiding in the formulation of the research idea and study design, reviewing all work before submission, giving corrections and feedback on work done.

Date: 24 December 2021

Nivana Mohan
216017401

Date: 24 December 2021

Prof L. Lazarus

Date: 24 December 2021

Prof A. Madaree

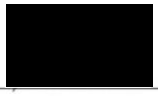

Date: 24 December 2021

Dr. R. Harrichandparsad.

DEDICATION

"*Believe in yourself, and you will achieve everything you yearn for and more*" – Mom and Dad. Without these words, I would not have been able to complete this journey, and I am forever thankful for all the love, support, encouragement, and comfort that you both have given me at every step of the way.

ACKNOWLEDGEMENTS

The author would like to place on record her gratitude to the following individuals and entities for their invaluable assistance in preparing this Master's thesis.

- First and foremost, I would like to praise and thank God, whose grace guided me from the inception to the completion of this research work.
- My parents, Anitha and Lesley Mohan, for their endless support. It was their love that raised me again when I got weary. I am forever indebted to my parents for giving me the opportunities and experiences to make me who I am.
- My supervisors, Professor Lelika Lazarus, Professor Anil Madaree and Dr Rohen Harrichandparsad, for their guidance and support. They have inspired me to become an independent researcher and helped me realize the power of critical reasoning. Thank you for the valuable inputs and for generously spending precious time giving me encouragement, suggestions, and comments for this thesis.
- I am grateful to Dr Partson Tinarwo for lending me his time, expertise, technical assistance, as well as assistance with statistical analysis.
- My sister, Nivita Mohan, for her invaluable support and steering me on when I needed it the most.
- I cannot forget friends who cheered me on, supported me and celebrated each accomplishment: Vensuya Bisetty, Kerissa Naidoo, Keegan Manilal, Livashin Naidu, Mikaela Jaganaikulu and Sumeera Partab. I am grateful to have a group of friends that inspire, motivate, and encourage me to become a better version of myself and who have stuck by my side through all the good and bad.
- The National Research Foundation (NRF), for the financial assistance of this project. Its contents are solely the authors' responsibility and do not necessarily represent the official views of the National Research Foundation.

TABLE OF CONTENTS

LIST OF FIGURES

LIST OF TABLES

LIST OF ACRONYMS AND ABBREVIATIONS

ACF	Anterior cranial fossa
ASP	Anterior synostotic plagiocephaly
CT	Computed tomography
DICOM	Digital Imaging and Communication in Medicine
EAM	External auditory meatus
FOAR	Fronto-orbital advancement and remodelling
IALCH	Inkosi Albert Luthuli Central Hospital
ICP	Intracranial pressure
IOR	Infraorbital rim
LUCS	Left unilateral coronal synostosis
MPR	Multiplanar reconstruction
PACS	Picture Archiving and Communication System
ROI	Region of interest
RUCS	Right unilateral coronal synostosis
SOR	Supraorbital rim
UCS	Unilateral coronal synostosis
UKZN	University of KwaZulu-Natal

ABSTRACT

Anterior synostotic plagiocephaly (ASP) is caused by the premature fusion of one coronal suture, which results in severe craniofacial asymmetry that can be challenging to correct. The various methods of the surgical procedures, as well as the distinctive facial characteristics of ASP, have been well documented. However, there is a paucity of literature pertaining to the quantitative analysis of the craniofacial features that are affected in ASP. This study used preoperative computed tomography (CT) scans to document and compare the morphometry of the anterior cranial fossa (ACF), orbit, and ear on the ipsilateral (synostotic) and contralateral (non-synostotic) sides in a select South African population of patients diagnosed with ASP.

The dimensions of the ACF, orbit and the position of the ear on the ipsilateral and contralateral sides were measured using a set of anatomical landmarks on two-dimensional (2D) CT scans of 18 consecutive patients diagnosed with non-syndromic ASP. The differences between the ipsilateral and contralateral sides were computed and expressed as a percentage of the contralateral side. The findings of this study revealed that there was side-to-side asymmetry in the ACF, orbit, and ear. All ACF parameters decreased significantly (t-test; $p<0.001$) on the ipsilateral side when compared to the contralateral side, resulting in the volume of the ACF being the most affected (-27.7%). In terms of the orbit, on the ipsilateral side, the length-infraorbital rim (IOR), height, and surface area parameters increased significantly (t-test; $p<0.001$), with the height being the most affected (24.6%). The remaining orbital parameters (length-supraorbital rim (SOR), breadth and volume) decreased significantly (t-test; $p<0.001$), with the length-SOR parameter being the most affected (-10.8%). Furthermore, the ipsilateral SOR was noted to be displaced more cranially by an average of 3.89mm from the contralateral SOR. With regards to the position of the ipsilateral ear, it was found to be displaced anteriorly (9.33mm) and caudally (5.87mm) from the contralateral ear.

This study augments the existing literature by providing actual values to corroborate the hallmark characteristics of ASP. These measures may help surgeons plan the technique and extent of surgical correction of the affected craniofacial structures during corrective surgery as it will provide them with an indication of the extent of the deformity on the ipsilateral side as compared to the contralateral side. The results of this study have the potential to propose a grading system in ASP patients according to severity of the condition if the sample size is increased.

CHAPTER 1: INTRODUCTION

1.1.Introduction

Craniosynostosis is one of the most common causes of craniofacial abnormalities in infants (Lee *et al*., 2021). It is a condition that involves the premature closure of one or many sutures of the cranial vault before the growth of the brain is complete; thereby, changing the growth pattern of the skull (Lee *et al*., 2021; Flaherty *et al*., 2016). Since the skull cannot expand perpendicular to the fused suture, it compensates by growing more in the direction parallel to the closed sutures (Van Veelen-Vincent *et al*., 2010). This results in an irregularly shaped skull and abnormal facial features (Kajdic *et al*., 2017). Craniosynostosis is classified according to the type of premature fused cranial suture involved, such as sagittal, metopic, coronal, or lambdoid types (Lee *et al*., 2021).

Anterior synostotic plagiocephaly (ASP) also known as unilateral coronal synostosis (UCS) is a rare pathological cranial malformation (Calandrelli *et al*., 2018). It is the third most prevalent type of simple craniosynostosis, following scaphocephaly and trigonocephaly, representing 13% to 16% of all craniosynostoses (Calandrelli *et al*., 2018). ASP is caused by premature ossification of the coronal suture on one side (Raposo-do-Amaral *et al*., 2011). This can result in left- or right-sided ASP, naturally depending on which side the suture is fused (Kronig *et al*., 2020). ASP occurs more frequently in females than in males and has an incidence of 1 per 10 000 live births (Spazzapan *et al*., 2017).

There are many side-to-side asymmetrical changes in the skull and face as a result of ASP (Calandrelli *et al*., 2018). The side of the head presented with the synostosis is referred to as "ipsilateral" and the opposite side is referred to as "contralateral" (Di Rocco *et al*., 2012). In ASP, most of the facial structures usually deviate towards the side of the synostosis (Marsh *et al*., 1986). Some of the clinical presentations include: shortened anterior cranial fossa (ACF) on the ipsilateral side; ipsilateral flattening and contralateral bossing of the forehead; high and flattened supraorbital rim (SOR) on the ipsilateral side; elongated and narrow ipsilateral orbital cavity; anterior displacement of the ear, petrous bone and zygoma on the ipsilateral side; ipsilateral deviation of the nasal root and contralateral deviation of the nasal septum and chin (Captier *et al*., 2003; Oh *et al*., 2008; Raposo-do-Amaral *et al*., 2011; Di Rocco *et al*., 2012; Spazzapan *et al*., 2017; Brown and Wetz, 2019). ASP may also be accompanied by various neurological and

developmental abnormalities, including behavioural, speech, intelligence, and learning difficulties (Becker et al., 2005).

Measurement of the craniofacial structures is essential for diagnosis and monitoring of changes in growth; moreover, it may indicate the effectiveness of surgical intervention (Raposo-do-Amaral *et al.*, 2011). Since ASP requires a surgical approach to correct these asymmetrical features, it is imperative for the morphometry of these craniofacial structures on the ipsilateral and contralateral sides to be documented. The morphometric data could aid surgeons in achieving normalcy of the affected structure by providing an indication of the degree of the asymmetry on the ipsilateral side compared to the contralateral side, thus making it easier to plan the surgical procedure and extent of the correction. The most common and current treatment for ASP is open cranial vault remodelling with fronto-orbital advancement, which is usually done between the ages of nine and twelve months (Brown and Wetz, 2019).

Due to the low prevalence of ASP, only a few previous studies quantitatively reported on the asymmetry of the craniofacial structures associated with this deformity (Bentley *et al*., 2002; Captier *et al*., 2003; Calandrelli *et al*., 2016; 2018; Dvoracek *et al*., 2021; Kronig *et al*., 2021). There are aspects of these asymmetric craniofacial structures for example, ACF width, length of curvature, volume and height; orbital length and surface area; and the position of the ears on the ipsilateral and contralateral sides that have yet to be reported. As a result, some of the parameters mentioned in this study are novel, and there is no previous research to report on.

Di Rocco and Velardi (1988) established a classification scheme for ASP to determine the severity of asymmetry in patients. Asymmetry was more noticeable in patients with higher severity of the deformity, suggesting that UCS had taken place earlier than it normally does (Calandrelli *et al.*, 2018). Captier *et al.* (2003) confirmed that ASP caused a significant asymmetry in the skull base, on the ipsilateral side, the skull base was always reduced, and all the midline features in front of the sella turcica deviated towards the ipsilateral side. This was also associated with the deviation of the facial structures to the ipsilateral side (Heuzé *et al.*, 2012; Calandrelli *et al.*, 2016).

Previous studies that investigated the asymmetry of the ACF on either side discovered that there was a significant decrease in the length of the ACF on the ipsilateral side when compared to the contralateral side (Captier *et al*., 2003; Calandrelli *et al*., 2016; 2018). The angle of the ACF was also reported to be significantly smaller on the ipsilateral side. These significant differences in the lengths and angles resulted in the asymmetry of the ACF with reduced growth on the

ipsilateral side (Marsh *et al*., 1986; Captier *et al*., 2003; Calandrelli *et al*., 2016; Calandrelli *et al*., 2018).

The volume of the orbit has been calculated in a variety of ways in the literature, with authors using their preferred orbital boundaries to segment the orbital cavity. Bentley *et al*. (2002), Beckett *et al*. (2013), Calandrelli *et al*. (2018) and Kronig *et al*. (2021) focused on orbital volumes stating that there was significant side-to-side asymmetry in the volume of the orbits, the ipsilateral orbit had a smaller orbital volume when compared to the volume of the contralateral orbit. Regarding orbital breadth and height, Dvoracek *et al*. (2021) found that the breadth decreased significantly and that the height increased significantly on the ipsilateral orbit. As a result of this, the ipsilateral orbit appeared to be narrow and elongated while the contralateral orbit appeared to be wide and short.

There were no studies that examined the asymmetry in the position of the SORs and the ears on either side quantitatively, however, a few anatomical changes were noticed: the ipsilateral orbit exhibited a higher SOR than the contralateral orbit (Marsh *et al*., 1986; Mesa *et al*., 2011). Pelo *et al*. (2011) and Spazzapan *et al*. (2017) examined the placement of the ears and discovered that the external auditory meatus (EAM) and petrous bone on the ipsilateral side were anteriorly displaced. Severe anteriorization and slight depression of the EAM on the ipsilateral side have been found in more severe cases of ASP (Pelo *et al*., 2011). In contrast to the findings of Pelo *et al*. (2011) on the vertical position of the affected ear, Bruneteau and Mulliken *et al*. (1992) discovered the ipsilateral ear to be superiorly positioned.

Distinctive craniofacial features and various methods of surgical treatments for ASP have been well documented in the literature (Captier *et al*., 2003; Oh *et al*., 2008; Jeyaraj, 2011; Raposo-do-Amaral *et al*., 2011; Di Rocco *et al*., 2012; Matushita *et al*., 2012; Spazzapan *et al*., 2017; Brown and Wetz, 2019). However, there is sparse literature available on the quantitative analysis of the craniofacial structures that are involved in this condition. Therefore, this proposed study is warranted as it will contribute to the literature by providing anthropometric measurements of the craniofacial features involved in ASP. This is a purely anatomical study that may be used as a reference in future studies to compare preoperative and postoperative findings to assess the improvement of the deformity and monitor surgical outcomes.

This study aimed to document and compare the morphometry of the ACF, orbit and ear on the ipsilateral and contralateral sides in a select cohort of South African patients with ASP, using

preoperative CT scans. Furthermore, this study proposed to compare the anthropometric measurements obtained in this study by age, sex, race and laterality.

1.1.1. Research question

What are the dimensions of the ACF, orbit and position of the ear on the ipsilateral side compared to the contralateral side in patients with untreated ASP?

1.1.2. Aim

This study aimed to document and compare the morphometry of the ACF, orbit and ear on the ipsilateral and contralateral sides in a select cohort of South African patients with ASP, using preoperative CT scans.

1.1.3. Objectives

Preoperative CT scans of patients with ASP will be used to achieve the following objectives:

i) To determine and compare the morphometry of the ACF on the ipsilateral and contralateral sides in terms of width, length, length of curvature, angle, volume, and height.

ii) To determine and compare the morphometry of the orbit on the ipsilateral and contralateral sides in terms of length, breadth, height, volume, surface area and the maximum vertical height between the supraorbital rims (SORs).

iii) To determine and compare the (a) maximum anteroposterior (AP) distance between the ipsilateral and contralateral ear; and (b) maximum vertical height between the ipsilateral and contralateral ear.

iv) To compare the aforementioned variables with regard to sex, age, race and laterality.

1.2. Literature review

1.2.1. Gross anatomy

1.2.1.1. ACF

The anterior, middle and posterior cranial fossae are the three distinct fossae that make up the floor of the cranial cavity (Moore *et al.*, 2010; Gray and Standring, 2016). Each fossa houses a

specific portion of the brain. The ACF is the most superior and shallowest of the three cranial fossae. Its function is to accommodate and provide support to the frontal lobes of the cerebral hemispheres (Moore *et al.*, 2010). The ACF is made up of three cranial bones viz.: the ethmoid bone, the orbital surface of the frontal bone, and part of the lesser wing of the sphenoid bone (Gray and Standring, 2016). It is bounded anteriorly and laterally by the inner surface of the frontal bone, posteriorly and laterally by the lesser wings of the sphenoid bone, and posteriorly and medially by the limbus of the sphenoid bone (Moore *et al.*, 2010; Gray and Standring, 2016). The floor of the ACF is composed of the orbital plate of the frontal bone, the crista galli and cribriform plate of the ethmoid bone, and the jugum sphenoidale, prechiasmatic sulcus, and lesser wings of the sphenoid bone. The landmarks of the ACF include the frontal crest, foramen caecum, anterior ethmoidal foramen, cribriform foramina, and jugum sphenoidale (Gray and Standring, 2016).

1.2.1.2. Orbit

The orbits are skeletal cavities that serve as sockets for the eyeballs and associated tissues (Moore *et al.*, 2010; Gray and Standring, 2016). Each orbital cavity is shaped like a quadrangular pyramid, having a base at the orbital opening and its apex along a posteromedially directed axis (Gray and Standring, 2016). The orbit is made up of four facial bones viz.: zygomatic bone, palatine bone, lacrimal bone, and maxilla and three cranial bones which are the sphenoid, ethmoid, and frontal bones (Moore *et al.*, 2010).

Each orbit has four walls (Moore *et al.*, 2010). The superior wall (roof) is formed by the orbital part of the frontal bone and the lesser wing of the sphenoid bone. The inferior wall (floor) is formed by the palatine bone, zygomatic bone, and mostly by the orbital plate of the maxilla. The medial wall curves inferolaterally into the floor of the orbit and is formed by the orbital plate of the ethmoid bone, lacrimal bone, greater wing of the sphenoid bone, and frontal process of the maxilla (Moore *et al.*, 2010; Gray and Standring, 2016). Most of the bone forming the medial wall of the orbit is paper-thin (Moore *et al.*, 2010). The lateral wall is the thickest and it is formed anteriorly by the frontal process of the zygomatic bone and posteriorly by the orbital surface of the greater wing of the sphenoid bone; these bones meet at the sphenozygomatic suture (Moore *et al.*, 2010; Gray and Standring, 2016). The base of the orbit is also known as the orbital margin or rim, it is quadrangular in shape. It protects the contents of the orbit and provides an attachment site for the orbital septum (Gray and Standring, 2016).

The orbit has four margins viz.: the infra-orbital margin formed by the zygomatic bone and zygomatic process of the maxilla, the supra-orbital margin formed by the frontal bone, the medial margin formed by the frontal process of the maxilla, and the lateral margin is formed largely by the frontal process of the zygomatic bone and is completed above by the zygomatic process of the frontal bone; these bones meet at the frontozygomatic suture, this suture lies in a palpable depression (Moore *et al.*, 2010). The landmarks and openings of the orbit consist of the superior and inferior orbital fissures, lacrimal groove, lacrimal fossa, trochlea, optic foramen (canal), and the anterior and posterior ethmoidal foramina (Gray and Standring, 2016).

1.2.1.3. Ear

The ear is situated bilaterally on the human skull, at the same level as the nose. It is responsible for hearing and maintaining balance (Moore *et al.*, 2010). The ear is composed of three parts viz.: the external, middle, and internal ear. The external ear consists of the auricle (pinna), external acoustic meatus, and tympanic membrane (eardrum). The middle ear is found mostly within the temporal bone and consists of the auditory ossicles (malleus, incus and stapes), muscles of the ossicles (stapedius and tensor tympani), and tympanic cavity. The internal ear is placed in the petrous part of the temporal bone and consists of the membranous labyrinth (semicircular ducts, sacculus, utriculus and cochlear duct) and bony labyrinth (semicircular canals, cochlear and vestibule) (Gray and Standring, 2016).

1.2.1.4. Temporal bone

The temporal bones are a pair of bilateral, symmetrical bones that form a large part of the lateral wall and base of the skull (Moore *et al.*, 2010). The ear is mostly, but not entirely, contained within the temporal bone. It houses and protects the structures and nerves that form the middle and internal ear. This bone consists of several parts viz.: the squamous part, petromastoid and tympanic parts which form most of the bone, and the styloid and zygomatic processes (Gray and Standring, 2016).

1.2.1.5. Coronal suture

The coronal suture is a dense, fibrous tissue joint (Gray and Standring, 2016). It marks the articulation between the posterior margin of the frontal bone and the anterior margins of the two parietal bones (Moore *et al.*, 2010). It descends across the calvaria, projecting inferiorly until it meets the junction between the greater wing of the sphenoid and the squamous part of the temporal bone at the pterion (Gray and Standring, 2016). The coronal suture remains unfused during childhood until around 24 years of age when it eventually closes (Idriz *et al.*, 2015).

1.2.1.6. Sphenofrontal suture

The sphenofrontal suture is a transverse cranial suture between the posterior margin of the horizontal orbital plates and the anterior margin of the lesser wings of the sphenoid bone (Gray and Standring, 2016). This suture plays an important role in the growth of the anterior cranial fossa and forms with the sphenoethmoidal synchondrosis (basal part of the coronal ring) (Captier *et al.*, 2003).

1.2.1.7. Frontozygomatic suture

The frontozygomatic suture is also known as the zygomaticofrontal suture, it is a cranial suture between the zygomatic process of the frontal bone and the frontal process of the zygomatic bone (Gray and Standring, 2016). It can be easily palpated on the lateral side of the eye; therefore, it serves as a significant reference point for orbital surgery (Hegazy, 2021).

1.2.2. Embryology

Lateral plate mesoderm in the neck region, paraxial mesoderm and neural crest cells all contribute to the development and existence of the skull in its entirety (Jin et al., 2016). The bones of the skull are created in two different ways; intramembranous ossification and endochondral ossification are responsible for producing compact cortical bone or spongy bone (Sadler et al., 2012). The skull is made up of two parts: the neurocranium, which protects and surrounds the brain, and the viscerocranium, which forms the skeleton of the face (Sadler et al., 2012; Jin et al., 2016). The neurocranium can be subdivided into the membranous part, which forms the cranial vault or calvarium and the cartilaginous part, or chondrocranium, which forms the base of the skull (Sadler et al., 2012). The membranous part is derived from neural crest cells and paraxial mesoderm. Mesenchyme from these two sources surrounds the brain and undergoes intramembranous ossification to form flat bones, which later ossify with needle-like spicules that radiate from the primary ossification centres towards the periphery. The cartilaginous part is composed of a number of separate cartilages. Cartilages that arise from neural crest cells and lie anterior to the pituitary fossa form the prechordal part. Cartilages lying posterior to this limit form the chordal part and arise from paraxial mesoderm. The cranial base is formed when these cartilages fuse and ossify by endochondral ossification (Sadler et al., 2012; Jin et al., 2016). The viscerocranium is formed mainly from the first two pharyngeal arches. The first arch forms the maxillary process (dorsal portion), which extends forward beneath the eye and gives rise to the maxilla, zygomatic bone, and part of the temporal bone. The mandibular process (ventral portion) contains the Meckel cartilage. The mandible is formed when the mesenchyme around the Meckel

cartilage condenses and ossifies by intramembranous ossification. The dorsal tip of the mandibular process, as well as the second pharyngeal arch, form the incus, malleus, and stapes. The three ossicles begin to ossify in the fourth month, making them the first bones to fully ossify. Neural crest cells produce mesenchyme, which is used to form the bones of the face, such as the nasal and lacrimal bones (Sadler et al., 2012).

Cranial sutures form at the junction of numerous osteogenic fronts by 16 weeks' gestation and are particularly active areas of bone formation and deposition, directly affected by underlying tension forces of brain growth and dural reflections as well as local growth factors (Sadler et al., 2012; Jin et al., 2016).

1.2.3. Overview of craniosynostosis

The cranial vault expands during infancy and childhood to support the growing brain. This growth occurs predominantly at the cranial sutures, which connect the bones of the skull (Johnson and Wilkie, 2011). The metopic and sagittal sutures separate the paired frontal and parietal bones in the midline, the coronal sutures separate the frontal and parietal bones, and the lambdoid sutures separate the parietal bones from the single occipital bone (Hegazy, 2021). Premature fusion of one or more of the cranial sutures is known as craniosynostosis. Craniosynostosis is one of the most common causes of craniofacial abnormalities in babies (Lee *et al.*, 2021). The skull compensates for its inability to expand perpendicular to the affected suture by growing more in the direction parallel to the unaffected sutures, resulting in facial and head shape abnormalities (Van Veelen-Vincent *et al.*, 2010). It is important to recognize and treat craniosynostosis since it can lead to a variety of issues that affect sensory, respiratory, and neurological functioning (Johnson and Wilkie, 2011). In cases of craniosynostosis, neurosurgery is frequently recommended to enable the 'release' of the suture and a return to normal growth trajectories (Derderian and Seaward, 2012).

Various classification systems have been devised to understand the variation in craniosynostosis phenotypes. Craniosynostosis can be characterized as primary or secondary. Primary craniosynostosis refers to cases in which suture fusion is a result of a developmental abnormality that affects the suture directly, whereas secondary craniosynostosis refers to cases in which premature suture fusion is secondary to another known defect, usually associated with the CNS, metabolic, or hematological illnesses and diseases. Craniosynostosis can also be classed as simple craniosynostosis which occurs when a single suture closes prematurely, or compound craniosynostosis which occurs when two or more sutures close prematurely (Flaherty *et al.*, 2016).

Craniosynostosis can be further classified as non-syndromic, when it occurs as an isolated disorder, or as syndromic, when it is caused by a hereditary or genetic disorder and occurs in conjunction with other abnormalities, usually involving multiple sutures (Derderian and Seaward, 2012).

The cause of craniosynostosis is unknown, however, it could be caused by a variety of factors such as genetic and environmental factors, teratogenic exposure during critical developmental stages, and gene mutations (Durham *et al.*, 2017). The reported incidence of craniosynostosis is approximately 1 in 2100 to 2500 live births (Johnson and Wilkie, 2011; Kajdic *et al.*, 2017). The frequency in which each of the skull sutures fuses varies; the most common non-syndromic craniosynostosis is sagittal synostosis, which is followed by metopic synostosis, uni- and bilateral-coronal synostosis, lambdoid, and other types of multiple suture synostosis (Van Veelen-Vincent *et al.*, 2010; Johnson and Wilkie, 2011).

1.2.4. Anterior synostotic plagiocephaly (ASP)

The term "plagiocephaly", derived from the Greek term "plagio kephale" which means slanted or oblique head, has been used to define either acquired or congenital developmental cranial deformities that cause severe asymmetry and scoliosis of the craniofacial skeleton (Di Rocco *et al.*, 2012). Plagiocephaly affects every part of the skull bone, especially the calvaria, which accounts for seven-eighths of the cranial volume in infants (Captier *et al.*, 2003).

Anterior synostotic plagiocephaly (ASP) also known as unilateral coronal synostosis (UCS) is a congenital deformation of the skull, caused by premature fusion of the coronal suture on one side (Fig. 1) (Calandrelli *et al.*, 2018). This can result in left- or right-sided UCS (LUCS or RUCS), naturally depending on which side the suture is fused (Kronig *et al.*, 2020). ASP may also occur in conjunction with synostosis of other coronal ring sutures, such as the frontoethmoidal or frontosphenoidal sutures (Calandrelli *et al.*, 2018). Regardless of whether one or more cranial sutures fuse prematurely, the brain continues to expand at the same rate, however, when one coronal suture fuses prematurely the remaining cranial sutures must compensate with increased growth to continue to allow for the expansion of the brain (Derderian and Seaward, 2012). The main goal of ASP is to increase the dimensions of the calvaria anteroposteriorly (Kabbani and Raghuveer, 2004). This growth pattern gives the skull and face an asymmetrical appearance because there is increased growth on one side of the skull and decreased growth on the other side of the skull (Fig. 1) and (Fig. 2A and B) (Heuzé *et al.*, 2012).

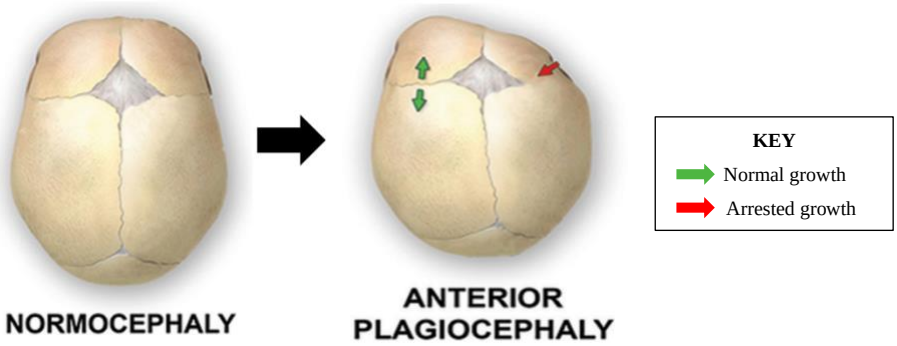

Figure 1: Skull deformity caused by premature fusion of one coronal suture.
(Adapted from Kajdic et al., 2017)

The side of the head that is presented with a fused coronal suture (premature synostosis) is regarded as “ipsilateral” and the side of the head opposite to the fused coronal suture is regarded as “contralateral”. The contralateral side only refers to the absence of a fused coronal suture, it does not imply that head shape is normal (Di Rocco *et al.*, 2012).

The clinical findings of ASP usually include:

- A "C-shaped" malformation or "facial twist" is always present on the face (Mesa *et al.*, 2011; Di Rocco *et al.*, 2012).
- The ipsilateral ear is slightly elevated and anteriorly displaced becoming attracted to the affected orbit (Fig. 2A) (Matushita *et al.*, 2012).
- Flattening of the forehead and SOR on the ipsilateral side due to arrested growth and bulging/ bossing of the forehead on the contralateral side (Fig. 2A and B) and (Fig. 3A-C, E, F) (Jeyaraj, 2011).
- The nasal root is constricted and deviates to the ipsilateral side while the nasal septum and vomer deviate towards the contralateral side (Fig. 2A and B) and (Fig. 3B) (Raposo-do-Amaral *et al.*, 2011).
- The zygoma is anteriorly displaced and the zygomatic arch is more curved and shorter on the ipsilateral side (Fig. 2B) and (Fig. 3A-C) (Goodrich, 2005).
- The SOR is retracted, elevated, and displaced laterally on the ipsilateral side (Fig. 2A-C). The ipsilateral orbit is shallow and is situated posterolaterally. It exhibits the typical “Harlequin” phenomenon (elevation of the large sphenoid wing) which can be observed radiographically (Fig. 2C) (Spazzapan *et al.*, 2017).
- The eyebrow is raised on the ipsilateral side (Fig. 2A) (Spazzapan *et al.*, 2017).

- Due to the abnormally configured orbital cavity, hypertelorism, astigmatism, and strabismus may be evident. On the ipsilateral side, proptosis of the eye is accompanied by a rounded and transversely shortened palpebral fissure (Di Rocco et al., 2012).
- The sphenotemporal fossa is deepened and forward deviation of the petrous part of the temporal bone occurs (Fig. 3 A, C, F) (Captier *et al.*, 2003).
- The ipsilateral side of the anterior cranial base is shortened, with ipsilateral deviation of the ethmoid bone and structures in front of the sella turcica (Fig. 3F) (Captier *et al.*, 2003).
- Anterior displacement of the temporomandibular joint on the ipsilateral side (Oh *et al.*, 2008).

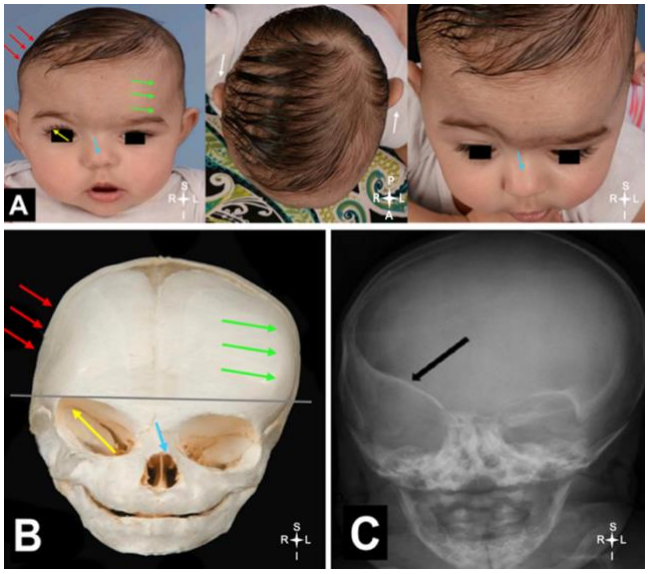

KEY

IMAGE A & B:
Red arrows – Head/face pushed inwards
Yellow arrow – Eye socket is elevated and pulled upwards
Grey line – Displaying the difference in the height between the right and left SOR
Blue arrows – Deviation of nasal root and nasal septum
Green arrows – Forehead pushed outwards
White arrows – Elevation and anterior displacement of the ear

IMAGE C:
Black arrow – Superior displacement of the large sphenoid wing causing a "Harlequin eye" deformity

Figure 2: (A) Anterior and superior views of an infant's head with right unilateral coronal synostosis (RUCS) showing the different presentations of ASP in soft tissue. **(B)** Anterior view of a skull with RUCS showing the different presentations of ASP. **(C)** Anterior view of an x-ray image showing a typical "Harlequin eye" deformity on the ipsilateral side. *(Adapted from Spazzapan et al., 2017 and Brown and Wetz, 2019)*

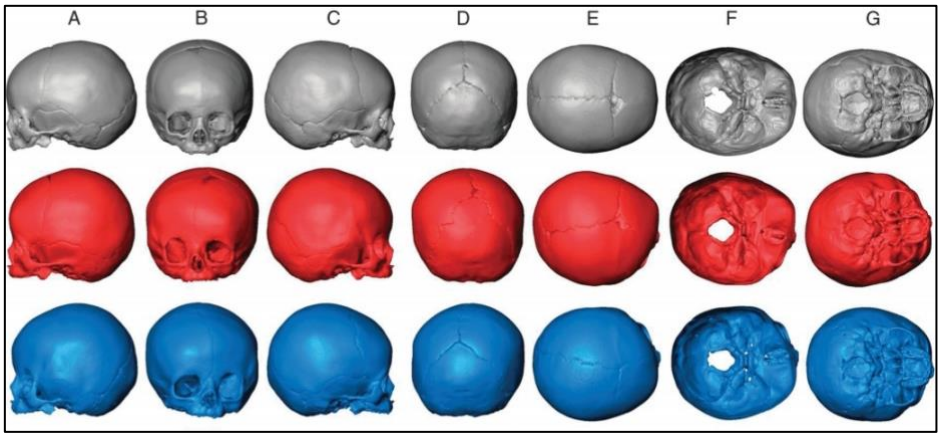

KEY

A – Lateral (left) view
B – Anterior view
C – Lateral (right) view
D – Posterior view
E – Superior view
F – Endocranial view
G – Ectocranial (inferior) view

Figure 3: Different presentations of a normal skull (grey), a skull with RUCS (red), and a skull with LUCS (blue) depicted in different views. *(Adapted from Heuzé et al., 2012)*

UCS may be associated with the following: craniofrontonasal dysplasia, Crouzon-, Muenke-, Apert-, Pfeiffer-, and Saethre-Chotzen syndromes (Raposo-do-Amaral *et al.*, 2011). These are genetic conditions generated by various mutations, some of which are located on the genes coding for the fibroblast growth factor receptors (FGFR) 1, 2 and 3 and the TWIST 1 gene. The FGFR signalling pathway plays a crucial role in different cellular processes and the TWIST 1 gene is responsible for supplying instructions to produce a protein that is required for early development (Derderian and Seaward, 2012; Heuzé *et al.*, 2012). UCS can also be accompanied by various neurological and/or developmental problems (Di Rocco *et al.*, 2012). Becker *et al.* (2005) stated that children with either right or left UCS displayed developmental problems related to behaviour, speech, intelligence, and learning. Di Rocco *et al.* (2012) reported that RUCS can increase the chances of non-verbal learning disorders, social perception, and functioning disorders whereas, LUCS accompanied by the restriction of frontal brain growth is associated with developmental reading disorders and language-based learning disorders. Neurocognitive development may also be affected due to the impaired visual-perceptual skills caused by changes in vision (Heuzé *et al.*, 2012).

1.2.4.1. Epidemiology

ASP is the third most prevalent type of simple craniosynostosis following scaphocephaly and trigonocephaly, representing 13% to 16% of all craniosynostosis. Approximately 61% of cases are non-syndromic, with the remaining 39% being syndromic (Calandrelli *et al.*, 2016). ASP has an incidence of 1 per 10 000 live births (Spazzapan *et al.*, 2017). The incidence of UCS is four to seven times that of bilateral coronal synostosis (Di Rocco *et al.*, 2012). RUCS is said to occur twice as often as LUCS (Heuzé *et al.*, 2012). ASP is diagnosed more commonly in females than males (2:1) (Heuzé *et al.*, 2012; Kajdic., *et al* 2017). Females are more likely to be affected by LUCS than males, whereas RUCS affects both males and females equally (Heuzé *et al.*, 2012). Cephalic index (CI) is the ratio of the maximum width of a skull to its maximum length. The CI for plagiocephaly is >76% - <90% (Kajdic., *et al* 2017).

1.2.4.2. Surgical intervention

The treatment for ASP is via surgical intervention. There are a variety of surgical methods to treat ASP and these include endoscopic suturectomy and helmet molding, springs, distraction and open correction (Oh *et al.*, 2008). Until now, the most common treatment has been open cranial vault remodelling with fronto-orbital advancement, allowing surgeons to overcorrect the fused side and reshape the orbital cavity to allow the patient to 'grow into' the correction (Oh *et al.*, 2008;

Matushita *et al.*, 2012). This is usually done around nine to twelve months of age (Brown and Wetz, 2019). Early diagnosis is important so that the infant is operated on within the first twelve months of age. If surgeries are performed too early there is a possibility of extreme blood loss and high recurrence of craniosynostosis (Spazzapan *et al.*, 2017). Therefore, the optimal time of surgery is between six to twelve months of age as children can tolerate major surgeries due to sufficient stability of the postorbital bar. In addition, surgeries are performed in this age range to avoid intracranial hypertension and to achieve better aesthetic results (Matushita *et al.*, 2012).

1.2.5. Craniofacial morphometry

The more severe the deformity in the skull, the more apparent ASP becomes (Calandrelli *et al.*, 2018). Calandrelli *et al.* (2016; 2018) confirmed that changes in the skull base tend to affect the growth of the skull and orbit. If synostosis takes place early, it has a greater effect (asymmetry) on the shape of the skull and face but if synostosis takes place later, the effect is lessened (Calandrelli *et al.*, 2018).

Di Rocco and Velardi (1988) classified ASP into three main groups according to severity as follows:

(i) *Group 1* – flattening of the frontal bone and elevation of the roof of the orbit on the ipsilateral side with no nasal pyramid deviation.

(ii) *Group 2* – orbital and frontal malformations with nasal pyramid deviation to the contralateral side and variable anterior displacement of the petrous bone/ ear on the ipsilateral side (Fig. 4a-f). This group has been further subdivided into two groups: *Group 2a* and *Group 2b*, according to the presence of the deviation of the vomer bone and severity of the anterior displacement of the petrous bone on the ipsilateral side.

- *Group 2a* – includes patients with mild/ absent anterior displacement of petrous bone on the ipsilateral side with the normal position of the vomer bone (Fig. 4a-c).
- *Group 2b* – includes patients with mild or severe anterior displacement of petrous bone with a moderate degree of vomer bone deviation to the ipsilateral side (Fig. 4d-f).

(iii) *Group 3* – occurrence of severe deviation of the nasal pyramid to the contralateral side associated with anterior displacement of the petrous bone and vomer on the ipsilateral side in addition to orbital bone abnormalities and unilateral flattening of the frontal bone with secondary asymmetry of the craniovertebral junction (Fig. 4g-i).

Di Rocco *et al.* (2012) stated that a classification scheme is important for the establishment of surgical planning and to forecast the late functional and cosmetic outcomes.

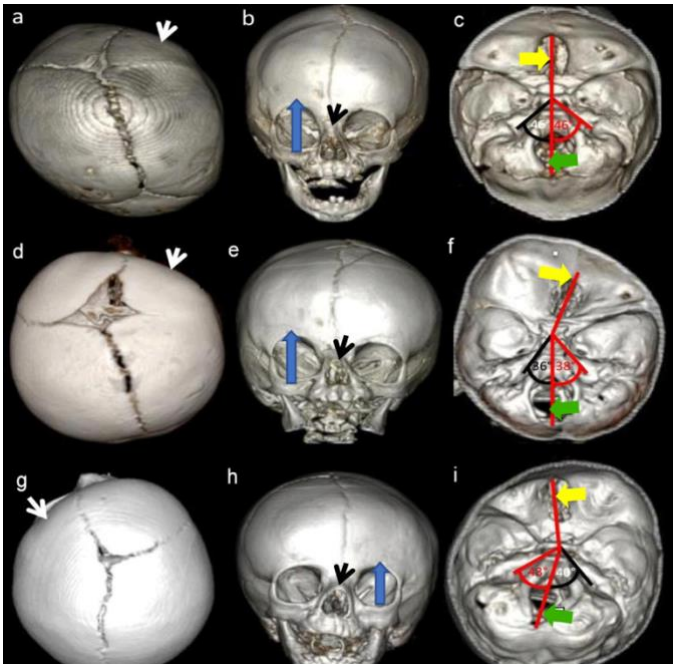

Figure 4: Displays the Di Rocco and Velardi classification scheme for ASP that was implemented in 1988 based on craniofacial dysmorphology. **(a-c)** and **(d-f)** Skulls presented with RUCS. **(g-i)** Skulls presented with LUCS. *(Adapted from Calandrelli et al., 2016)*

KEY

Superior view – **a, d, g**
Anterior view – **b, e, h**
Endocranial view – **c, f, i**

(a, b, c) ***Group 2a***
White arrow = Flattening of frontal bone on ipsilateral side
Blue arrow = Elevated roof of orbit on ipsilateral side
Black arrow = Normal position of the nasal pyramid
Yellow arrow = Normal positioned vomer
Green arrow = Normal position of sphenobasilar line
Angles = Mild/absent anterior displacement of petrous bone on ipsilateral side

(d, e, f) ***Group 2b***
White arrow = Flattening of frontal bone on ipsilateral side
Blue arrow = Elevated roof of orbit on ipsilateral side
Black arrow = Deviation of the nasal pyramid to contralateral side
Yellow arrow = Moderate degree of vomer deviation to ipsilateral side
Green arrow = Normal position of sphenobasilar line
Angles = Mild anterior displacement of petrous bone on ipsilateral side

(g, h, i) ***Group 3***
White arrow = Flattening of frontal bone on ipsilateral side
Blue arrow = Elevated roof of orbit on ipsilateral side
Black arrow = Severe deviation of the nasal pyramid to contralateral side
Yellow arrow = Deviation of vomer to ipsilateral side
Green arrow = Deviation of sphenobasilar line to the ipsilateral side
Angles = Sever anterior displacement of petrous bone on ipsilateral side

1.2.5.1. ACF

Captier *et al.* (2003) verified that ASP caused an asymmetrical skull base, which was very significant. It was also confirmed that the ipsilateral side of the skull base is usually smaller and the midline structures in front of the sella turcica, from the tuberculum sellae to the foramen cecum, deviate to the ipsilateral side (Marsh *et al.*, 1986; Captier *et al.*, 2003). Contralateral frontal bossing and ipsilateral frontal bone retrusion was also identified (Marsh *et al.*, 1986; Heuzé *et al.*, 2012; Dvoracek *et al.*, 2021).

- ACF length

Previous studies measured the length of the ACF from the anterior edge of the crista galli to the xiphoid of the lesser wing (Fig. 5) (Captier *et al.*, 2003; Calandrelli *et al.*, 2016; 2018). They

reported that there was a significant decrease in length of the ACF on the ipsilateral side when compared to the contralateral side (Table 1).

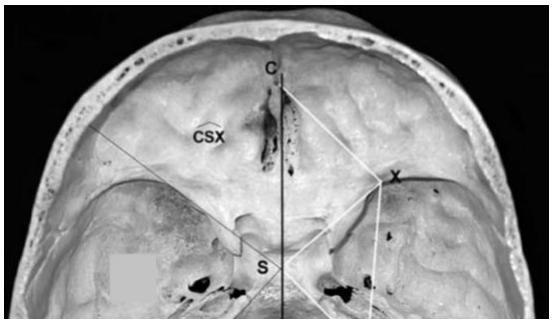

KEY
C – Crista galli
S – The centre of the sella turcica
X – The xiphoid of the lesser wing of the sphenoid
∠CSX – Angle of ACF

Figure 5: Displays the landmarks used to measure the length and angle of the ACF. *(Adapted from Captier et al*., 2003)

- ACF angle

In literature, the angle of the ACF was measured from the anterior edge of the crista galli to the centre of the sella turcica and to xiphoid of the lesser wing (Fig. 5) (Captier *et al.*, 2003; Calandrelli *et al.*, 2016; 2018). The angle of the ACF on the ipsilateral side compared to the contralateral side, resulted in a significant difference; the ipsilateral angle was reported to be smaller than the contralateral angle according to Marsh *et al.* (1986), Captier *et al.* (2003), Calandrelli *et al.* (2016; 2018). Marsh *et al.* (1986) also discovered that the angles of the ACF on the ipsilateral side are more acute, hence the decrease in the degree of the angles. Calandrelli *et al.* (2016; 2018) employed the Di Rocco and Velardi (1988) classification to assess the asymmetry in ASP patients according to severity. The asymmetry of the angle was more evident in infants with higher severity of the deformity, such as those in group 3 (Table 2).

In Tables 1 and 2, the lengths and angles of the ACF were significantly decreased on the ipsilateral side when compared to the contralateral side, this resulted in the asymmetry of the ACF with reduced growth on the ipsilateral side (Captier *et al.*, 2003; Calandrelli *et al.*, 2016; 2018).

Sgouros *et al.* (1999) and Bentley *et al.* (2002) reported that in infants with ASP, the dimensions of the ACF reached normal values in males within the first few months of life, but remained underdeveloped (shallow) in females; however, this did not appear to have a direct impact on the patterns of orbital growth, as orbital volume reaches normal values before the end of the first year of life in both sexes.

1.2.5.2. Orbit

- Orbital volume

Previous studies that investigated the volume of the orbit, segmented the orbital cavity using their preferred orbital boundaries to compute the volume. Bentley *et al.* (2002) and Calandrelli *et al.* (2018) calculated the orbital volume by outlining the interface between the inner walls of the bony orbit and the soft tissue contents of the orbit. The anterior boundary was defined as the line extending between the medial and lateral canthi and the posterior boundary was defined as the line connecting the medial and lateral walls of optic foramen within the orbit (Fig. 6A). Kronig *et al.* (2021) included the intraorbital soft tissues but excluded the bony boundaries. They defined the anterior boundary as a straight line connecting the most antero-inferior point of the SOR and the most antero-superior point of the IOR in the sagittal plane. The anterior segment of the optic canal was identified as the posterior boundary, therefore excluding the optic canal from the volume calculation (Fig. 6B). Beckett *et al.* (2013) and Dvoracek *et al.* (2021) defined orbital volume as the volume of the soft-tissue contents of the orbit, bounded by a plane connecting the medial and lateral walls of the orbit anteriorly, and the posterior orbital openings (Fig. 6C).

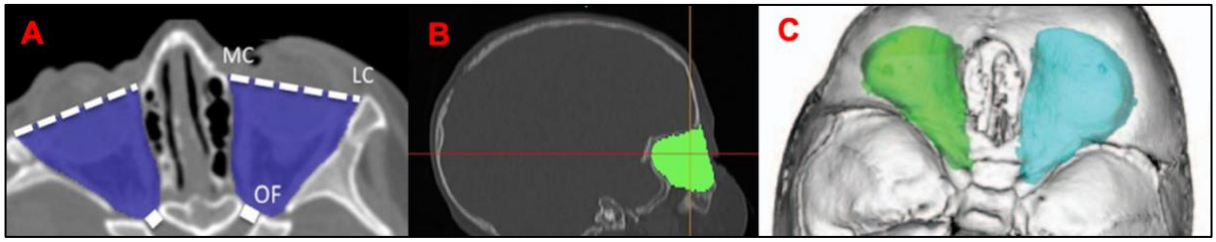

Figure 6 A-C: Displays the orbital boundaries that were segmented to calculate orbital volume in the literature. *(Adapted from Calandrelli et al., 2018; Dvoracek et al., 2021; Kronig et al.,2021)*
KEY: **A**- Axial view, **B**- Sagittal view, **C**- Superior view, **MC**- Medial canthus, **LC**- Lateral canthus, **OF**- Optic foramen, **Shaded areas**- Segmented orbital areas.

Despite the fact that the authors used different segmentation techniques, they all observed the same pattern: there was asymmetry between the ipsilateral and contralateral orbits, and the volume of the ipsilateral orbit was much smaller than the contralateral orbit (Table 3) (Bentley *et al.*, 2002; Beckett *et al.*, 2013; Calandrelli *et al.*, 2018; Dvoracek *et al.*, 2021; Kronig *et al.*, 2021). Bentley *et al.* (2002), assessed their patients separately and noted that in all 12 patients, the volume of the ipsilateral orbit was smaller than the contralateral orbit with a mean difference of 1.31±1.05 cm^3 (Table 3). Lo *et al.* (1996), also noted that the volume of the ipsilateral orbit was less than the contralateral orbit but there was no significant association between orbital volume and the ipsilateral side.

In patients with ASP, only a few studies calculated orbital volume and orbital volume ratios (ipsilateral-contralateral side). Bentley *et al.* (2002) found a mean ratio of 92.0 and Beckett *et al.* (2013) reported a mean ratio of 93.8. Calandrelli *et al.* (2018) employed the Di Rocco and Velardi (1988) classification scheme to link calculated orbital volumes to ASP severity, resulting in ratios of 92.0 in groups 2a and 2b (moderate) and 91.0 in group 3 (severe). On the ipsilateral side, they found that orbital volume was not significantly reduced although a trend in progressively reducing volumes was noticed according to the severity of the group (Table 3).

Kronig *et al.* (2021) aimed to link calculated orbital volumes to Utrecht Cranial Shape Quantifier (UCSQ) severity levels. There were no significant variations in group means of orbital volume ratio between different UCSQ severity levels, both the mild and moderate groups had a mean orbital volume ratio of 0.92, while the severe group had a mean orbital volume ratio of 0.93.

Escaravage and Dutton (2013) reported on normal orbits, during the first twelve to twenty-four months of life, orbital growth was most rapid, and orbital volumes were smaller in females than in males throughout childhood. Bentley *et al.* (2002) further added that in their study the normal mean orbital volumes in patients with UCS were not reached until eleven months of age, they also stated that if surgery is performed before this time, when the synostosis process is still active, improving the ratio of the ipsilateral to contralateral side will be extremely difficult. Heuzé *et al.* (2012) reported that on the ipsilateral side the orbit was shifted posterolaterally and on the contralateral side the orbit was shifted anteromedially.

- Orbital breadth

Dvoracek *et al.* (2021) measured the orbital breadth as the horizontal distance between the most lateral and medial points along the lateral and medial orbital rim. They reported that the breadth of the orbit was significantly decreased on the ipsilateral side when compared to the contralateral side. As a result, the ipsilateral orbit appeared to be very narrow, while the contralateral orbit appeared to be expanded (Fig. 7) (Table 4).

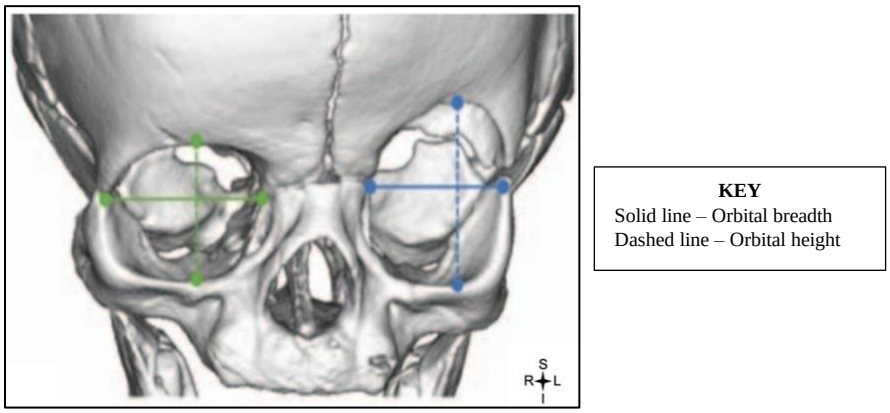

Figure 7: Anterior view of skull with LUCS showing the landmarks used to measure the breadth and height of the orbital cavity. *(Adapted from Dvoracek et al., 2021)*

- Orbital height

Orbital height was measured as the vertical distance between the highest and lowest points along the SOR and infraorbital rim (IOR) (Dvoracek *et al.*, 2021). Orbital height was significantly increased on the ipsilateral side compared to the contralateral side, as a result, the ipsilateral orbit appeared to be elongated, while the contralateral orbit appeared to be shortened (Fig. 7) (Table 5) (Dvoracek *et al.*, 2021).

- Supraorbital rims

No measurements have been documented in literature regarding the position of the SORs; however, Marsh *et al.* (1986) and Mesa *et al.* (2011) reported that the ipsilateral orbit had a higher SOR than the contralateral orbit. According to Dvoracek *et al.* (2021), the contralateral orbit had increased brow protrusion, while the ipsilateral orbit had mild and inconsistent brow retrusion.

1.2.5.3. Position of the ear

There were no studies that examined the position of the ears on either side quantitatively, however a few previous studies have reported on the horizontal and vertical position of the ears. It was noted that the EAM was anteriorly displaced on the ipsilateral side (Pelo *et al.*, 2011; Spazzapan *et al.*, 2017). In more severe cases of ASP, the EAM on the ipsilateral side was more anterior and slightly depressed (Pelo *et al.*, 2011). A study by Bruneteau and Mulliken *et al.* (1992) reported that the ipsilateral ear was anteriorly and superiorly positioned based on physical examination. The parietal bone and squamous part of the temporal bone were shifted anteromedially on the ipsilateral side and posterolaterally on the contralateral side, according to Di Rocco *et al.* (2012)

and Heuzé *et al.* (2012). The upward and forward deviation of the petrous part of the temporal bone was also documented by Captier *et al.* (2003).

1.2.6. Summary of literature

Table 1: Lengths of the ACF on the ipsilateral and contralateral sides in patients with ASP

Author	Year	Sample size (N)	Sex	Age (months)	Classification system used	Degree of severity	ACF length (mm) (Ipsilateral side)	ACF length (mm) (Contralateral side)
Calandrelli *et al.*	2016	Total: 36 (18 ASP subjects and 18 healthy subjects)	Male and Female	Mean age: 5.92	Di Rocco and Velardi (1988)	Group 2 Group 3	31.50 29.00	36.50 37.00
Calandrelli *et al.*	2018	Total: 50 (26 ASP subjects and 24 healthy subjects)	Male and Female	Mean age: 5.34	Di Rocco and Velardi (1988)	Group 2a Group 2b Group 3	32.10 32.70 29.50	39.70 40.60 39.20

Note: ACF = Anterior cranial fossa
ASP = Anterior synostotic plagiocephaly
mm = millimeter

Table 2: Angles of the ACF on the ipsilateral and contralateral sides in patients with ASP

Author	Year	Sample size (N)	Sex	Age (months)	Classification system used	Degree of severity	ACF Angle (Degrees) (Ipsilateral side)	(Contralateral side)
Captier *et al.*	2003	Total: 102 (18 cases of ASP)	Male and Female	Mean age: 15.1 (Mean age for ASP cases: 4.8)	Not applicable	Not applicable	54.40	71.40
Calandrelli *et al.*	2016	Total: 36 (18 ASP subjects and 18 healthy subjects)	Male and Female	Mean age: 5.92	Di Rocco and Velardi (1988)	Group 2 Group 3	53.65 49.00	65.75 65.25
Calandrelli *et al.*	2018	Total: 50 (26 ASP subjects and 24 healthy subjects)	Male and Female	Mean age: 5.34	Di Rocco and Velardi (1988)	Group 2a Group 2b Group 3	50.50 50.99 46.24	63.71 68.01 68.48

Note: ACF = Anterior cranial fossa
ASP = Anterior synostotic plagiocephaly

Table 3: Volume of the orbits on the ipsilateral and contralateral sides in patients with ASP

Author	Year	Sample size (N)	Sex	Age (months)	Classification system used	Degree of severity	Orbital volume (cm^3) (Ipsilateral side)	Orbital volume (cm^3) (Contralateral side)
Bentley *et al.*	2002	Total: 50 (12 cases of ASP)	Male Female	Mean age: 13.10	Not applicable	Not applicable	14.83 15.85	16.09 17.33
Calandrelli *et al.*	2018	Total: 50 (26 ASP subjects and 24 healthy subjects)	Male and Female	Mean age: 5.34	Di Rocco and Velardi (1988)	Group 2a Group 2b Group 3	11,561.85 11,259 10,513.57	12,471.14 12,127 11,462.85
Dvoracek *et al.*	2021	Total: 46 (23 ASP subjects and 23 healthy subjects)	Male and Female	Not stated	Not applicable	Not applicable	11.02	11.85
Kronig *et al.*	2021	Total: 19 ASP subjects	Male and Female	Mean age: 6.53	Utrecht Cranial Shape Quantifier	Mild Moderate Severe	12.43 13.66 13.36	13.47 14.87 14.32

Note: ASP = Anterior synostotic plagiocephaly
cm^3 = Cubic centimeter

Table 4: Breadth of the orbits on the ipsilateral and contralateral sides in patients with ASP

Author	Year	Sample size (N)	Sex	Age (months)	Classification system used	Degree of severity	Orbital breadth (mm) (Ipsilateral side)	Orbital breadth (mm) (Contralateral side)
Dvoracek *et al.*	2021	Total: 46 (23 ASP subjects and 23 healthy subjects)	Male and Female	-	Not applicable	Not applicable	26.32	28.03

Note: ASP = Anterior synostotic plagiocephaly
mm = millimeter

Table 5: Height of the orbits on the ipsilateral and contralateral sides in patients with ASP

Author	Year	Sample size (N)	Sex	Age (months)	Classification system used	Degree of severity	Orbital height (mm) (Ipsilateral side)	Orbital height (mm) (Contralateral side)
Dvoracek *et al.*	2021	Total: 46 (23 ASP subjects and 23 healthy subjects)	Male and Female	-	Not applicable	Not applicable	28.73	23.97

Note: ASP = Anterior synostotic plagiocephaly
mm = millimeter

1.3. Materials and methods

This study is a retrospective, descriptive observational (cross-sectional) study. Eighteen preoperative CT scans, with an axial slice thickness range of 1-5mm were obtained from the database of the Department of Plastic and Reconstructive Surgery at the Inkosi Albert Luthuli Central Hospital (IALCH), Durban, South Africa. The analysis was limited to patients who met the inclusion criteria. The Horos Project (Version 3.3.6) DICOM (Digital Imaging and Communication in Medicine) viewer was used to review and analyse these scans. The morphometry of the ACF, orbit and ear on the ipsilateral and contralateral sides were determined using anatomical landmarks in the axial, sagittal, or coronal planes on two-dimensional (2D) CT scans. Each measurement was repeated three times by the candidate (intra-observer analysis) as well as by a second observer (inter-observer analysis) to ensure accuracy and reliability. Relevant gatekeeper permissions were acquired, and institutional ethical clearance for this study was obtained from the Biomedical Research Ethics Committee of the University of KwaZulu-Natal (UKZN) (BREC/00002129/2020) and relevant authorities.

1.3.1. Inclusion & exclusion criteria

1.3.1.1. Inclusion criteria

- Patients with premature fusion of either the right or left coronal suture (RUCS or LUCS)
- Patients with non-syndromic (isolated) ASP
- Patients with preoperative CT scans only
- Patients with fine CT slices (1-5 mm thickness) which were of acceptable quality for assessment of craniofacial asymmetry

1.3.1.2. Exclusion criteria

- Patients with synostosis affecting multiple cranial sutures or with synostosis affecting more than one coronal suture (any other type of craniosynostosis other than ASP)
- Patients with any known or suspected craniofacial syndrome
- Patients who had undergone surgical correction, postoperative CT scans
- Patients with poor CT image resolution or slice thickness greater than 5mm

1.3.2. Ethics and regulatory approvals

Relevant gatekeeper permissions were acquired, and institutional ethical clearance for this study was obtained from the Biomedical Research Ethics Committee of the University of KwaZulu-Natal (UKZN) (BREC/00002129/2020) and relevant authorities.

1.3.3. Anonymity and confidentially

The study involved the use of retrospective CT scans and there was no known risk to patients or direct patient contact. Patient information and collected data were held anonymously and stored in password protected electronic devices.

1.3.4. Anatomical landmarks

A set of select standardized anatomical landmarks consistent with the characteristic features of anterior plagiocephaly were located and marked by three individuals, a plastic surgeon (AM), neurosurgeon (RH), and an anatomist (LL) as they were easily identifiable, reproducible, and deemed to be the best points to investigate the dimensions being studied. To ensure repeatability and reproducibility of the landmarks, each measurement was repeated three times by the candidate and a second observer in different settings and the intra- and inter-observer reliability coefficients were calculated.

1.3.5. Image acquisition and analysis

CT scans of patients were retrieved from a Picture Archiving and Communication System (PACS) at the hospital and saved as a DICOM file. The CT images were acquired in the clinical routine with either a 128-slice SOMATOM Definition AS scanner or SOMATOM Definition Flash CT Scanner (Siemens Healthineers, Forcheim, Germany).

All the CT images were automatically calibrated by the Horos Project DICOM viewer. This was verified manually. Slice orientation was standardized to reduce measurement errors by loading the images into a 3D multiplanar reconstruction (MPR) view and aligning them parallel to the orbitomeatal plane. The orbitomeatal line, also known as the canthomeatal line is a positioning line used in skull radiography. It runs through the outer canthus of the eye and the midpoint of the EAM. This line is used to position the patient for various radiological views (Otake *et al.*, 2018). All volume measurements were performed on 2D axial slices with the use of two tools in the Horos Project DICOM viewer: the 'closed polygon' tool for manual segmentation of a specific

region and the region of interest (ROI) volume tool for automatic volume calculation of the total selected regions. All scans were analyzed using bone-window settings.

1.3.6. Morphometric analysis

1.3.6.1. ACF dimensions

- Width (transverse diameter) and length (anteroposterior diameter):

These measurements were taken in the axial plane at the level where the inferior extent of the fused coronal suture was first observed to be the most prominent. The posterior margin of the crista galli was used as a reference landmark. This landmark was transcended to the level at which the inferior extent of the fused coronal suture was first observed to be the most prominent. At that level, the width was determined on the contralateral side by constructing a line from the coronal suture to the transcended landmark, whereas on the ipsilateral side, a line was constructed from the inferior extent of the fused coronal suture to the transcended landmark (Fig. 8). The midpoints of those two lines created by the width were calculated and the length of the ACF on either side was measured by constructing a perpendicular line from the midpoint to the inner table of the ACF (Fig. 8).

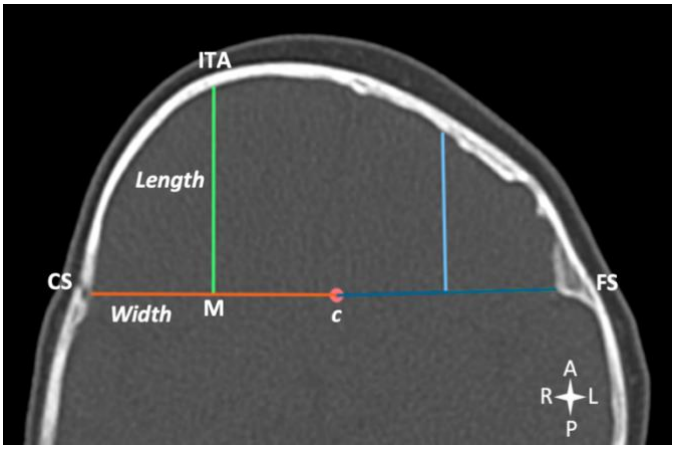

KEY
ITA - Inner table of ACF
CS - Coronal suture
FS - Fused coronal suture
M - Midpoint
c - Transcended point of posterior margin of crista gali

Figure 8: ACF width (CS - c) and length (M - ITA) measurements in a patient with LUCS *(axial view).*

- Length of ACF curve:

This measurement was taken in the axial plane at the level where the inferior extent of the fused coronal suture was first observed to be the most prominent. A midline that divided the ACF into right and left sides and a posterior boundary/limitation that separated the ACF from the rest of the skull base was created. The midline was determined by using two reference landmarks; the nasion

and the midpoint of the sella turcica when it was first observed to be the most prominent. These landmarks were transcended to the level at which the inferior extent of the fused coronal suture was first observed to be the most prominent. At that level, the two transcended landmarks were connected, and the midline reference was formed. The posterior boundary was determined as the coronal suture on the contralateral side and the fused coronal suture on the ipsilateral side. On the contralateral side, the length of the curve was measured from the midline to the coronal suture, whereas on the ipsilateral side, the length of the curve was measured from the midline to the fused coronal suture (Fig. 9).

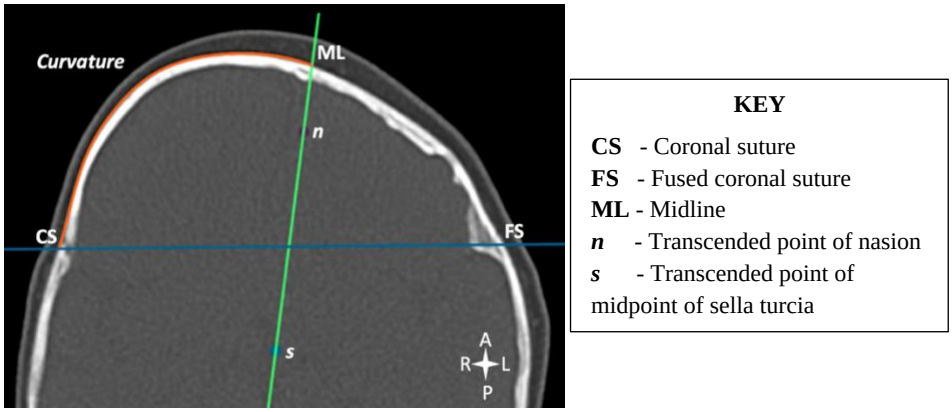

Figure 9: Measurement of the length of the ACF curvature (CS - ML) in a patient with LUCS *(axial view)*.

- Angle:

This measurement was taken in the axial plane at the level where the inferior extent of the fused coronal suture was first observed to be the most prominent. The first ray of the angle was determined by constructing a line from the coronal suture on the contralateral side to the fused coronal suture on the ipsilateral side. This line was extended to the border of overlying skin and marked off as a point on either side. The angle's second ray was determined by constructing a tangent from the point at the border of the overlying skin to the curve of the ACF. The common vertex of the angle on both sides was the point at the border of the overlying skin. The inter-tangential angle of the ACF was determined by extending the tangents on either side anteriorly until they intersect. This angle was manually calculated by subtracting 180° from the sum of the angle values acquired on each side (Fig. 10).

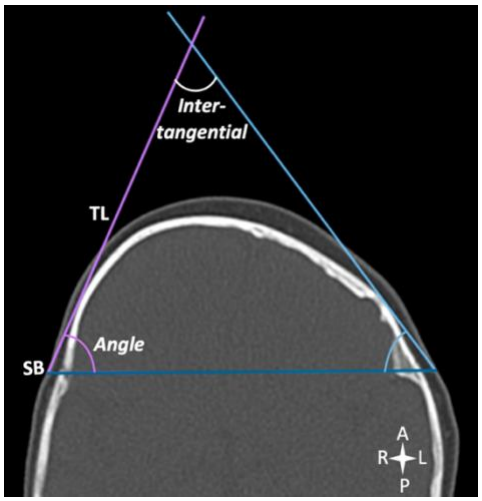

KEY
TL - Tangent line
SB - Overlying skin border

Figure 10: ACF angle and inter-tangential angle measurements in a patient with LUCS *(axial view)*.

- Height:

This measurement was taken in the coronal plane at the level where the posterior margin of the crista galli was first observed to be the most prominent. Two approaches were used to measure the height:

(a) By constructing a perpendicular line from the midpoint of the orbital roof to the inner table of the ACF on either side (Fig. 11).

(b) By constructing a perpendicular line from the superolateral border of the orbit to the inner table of the ACF (Fig. 11).

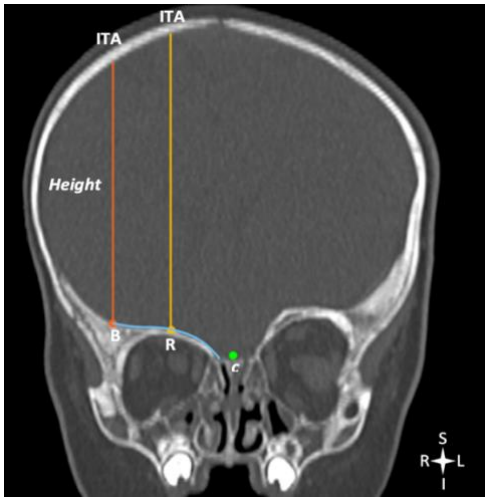

KEY
ITA - Inner table of ACF
B - Superolateral border of orbit
R - Midpoint of the roof of orbit
c - Posterior margin of crista gali

Figure 11: Measurements of the height of the ACF from superolateral border of orbit (B - ITA) and the height of the ACF from midpoint of the roof of orbit (R - ITA) in a patient with LUCS *(coronal view)*.

- Volume:

This measurement was taken on 2D axial slices. The ACF was manually segmented in every slice of the CT images. A midline that divided the ACF into right and left sides and a posterior boundary/limitation that separated the ACF from the rest of the skull base was created. The midline was created by using two reference landmarks; the nasion and the midpoint of the sella turcica when it was first observed to be the most prominent. These landmarks were transcended to the level at which the inferior extent of the fused coronal suture was first observed to be the most prominent. At that level, the two transcended landmarks were connected, and the midline reference was formed. The posterior boundary was determined by connecting the coronal suture on the contralateral side to the fused coronal suture on the ipsilateral side. The midline and posterior boundary lines were transcended onto every slice of the CT images where the ACF was visible. When the ACF was visible, the start slice was chosen, and when the posterior margin of the crista galli was no longer visible or shortly before the sinuses were apparent, the end slice was chosen. The right and left segments of the ACF (ROIs) were manually outlined on each consecutive slice by using the 'closed polygon' tool. All ROIs were selected and the volume on either side was automatically calculated using the ROI volume tool (Fig. 12).

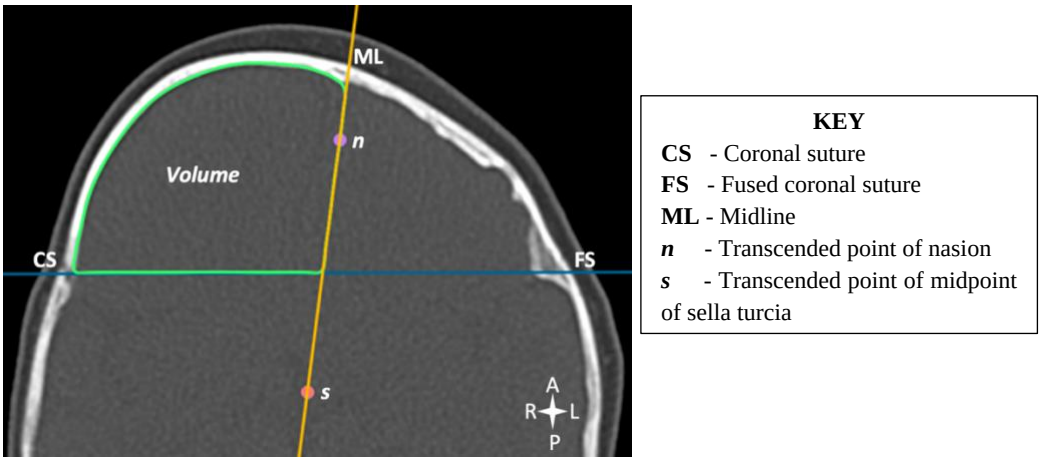

Figure 12: Segmentation technique used to outline the ACF on either side in a patient with LUCS *(axial view)*.

1.3.6.2. Orbital dimensions

- Length (anteroposterior diameter):

This measurement was taken in the sagittal plane at the level where the maximum diameter of the optic canal was observed on each orbit. The orbital length was measured in relation to the SOR and IOR. The purpose of using these two approaches was to examine the anatomical changes that

may have occurred to the SOR and IOR on the ipsilateral side when compared to the contralateral side as these structures are usually severely impacted in ASP patients.

The slice that portrayed the maximum diameter of the optic canal on each orbit was chosen and the midpoint of the optic canal was used as a landmark. At that level, a line was drawn vertically downwards from the most anterior portion of the SOR to mark the point of the SOR and another line was drawn vertically upwards from the most anterior portion of the IOR to mark the point of the IOR. The orbital length on either side was determined by constructing a perpendicular line anteriorly from the midpoint of the optic canal until it met with the vertical lines that marked the points of the SOR and IOR (Fig. 13).

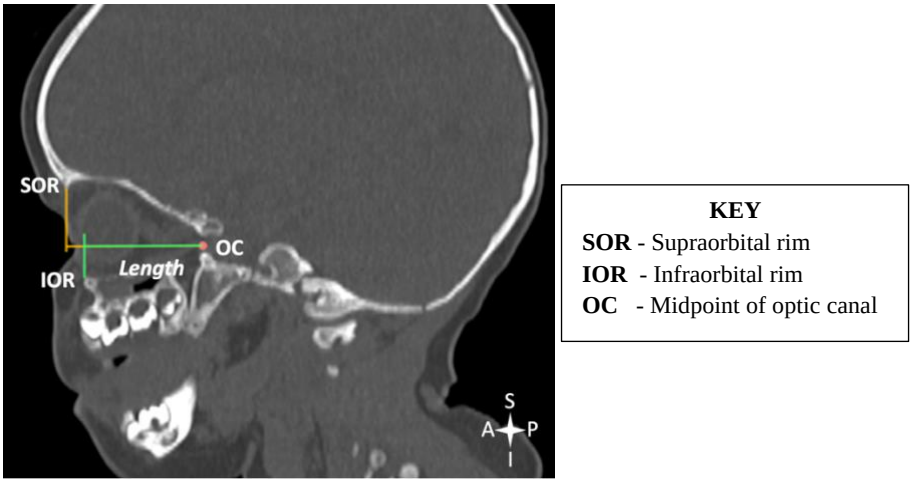

Figure 13: Measurements of the orbital length in relation to the SOR (OC - SOR) and in relation to the IOR (OC - IOR) in a patient with LUCS *(sagittal view).*

- Breadth (transverse diameter) and height (maximum vertical height):

These two measurements were taken in the coronal plane at the level where the frontozygomatic suture was first observed to be the most prominent on each orbit. The breadth of each orbit was determined by constructing a horizontal line from the anterior margin of the frontozygomatic suture to the medial wall of the orbit (Kronig et al., 2021). The height of each orbit was determined by taking a point from the inferior orbital margin, marking the infraorbital foramen to the highest point of each orbit on the superior orbital margin (Fig. 14).

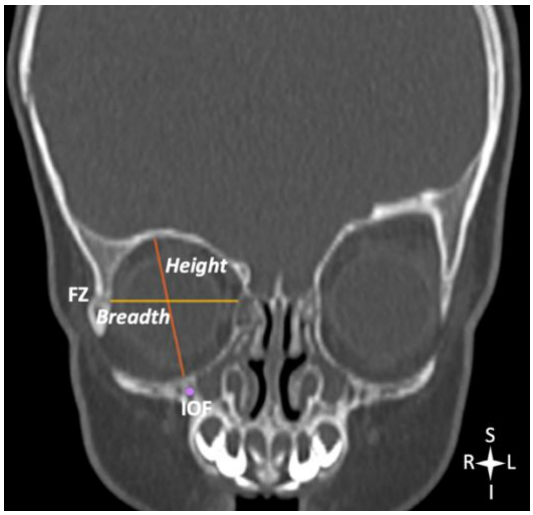

KEY
FZ - Frontozygomatic suture
IOF - Infraorbital foramen

Figure 14: Orbital breadth (FZ - Medial wall) and height (IOR - SOR) measurements in a patient with LUCS *(coronal view)*.

- Surface area:

This measurement was taken in the coronal plane at the level where the frontozygomatic suture was first observed to be the most prominent on each orbit. The surface area of each orbit was determined by manually tracing the orbital rim with the 'closed polygon' tool. This tool automatically calculated the surface area for each orbit (Fig. 15).

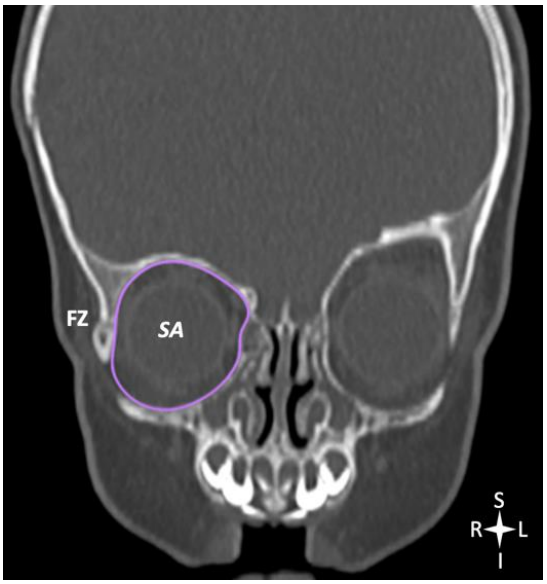

Figure 15: Segmentation of the orbital surface area (SA) in a patient with LUCS *(coronal view)*.

- Volume:

This measurement was taken on 2D axial slices. The interface between the inner bony walls and the soft tissue contents of each orbit was manually delineated on every slice of the CT images using the 'closed polygon' tool to determine the orbital volume. The anterior boundary of the orbit was defined as the inner surface of the eyelid, this landmark was used to account for the spaces around the globe due to its variable location in the orbital cavity. The posterior boundary was defined by a line connecting the lateral and medial walls of the optic foramen within the orbital cavity. The segmented orbital areas (ROIs) on each consecutive slice were selected, and the volume of each orbit was automatically calculated using the ROI volume tool (Fig. 16).

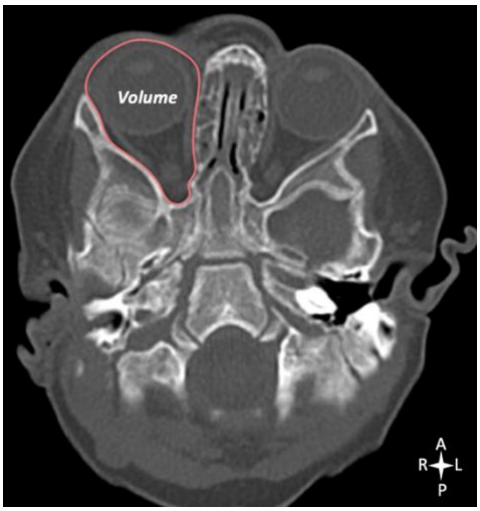

Figure 16: Segmentation technique used to outline the orbital cavity in a patient with LUCS *(axial view)*.

- Maximum vertical height between the supraorbital rims:

This measurement was taken in the coronal plane at the level where the frontozygomatic suture was first observed to be the most prominent on each orbit. Two horizontal lines were drawn, one from the highest point of the SOR on the ipsilateral side extending to the contralateral side (cranial line), and the other was drawn from the highest point of the SOR on the contralateral side extending to the ipsilateral side (caudal line). The distance between the cranial and caudal lines calculated the maximum vertical height between the SORs (Fig. 17).

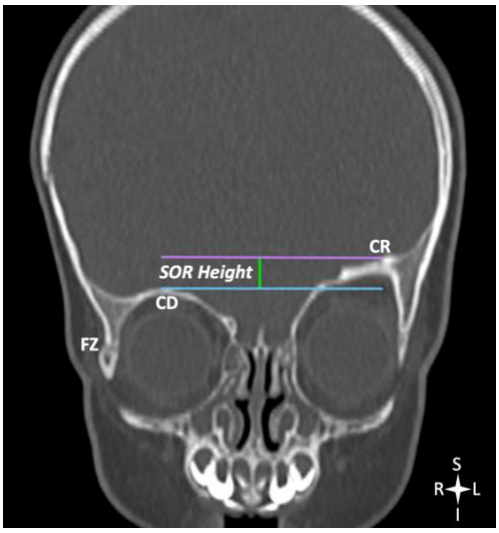

KEY
FZ - Frontozygomatic suture
CR - Cranial line
CD - Caudal line

Figure 17: Maximum vertical height between the SORs (CR - CD) in a patient with LUCS *(coronal view)*.

1.3.6.3. Position of the ear

The maximum AP distance and vertical height measurements of the ear were taken at the level where the maximum diameter of the EAM was observed on each ear (Fig. 18 and 19).

- Maximum AP distance:

The axial slice that portrayed the maximum diameter of the EAM on each ear was chosen and the midpoint of the EAM was used as a landmark. Two horizontal lines were drawn, one from the midpoint of the EAM on the ipsilateral side extending to the contralateral side (anterior line), and the other was drawn from the midpoint EAM on the contralateral side extending to the ipsilateral side (posterior line). The distance between these anterior and posterior lines calculated the maximum AP distance between the ipsilateral and contralateral ear (Fig. 18).

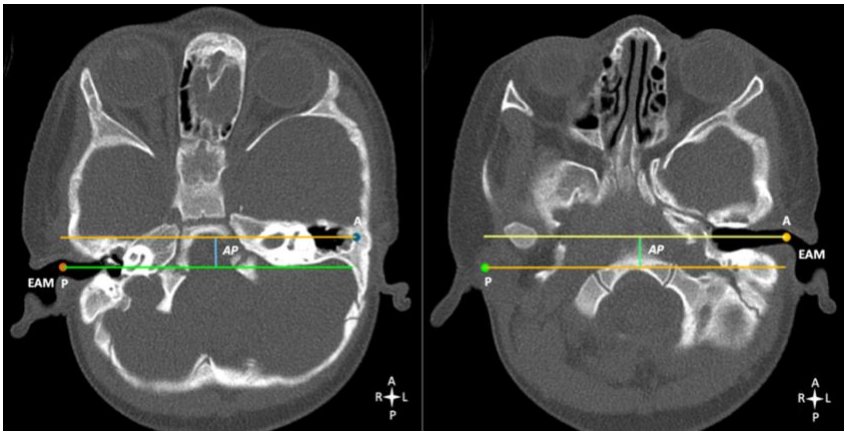

KEY
EAM - External auditory meatus
AP - Anteroposterior distance
A - Anterior line
P - Posterior line

Figure 18: Maximum AP distance between the ears (A - P) of a patient with LUCS *(axial view)*.

- Maximum vertical height:

The coronal slice that portrayed the maximum diameter of the EAM on each ear was chosen and the midpoint of the EAM was used as a landmark. Two horizontal lines were drawn, one from the midpoint of the EAM on the ipsilateral side extending to the contralateral side (caudal line), and the other was drawn from the midpoint EAM on the contralateral side extending to the ipsilateral side (cranial line). The distance between the cranial and caudal lines calculated the maximum vertical height between the ipsilateral and contralateral ear (Fig. 19).

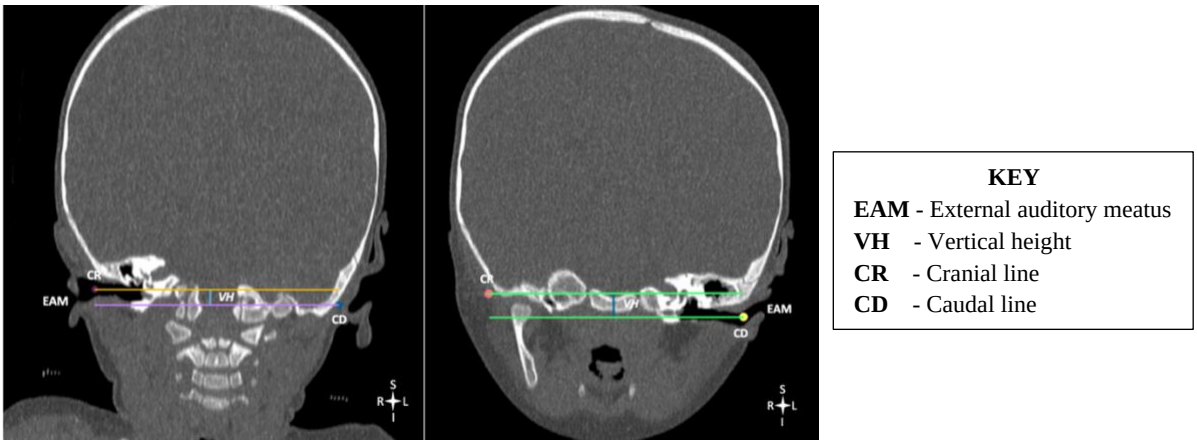

Figure 19: Maximum vertical height between the ears (CR - CD) of a patient with LUCS *(coronal view)*.

1.3.7. Variables

1.3.7.1. Demographic Factors

Demographic factors such as age, sex and race were documented and variations with regards to these factors were recorded.

1.3.7.2. Laterality

The fusion of either the right or left coronal suture was documented and variation with regards to this was recorded.

1.3.8. Sample size

This study included all patients with untreated, non-syndromic ASP who presented to the IALCH Craniofacial Unit between 2004 and 2020 and met the inclusion criteria. During this time, preoperative CT scans of 18 individuals with a confirmed diagnosis of non-syndromic ASP were obtained. This study initially acquired 29 cases of ASP, but 11 were eliminated because they were either syndromic or had multiple-suture synostosis, and thus did not fit the inclusion criteria.

A power analysis could not be calculated as studies with rare conditions require an analysis of what is available. The small sample size was attributable to the low prevalence of ASP (1 per 10,000 live births) and the study's focus on one specific cohort of craniosynostosis. Data was acquired from a single site, as this is a Masters dissertation and IALCH is the only Craniofacial Unit in KwaZulu-Natal. There are only three Craniofacial Units in South Africa. Scans performed prior to 2004 were not of the same quality and had poor resolution. Prior to 2003, the Craniofacial Unit was also housed at a different hospital, which provided scans of varying types and quality. Since the Craniofacial Unit relocated to Inkosi Albert Luthuli Central Hospital in 2003, only scans from 2004 onwards were collected because the scans were of greater quality and standardisation, hence the time span from 2004 to 2020 was chosen.

1.3.9. Statistical analysis

Statistical data analysis was performed by using R Statistical Computing Software of the R Core Team, 2020, version 3.6.3. A p-value of less than 0.05 was considered statistically significant. The results were presented in the form of descriptive and inferential statistics. Multidimensional numerical variables were presented as parallel plots. Depending on the distribution of the differences in the before and after numerical values, the differences were assessed using either the paired t-test or Wilcoxon respectively. In addition, boxplots were used for the visual display of the descriptive patterns as well as a paired test. To determine the reliability of the morphometrical data, intra-observer and inter-observer reliability were calculated and represented as intraclass correlation coefficient (ICC) values. All statistical methods and analyses were conducted in consultation with a university statistician.

1.4. Structure of thesis

This masters thesis was prepared according to the guidelines outlined by the College of Health Sciences, University of KwaZulu-Natal, South Africa. The manuscript has been structured and formatted according to the guidelines of the Journal of Craniofacial Surgery.
The structural outline of the thesis is as follows:

1.4.1. Chapter 1: Introduction

This chapter provided insight into the development of anterior synostotic plagocephaly and the craniofacial features associated with it as well as a comprehensive literature review and an

overview of the study. The aims, objectives, research question and the overview of methodology are included in this chapter.

1.4.2. Chapter 2: Scientific Manuscript

This chapter comprised of an original scientific manuscript entitled: Anterior synostotic plagiocephaly – A quantitative analysis of craniofacial features using computed tomography. This manuscript investigated and compared the morphometry of the anatomical parameters of the anterior cranial fossa, orbit and ear on the ipsilateral and contralateral sides in a select cohort of South African patients with anterior synostotic plagiocephaly. These results were compared by age, sex, race and laterality to determine statistically significant relationships. This manuscript was submitted to the Journal of Craniofacial Surgery for review and possible publication (Manuscript number: SCS-22-0062).

1.4.3. Chapter 3: Synthesis

This chapter further discussed the findings of Chapter 2 and concluded the findings of the morphometry of the anterior cranial fossa, orbit and ear between the ipsilateral and contralateral sides in anterior synostotic plagiocephaly patients. Limitations encountered and recommendations for future research have been outlined and explained in this chapter.

Please note: The references are listed after each Chapter.

1.5. References

1. Becker, D., Petersen J., Kane, A., Cradock M., Pilgram, T. and Marsh, J. (2005). Speech, cognitive, and behavioral outcomes in nonsyndromic craniosynostosis. *Plast Reconstr Surg*, 116, pp.400–407
2. Beckett, J., Persing, J. and Steinbacher, D. (2013). Bilateral Orbital Dysmorphology in Unicoronal Synostosis. *Plastic and Reconstructive Surgery*, 131(1), pp.125-130.
3. Bentley, R., Sgouros, S., Natarajan, K., Dover, M. and Hockley, A. (2002). Changes in orbital volume during childhood in cases of craniosynostosis. *Journal of Neurosurgery*, 96(4), pp.747-754.
4. Brown, S. and Wetz, E. (2019). *Https://Www.Childrens.Com/*. [ebook] pp.39-46. Available at: <https://www.childrens.com/> [Accessed 3 May 2020].

5. Bruneteau, R. and Mulliken, J. (1992). Frontal Plagiocephaly: Synostotic, Compensational, or Deformational. *Plastic and Reconstructive Surgery*, 89(1), pp.21-31.
6. Calandrelli, R., D'Apolito, G., Massimi, L., Gaudino, S., Visconti, E., Pelo, S., Di Rocco, C. and Colosimo, C. (2016). Quantitative analysis of craniofacial dysmorphology in infants with anterior synostotic plagiocephaly. *Child's Nervous System*, 32(12), pp.2339-2349.
7. Calandrelli, R., Pilato, F., Massimi, L., Panfili, M., Di Rocco, C. and Colosimo, C. (2018). Quantitative analysis of cranial-orbital changes in infants with anterior synostotic plagiocephaly. *Child's Nervous System*, 34(9), pp.1725-1733.
8. Captier, G., Leboucq, N., Bigorre, M., Canovas, F., Bonnel, F., Bonnafé, A. and Montoya, P. (2003). Plagiocephaly: morphometry of skull base asymmetry. *Surgical and Radiologic Anatomy*, 25(3-4), pp.226-233.
9. Derderian, C. and Seaward, J. (2012). Syndromic Craniosynostosis. *Seminars in Plastic Surgery*, 26(02), pp.064–075.
10. Di Rocco, C. and Velardi, F. (1988). Nosographic identification and classification of plagiocephaly. *Child's Nervous System*, 4(1), pp.9-15.
11. Di Rocco, C., Paternoster, G., Caldarelli, M., Massimi, L. and Tamburrini, G. (2012). Anterior plagiocephaly: epidemiology, clinical findings, diagnosis, and classification. A review. *Child's Nervous System*, 28(9), pp.1413-1422.
12. Durham, E., Howie, R. and Cray, J. (2017). Gene/environment interactions in craniosynostosis: A brief review. *Orthodontics & Craniofacial Research*, 20, pp.8-11.
13. Dvoracek, L., Bykowski, M., Foglio, A., Ayyash, A., Pfaff, M., Losee, J. and Goldstein, J. (2021). Objective Analysis of Fronto-Orbital Dysmorphology in Unilateral Coronal Craniosynostosis. *Journal of Craniofacial Surgery*, 32(7), pp.2266-2272.
14. Escaravage, G. and Dutton, J. (2013). Age-related Changes in the Pediatric Human Orbit on CT. *Ophthalmic Plastic and Reconstructive Surgery*, 29(3), pp.150-156.
15. Flaherty, K., Singh, N. and Richtsmeier, J. (2016). Understanding craniosynostosis as a growth disorder. *WIREs Developmental Biology*, 5(4), pp.429-459.
16. Goodrich, J. (2005). Skull base growth in craniosynostosis. *Child's Nervous System*, 21(10), pp.871-879.
17. Gray, H. and Standring, S. (2016). *Gray's anatomy: The anatomical basis of clinical practice*. 41st ed. Amsterdam: Elsevier.
18. Hegazy, A. (2021). Skull Sutures as Anatomical Landmarks. *The Sutures of the Skull*, pp.129-146.
19. Heuzé, Y., Martínez-Abadías, N., Stella, J., Senders, C., Boyadjiev, S., Lo, L. and Richtsmeier, J. (2012). Unilateral and bilateral expression of a quantitative trait: asymmetry

and symmetry in coronal craniosynostosis. *Journal of Experimental Zoology Part B: Molecular and Developmental Evolution*, 318(2), pp.109-122.

20. Idriz, S., Patel, J., Ameli Renani, S., Allan, R. and Vlahos, I. (2015). CT of Normal Developmental and Variant Anatomy of the Pediatric Skull: Distinguishing Trauma from Normality. *RadioGraphics*, 35(5), pp.1585-1601.
21. Jeyaraj, P. (2011). A Modified Approach to Surgical Correction of Anterior Plagiocephaly. *Journal of Maxillofacial and Oral Surgery*, 11(3), pp.358-363.
22. Jin, S., Sim, K. and Kim, S. (2016). Development and Growth of the Normal Cranial Vault : An Embryologic Review. *Journal of Korean Neurosurgical Society*, 59(3), p.192.
23. Johnson, D. and Wilkie, A. (2011). Craniosynostosis. *European Journal of Human Genetics*, 19(4), pp.369-376.
24. Kabbani, H. and Raghuveer, T. (2004). Craniosynostosis. *Am Fam Physician*, 69(12), pp.2863-2870.
25. Kajdic, N., Spazzapan, P. and Velnar, T. (2017). Craniosynostosis - Recognition, clinical characteristics, and treatment. *Bosnian Journal of Basic Medical Sciences*, 18(2), pp.110-116.
26. Kronig, S., Kronig, O., Vrooman, H., Veenland, J. and Van Adrichem, L. (2020). Quantification of Severity of Unilateral Coronal Synostosis. *The Cleft Palate-Craniofacial Journal*, 58(7), pp.832-837.
27. Kronig, S., Kronig, O., Zurek, M. and Van Adrichem, L. (2021). Orbital volume, ophthalmic sequelae and severity in unilateral coronal synostosis. *Child's Nervous System*, 37(5), pp.1687-1694.
28. Lee, M., Hong, H. and Shim, K. (2021). Quantitative Assessment of Shape Deformation of Regional Cranial Bone for Evaluation of Surgical Effect in Patients with Craniosynostosis. *Applied Sciences*, 11(3), p.990.
29. Lo, L., Marsh, J., Kane, A. and Vannier, M. (1996). Orbital Dysmorphology in Unilateral Coronal Synostosis. *The Cleft Palate-Craniofacial Journal*, 33(3), pp.190-197.
30. Marsh, J., Gado, M., Vannier, M. and Stevens, W. (1986). Osseous Anatomy of Unilateral Coronal Synostosis. *Cleft Palate Journal*, 23, pp.87-100.
31. Matushita, H., Alonso, N., Cardeal, D. and de Andrade, F. (2012). Frontal–orbital advancement for the management of anterior plagiocephaly. *Child's Nervous System*, 28(9), pp.1423-1427.
32. Mesa, J., Fang, F., Muraszko, K. and Buchman, S. (2011). Reconstruction of unicoronal plagiocephaly with a hypercorrection surgical technique. *Neurosurgical Focus*, 31(2), p.e.4.
33. Moore, K., Agur, A. and Dalley, A. (2010). *Clinically oriented anatomy*. 6th ed. Philadelphia: Wolters Kluwer Health: Lippincott, Williams and Wilkins.

34. Oh, A., Wong, J., Ohta, E., Rogers, G., Deutsch, C. and Mulliken, J. (2008). Facial Asymmetry in Unilateral Coronal Synostosis: Long-Term Results after Fronto-orbital Advancement. *Plastic and Reconstructive Surgery*, 121(2), pp.545-562.
35. Otake, S., Taoka, T., Maeda, M. and Yuh, W. (2018). A guide to identification and selection of axial planes in magnetic resonance imaging of the brain. *The Neuroradiology Journal*, 31(4), pp.336-344.
36. Pelo, S., Tamburrini, G., Marianetti, T., Saponaro, G., Moro, A., Gasparini, G. and Di Rocco, C. (2011). Correlations between the abnormal development of the skull base and facial skeleton growth in anterior synostotic plagiocephaly: the predictive value of a classification based on CT scan examination. *Child's Nervous System*, 27(9), pp.1431-1443.
37. Raposo-do-Amaral, C., Silva, M., Menon, D., Somensi, R., Raposo-do-Amaral, C. and Buzzo, C. (2011). Anthropometric Study of Craniofacial Asymmetry in Unilateral Coronal Craniosynostosis. *Brazilian Journal of Plastic Surgery*, 26(1), pp.27-31
38. Sadler, T., Leland, J., Sadler-Redmond, S., Tosney, K., Chescheir, N., Imseis, H. and Langman, J. (2012). *Langman's medical embryology*. 12th ed. Philadelphia, Pa.: Wolters Kluwer/Lippincott Williams & Wilkins, pp.133-138.
39. Sgouros, S., Natarajan, K., Hockley, A., Goldin, J. and Wake, M. (1999). Skull Base Growth in Craniosynostosis. *Pediatric Neurosurgery*, 31(6), pp.281-293.
40. Spazzapan, P., Bošnjak, R., Velnar, T. and Cassisi, A. (2017). Anterior Plagiocephaly - A report of a case and operative technique. *Slovenian Medical Journal*, 86(1-2).
41. Van Veelen-Vincent, M., Mathijssen, I., Arnaud, E., Renier, D. and Di Rocco, F. (2010). Craniosynostosis. *Neurosurgery*, pp.501-528.

CHAPTER 2: SCIENTIFIC MANUSCRIPT

Chapter 1 provided a review of published literature on anterior synostotic plagiocephaly, which demonstrated that literature on the quantitative analysis of the craniofacial features associated with this deformity is sparse.

Contributions of this chapter

This chapter investigated and compared the morphometry of the anatomical parameters of the anterior cranial fossa, orbit and ear on the ipsilateral and contralateral sides in a select cohort of South African patients with anterior synostotic plagiocephaly. These results were compared by age, sex, race and laterality to determine statistically significant relationships. The following manuscript has been formatted according to the guidelines outlined by the journal, with references set using the American Medical Association Manual of Style.

Title:	Anterior synostotic plagiocephaly – A quantitative analysis of craniofacial features using computed tomography.
Authors:	N. Mohan, R Harrichandparsad, L Lazarus, A Madaree
Journal:	Journal of Craniofacial Surgery
Manuscript Number:	SCS-22-0062

Anterior synostotic plagiocephaly - A quantitative analysis of craniofacial features using computed tomography

Nivana Mohan B. Med Sci; H. Med Sci[1], Lelika Lazarus B. Med Sci; M Med Sci; PD Dip in HE, PhD[1], Rohen Harrichandparsad MBChB; FC Neurosurg; MMed[2], Anil Madaree MBChB; M Med; FRCS[3]

[1] Department of Clinical Anatomy, School of Laboratory Medicine and Medical Sciences, University of Kwazulu-Natal, Durban. South Africa.

[2] Department of Neurosurgery, University of Kwazulu-Natal, Durban. South Africa

[3] Department of Plastic and Reconstructive Surgery, University of Kwazulu-Natal, Durban. South Africa.

Corresponding Author: Prof Anil Madaree MBChB; M Med; FRCS[3]
Department of Plastic and Reconstructive Surgery,
University of Kwazulu-Natal, Durban, South Africa
MADAREE@ukzn.ac.za
+27 (0)31 240 1168, +27 (0)83 625 0629

Financial disclosure statement: The authors have nothing to disclose. The financial assistance of the National Research Foundation (NRF) towards this research is hereby acknowledged. Opinions expressed and conclusions arrived at, are those of the author and are not necessarily to be attributed to the NRF.

2.1. Abstract

The premature fusion of one coronal suture causes anterior synostotic plagiocephaly (ASP), which results in overt craniofacial dysmorphology that could be challenging to correct. This study aimed to document and compare the morphometry of the anterior cranial fossa (ACF), orbit, and ear on the ipsilateral (synostotic) and contralateral (non-synostotic) sides in a select cohort of South African patients with ASP, using computed tomography (CT) scans.

The dimensions of the ACF, orbit and the position of the ear on the ipsilateral and contralateral sides were measured using a set of anatomical landmarks on two-dimensional (2D) CT scans of 18 consecutive patients diagnosed with non-syndromic ASP. The differences between the ipsilateral and contralateral sides were calculated and expressed as a percentage of the contralateral side.

All ACF parameters decreased significantly on the ipsilateral side when compared to the contralateral side, resulting in the volume of the ACF being the most affected (-27.7%). In terms of the orbit, on the ipsilateral side, the length-infraorbital rim (IOR), height, and surface area parameters increased significantly, with the height being the most affected (24.6%). The remaining orbital parameters (length-supraorbital rim (SOR), breadth and volume) decreased significantly, with the length-SOR parameter being the most affected (-10.8%). The ipsilateral ear was found to be displaced anteriorly (9.33mm) and caudally (5.87mm) from the contralateral ear.

These measures may be useful to surgeons during corrective surgery by indicating the degree of the asymmetry on each side, making it easier to plan the technique and extent of surgical correction of the affected structures.

Keywords: Anterior synostotic plagiocephaly (ASP), craniofacial, dysmorphology, ipsilateral, contralateral

2.2. Introduction

Craniosynostosis is a developmental craniofacial deformity characterized by premature fusion of one or more of the cranial sutures before the growth of the brain is complete.[1] Premature fusion causes abnormal skull growth, resulting in a deformed head and face shape, and an increased risk of elevated intracranial pressure (ICP).[2] This study focuses on anterior synostotic plagiocephaly (ASP); the third most common form of isolated single suture craniosynostosis, following scaphocephaly and trigonocephaly, accounting for 13% -16% of all craniosynostoses.[3] ASP, also known as unilateral coronal synostosis (UCS) is the premature fusion of one of the coronal sutures, resulting in either left- or right-sided UCS (LUCS or RUCS).[4] The incidence of ASP is 1 per 10 000 live births, with a 1.6 to 3.6:1 female preponderance.[5] Furthermore, right-sided ASP is reported to occur twice as often as left-sided ASP.[6]

ASP results in pronounced side-to-side craniofacial asymmetry, consisting of a spectrum of features, varying from mild to severe asymmetry.[7] It involves vertical, transverse, and sagittal facial asymmetry, as well as lower facial asymmetry, resulting in a 'C-shaped' malformation that is always visible on the face.[4,8] This asymmetrical appearance results in constricted growth on one side and compensatory growth on the other side of the skull.[7] The side of the head presented with the fused coronal suture is defined as “ipsilateral” and the opposite side is defined as “contralateral”.[9] Characteristic features on the ipsilateral side include flattened forehead; shortened anterior cranial fossa (ACF); temporal constriction; elevated, retracted, and laterally displaced supraorbital rim (SOR); shallow, elongated, and narrow orbital cavity (“harlequin” orbit); anterior shift of ear, petrous bone, and zygoma; and ipsilateral deviation of the nasal root.[9-12] Frontal and temporal bossing is present on the contralateral side; deviation of nasal tip and chin, as well as a rotation of the middle and lower face toward the non-fused side, occurs.[13]

If ASP is left untreated, it can lead to severe cosmetic defects and psychosocial sequelae, as well as increased ICP.[7] Since surgical intervention is indicated in ASP, it is imperative for the morphometry of the craniofacial features that are affected in ASP to be documented. Providing anthropometric data of these features to surgeons would allow them to define the degree of asymmetry on the ipsilateral side versus the contralateral side, which could be important during corrective surgery to restore normalcy to the distorted craniofacial structure. Fronto-orbital advancement and remodelling (FOAR) are the most common surgical treatments for ASP which is usually done around nine to twelve months of age.[13,14]

To determine the severity of asymmetry in patients, Di Rocco and Velardi[15] developed a classification scheme for ASP. Asymmetry was more apparent in patients with higher severity of the deformity, implying an earlier onset of UCS.[3] A study conducted by Captier *et al.*[10] noted that significant side-to-side asymmetry in the base of the skull was generated by ASP, the skull base was invariably reduced on the ipsilateral side, and the midline features in front of the sella turcica, from the tuberculum sellae to the foramen cecum, were deviated to the ipsilateral side. Deviation of the facial structures is also attributed to the asymmetry in the skull base.[6,16] There is also a notion that most forms of craniosynostosis have their origin in deformities in the skull base.[16]

Due to the relatively small numbers of ASP cases in single institutions, only a few previous studies quantitatively reported on the asymmetry of the craniofacial structures involved this condition. Many variables of these asymmetric craniofacial features (for example, ACF width, length of curvature, volume, and height; orbital length and surface area; and position of the ears) are not included in the literature and have yet to be reported on.[3,8] In terms of the ACF, the length was measured, and it was observed that the ipsilateral side was shorter than the contralateral side, resulting in a significant difference.[3,10,16] The ipsilateral and contralateral ACF angles were also significantly different; the ipsilateral angle was smaller since it is usually more acute than the contralateral angle. The asymmetry of the ACF was caused by these substantial differences in ACF lengths and angles, which resulted in decreased growth on the ipsilateral side and increased growth on the contralateral side.[3,10,16,17]

Previous research that focused on orbital volume employed their desired orbital boundaries when segmenting the orbital cavity to compute the volume. Despite this, these investigations found a similar pattern; the volume of the orbit on the ipsilateral and contralateral sides differed significantly, with the volume on the ipsilateral orbit being smaller than the volume on the contralateral orbit.[3,16,19,20] Since Calandrelli *et al.*[3] classified their patients using the Di Rocco and Velardi[15] classification scheme, they found a steady decrease in the volume on the ipsilateral orbits as the severity of ASP increased. Dvoracek *et al.*[8] reported on orbital height and breadth and discovered that the height significantly increased, and the breadth significantly decreased on the ipsilateral orbit. Marsh *et al.*[17] and Mesa *et al.*[21] found that the SOR of the ipsilateral orbit was higher than the SOR of the contralateral orbit.

In terms of the position of the ears, studies stated that the external auditory meatus (EAM) on the ipsilateral ear was displaced anteriorly.[12,22] In addition, Pelo *et al.*[22] reported that in more severe cases of ASP, the EAM on the ipsilateral ear had extreme anteriorization and a slight caudal

displacement. Bruneteau and Mulliken[23] physically examined the ears of patients with ASP and reported that the ipsilateral ear was anterosuperiorly positioned.

The various methods of surgical treatments of ASP have been well documented in the literature; however, there is a paucity of data regarding the quantitative analysis of the craniofacial features that are involved in ASP.[9-14] This study intends to provide anthropometric measurements of the craniofacial features associated with ASP. This investigation provides an anatomical base in patients with ASP to be used as a potential reference to compare preoperative and postoperative findings and to examine how effectively the corrected craniofacial features have been normalized (clinical outcome). To date, computed tomography (CT) imaging has yielded the most reliable and reproducible measurements of the craniofacial skeleton, as well as by providing the clearest identification of all the characteristics of ASP.[3]

This study aimed to document and compare the morphometry of the ACF, orbit, and ear on the ipsilateral and contralateral sides in a select cohort of South African patients with ASP, using preoperative CT scans. The objectives were to (i) measure the ACF width, length, length of curvature, angle, volume, and height on either side of the ACF (ii) measure the orbital length, breadth, height, volume, surface area, and maximum vertical height between the SOR on each orbit (iii) measure the maximum vertical height and anteroposterior (AP) distance between the ears. In addition, this study also compared the aforementioned variables with regard to age, sex, race and laterality.

2.3. Materials and methods

This study was a retrospective, descriptive observational study that was cross-sectional in nature, assessing the degree of craniofacial asymmetry on the ipsilateral and contralateral sides in a select cohort of South African patients presenting with ASP, using preoperative CT scans.

2.3.1. Participants

The study included 18 children (≤69 months) with CT confirmed non-syndromic, untreated ASP who presented to the Inkosi Albert Luthuli Central Hospital (IALCH) craniofacial unit between 2004 and 2020 and met the inclusion criteria.

2.3.2. Inclusion criteria

Participants were included if they:

- had premature fusion of one of the coronal sutures (LUCS or RUCS)
- had non-syndromic (isolated) ASP
- had preoperative CT scans only
- had fine CT slices (1-5 mm thickness) which were of acceptable quality for assessment of craniofacial asymmetry

2.3.3. Exclusion criteria

Participants were excluded if they:

- had synostosis affecting cranial sutures other than a single coronal suture or if they had multiple suture involvement (any other type of craniosynostosis other than ASP)
- had any known or suspected craniofacial syndrome
- had undergone surgical correction, postoperative CT scans
- had poor CT image resolution or slice thickness greater than 5mm

2.3.4. Ethics and regulatory approvals

Relevant gatekeeper permissions were acquired, and institutional ethical clearance for this study was obtained from the Biomedical Research Ethics Committee of the University of KwaZulu-Natal (UKZN) (BREC/00002129/2020) and relevant authorities.

2.3.5. Anonymity and confidentially

The study involved the use of retrospective CT scans and there was no known risk to patients or direct patient contact. Patient information and collected data were held anonymously and stored in password protected electronic devices.

2.3.6. Anatomical landmarks

A plastic surgeon, a neurosurgeon, and an anatomist located and marked a set of select standardized anatomical landmarks consistent with the characteristic features of anterior plagiocephaly as they were easily identifiable, reproducible, and deemed to be the best points to investigate the dimensions being studied. To ensure repeatability and reproducibility of the landmarks, each measurement was repeated three times by the candidate and a second observer in different settings and the intra- and inter-observer reliability coefficients were calculated.

2.3.7. Image acquisition and analysis

Preoperative CT scans, with an axial slice thickness range of 1-5mm were retrieved from the database of the Department of Plastic and Reconstructive Surgery at IALCH, Durban, South Africa, using the Picture Archiving and Communication System (PACS) and saved as a DICOM (Digital Imaging and Communication in Medicine) file. CT images were acquired in the clinical routine with either a 128-slice SOMATOM Definition AS scanner or SOMATOM Definition Flash CT Scanner (Siemens Healthineers, Forcheim, Germany).

The Horos Project (Version 3.3.6) DICOM viewer was used to review and analyse these scans. All the CT images were automatically calibrated by the DICOM viewer and verified manually. Slice orientation was standardized to reduce measurement errors by loading the images into a 3D multiplanar reconstruction (MPR) view and aligning them parallel to the orbitomeatal plane. The orbitomeatal line, also known as the canthomeatal line is a positioning line used in skull radiography. It runs through the eye's outer canthus and the midpoint of the EAM. This line is used to position the patient for various radiological views.[24] All volume measurements were performed on 2D axial slices with the use of two tools in the Horos Project DICOM viewer: the 'closed polygon' tool for manual segmentation of a specific region and the region of interest (ROI) volume tool for automatic volume calculation of the total selected regions. All scans were analysed using bone-window settings.

2.3.8. Morphometric analysis

The morphometry of the ACF, orbit and ear on the ipsilateral and contralateral sides were determined using anatomical landmarks in the axial, sagittal, or coronal planes on two-dimensional (2D) CT scans. Each measurement was repeated three times to ensure accuracy and reliability. Differences were calculated between the ipsilateral and contralateral sides and expressed as a percentage of the contralateral side. Results were statistically compared against age, sex, race and laterality.

2.3.8.1. ACF dimensions

- Width (transverse diameter) and length (anteroposterior diameter):

These measurements were taken in the axial plane at the level where the inferior extent of the fused coronal suture was first observed to be the most prominent. The posterior margin of the crista galli was used as a reference landmark. This landmark was transcended to the level at which the inferior extent of the fused coronal suture was first observed to be the most prominent. At that

level, the width was determined on the contralateral side by constructing a line from the coronal suture to the transcended landmark, whereas on the ipsilateral side, a line was constructed from the inferior extent of the fused coronal suture to the transcended landmark (Fig. 1). The midpoints of those two lines created by the width were calculated and the length of the ACF on either side was measured by constructing a perpendicular line from the midpoint to the inner table of the ACF (Fig. 1).

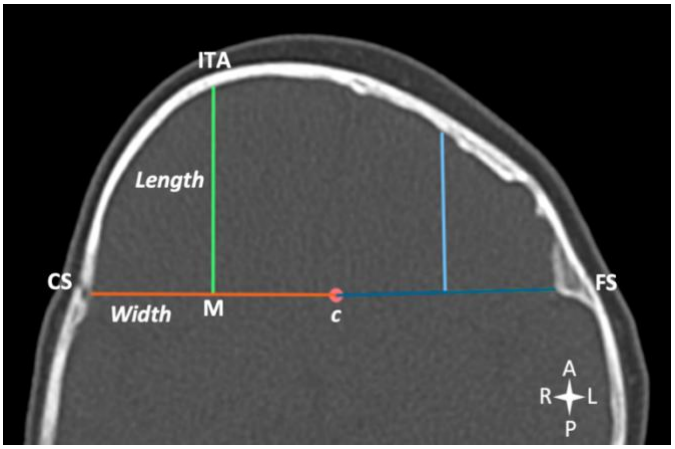

KEY
ITA - Inner table of ACF
CS - Coronal suture
FS - Fused coronal suture
M - Midpoint
c - Transcended point of posterior margin of crista gali

Figure 1: ACF width (CS - c) and length (M - ITA) measurements in a patient with LUCS *(axial view)*.

- Length of ACF curve:

This measurement was taken in the axial plane at the level where the inferior extent of the fused coronal suture was first observed to be the most prominent. A midline that divided the ACF into right and left sides and a posterior boundary/limitation that separated the ACF from the rest of the skull base was created. The midline was determined by using two reference landmarks; the nasion and the midpoint of the sella turcica when it was first observed to be the most prominent. These landmarks were transcended to the level at which the inferior extent of the fused coronal suture was first observed to be the most prominent. At that level, the two transcended landmarks were connected, and the midline reference was formed. The posterior boundary was determined as the coronal suture on the contralateral side and the fused coronal suture on the ipsilateral side. On the contralateral side, the length of the curve was measured from the midline to the coronal suture, whereas on the ipsilateral side, the length of the curve was measured from the midline to the fused coronal suture (Fig. 2).

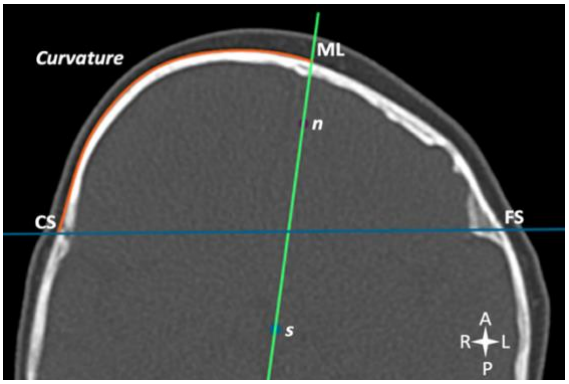

KEY

CS - Coronal suture
FS - Fused coronal suture
ML - Midline
n - Transcended point of nasion
s - Transcended point of midpoint of sella turcia

Figure 2: Measurement of the length of the ACF curvature (CS - ML) in a patient with LUCS *(axial view)*.

- Angle:

This measurement was taken in the axial plane at the level where the inferior extent of the fused coronal suture was first observed to be the most prominent. The first ray of the angle was determined by constructing a line from the coronal suture on the contralateral side to the fused coronal suture on the ipsilateral side. This line was extended to the border of overlying skin and marked off as a point on either side. The angle's second ray was determined by constructing a tangent from the point at the border of the overlying skin to the curve of the ACF. The common vertex of the angle on both sides was the point at the border of the overlying skin. The inter-tangential angle of the ACF was determined by extending the tangents on either side anteriorly until they intersect. This angle was manually calculated by subtracting 180° from the sum of the angle values acquired on each side (Fig. 3).

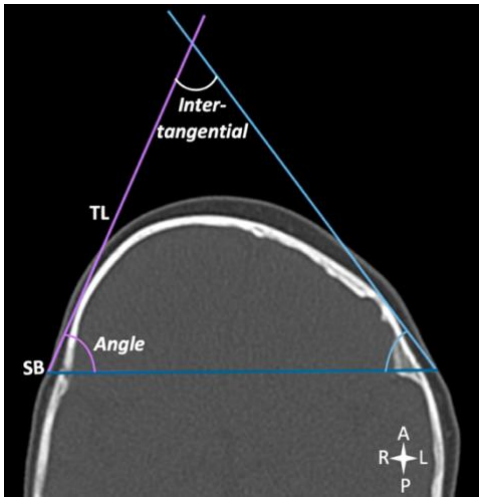

KEY

TL - Tangent line
SB - Overlying skin border

Figure 3: ACF angle and inter-tangential angle measurements in a patient with LUCS *(axial view)*.

- Height:

This measurement was taken in the coronal plane at the level where the posterior margin of the crista galli was first observed to be the most prominent.

ACF height from the midpoint of the orbital roof (R - ITA):

On either side, the height was measured by constructing a perpendicular line from the midpoint of the orbital roof to the inner table of the ACF (Fig. 4).

ACF height from the superolateral border of the orbit (B - ITA):

On either side, the height was measured by constructing a perpendicular line from the superolateral border of the orbit to the inner table of the ACF (Fig. 4).

The purpose of using these two approaches was to examine the anatomical changes that may have occurred to the SOR of each orbit.

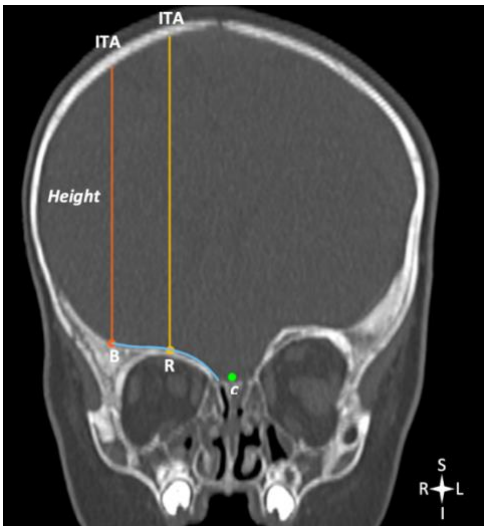

KEY

ITA - Inner table of ACF
B - Superolateral border of orbit
R - Midpoint of the roof of orbit
c - Posterior margin of crista gali

Figure 4: Measurements of the height of the ACF from superolateral border of orbit (B - ITA) and the height of the ACF from midpoint of the roof of orbit (R - ITA) in a patient with LUCS *(coronal view)*.

- Volume:

This measurement was taken on 2D axial slices. The ACF was manually segmented in every slice of the CT images. A midline that divided the ACF into right and left sides and a posterior boundary/limitation that separated the ACF from the rest of the skull base was created. The midline was created by using two reference landmarks; the nasion and the midpoint of the sella turcica when it was first observed to be the most prominent. These landmarks were transcended to the level at which the inferior extent of the fused coronal suture was first observed to be the

most prominent. At that level, the two transcended landmarks were connected, and the midline reference was formed. The posterior boundary was determined by connecting the coronal suture on the contralateral side to the fused coronal suture on the ipsilateral side. The midline and posterior boundary lines were transcended onto every slice of the CT images where the ACF was visible. When the ACF was visible, the start slice was chosen, and when the posterior margin of the crista galli was no longer visible or shortly before the sinuses were apparent, the end slice was chosen. The right and left segments of the ACF (ROIs) were manually outlined on each consecutive slice by using the 'closed polygon' tool. All ROIs were selected and the volume on either side was automatically calculated using the ROI volume tool (Fig. 5).

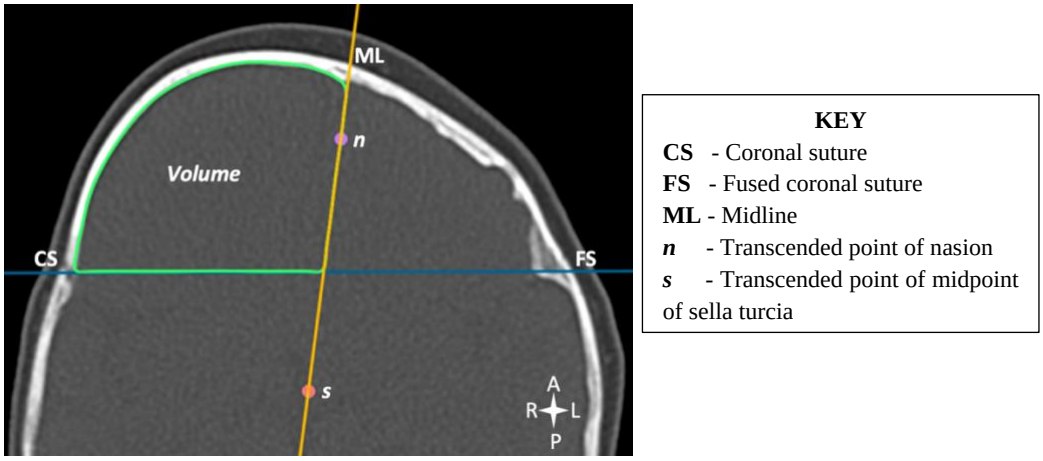

Figure 5: Segmentation technique used to outline the ACF on either side in a patient with LUCS *(axial view)*.

2.3.8.2. Orbital dimensions

- Length (anteroposterior diameter):

This measurement was taken in the sagittal plane at the level where the maximum diameter of the optic canal was observed on each orbit. This measurement was taken on a slice above and below the selected slice to ensure that the maximum diameter was chosen. The orbital length was measured in relation to the SOR and infraorbital rim (IOR). The purpose of using these two approaches was to examine the anatomical changes that may have occurred to the SOR and IOR on the ipsilateral side when compared to the contralateral side as these structures are usually severely impacted in ASP patients.

The slice that portrayed the maximum diameter of the optic canal on each orbit was chosen and the midpoint of the optic canal was used as a landmark. At that level, a line was drawn vertically

downwards from the most anterior portion of the SOR to mark the point of the SOR and another line was drawn vertically upwards from the most anterior portion of the IOR to mark the point of the IOR. The orbital length on either side was determined by constructing a perpendicular line anteriorly from the midpoint of the optic canal until it met with the vertical lines that marked the points of the SOR and IOR (Fig. 6).

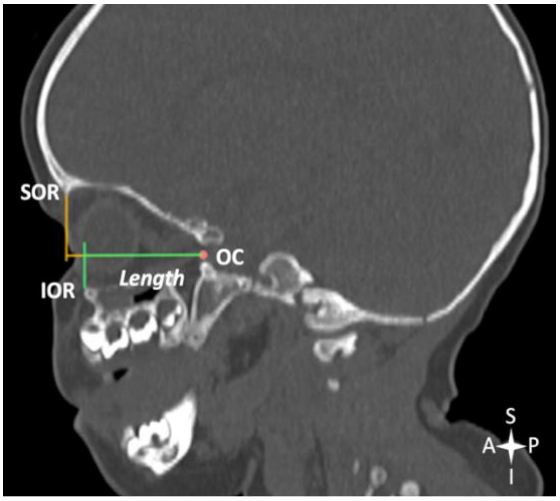

KEY
SOR - Supraorbital rim
IOR - Infraorbital rim
OC - Midpoint of optic canal

Figure 6: Measurements of the orbital length in relation to the SOR (OC - SOR) and in relation to the IOR (OC - IOR) in a patient with LUCS *(sagittal view).*

- Breadth (transverse diameter) and height (maximum vertical height):

These two measurements were taken in the coronal plane at the level where the frontozygomatic suture was first observed to be the most prominent on each orbit. The breadth of each orbit was determined by constructing a horizontal line from the anterior margin of the frontozygomatic suture to the medial wall of the orbit.[20] The height of each orbit was determined by taking a point from the inferior orbital margin, marking the infraorbital foramen to the highest point of each orbit on the superior orbital margin (Fig. 7).

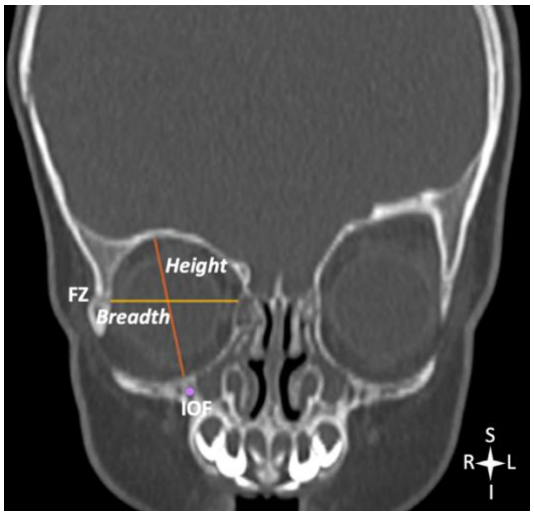

KEY
FZ - Frontozygomatic suture
IOF - Infraorbital foramen

Figure 7: Orbital breadth (FZ - Medial wall) and height (IOR - SOR) measurements in a patient with LUCS *(coronal view)*.

- Surface area:

This measurement was taken in the coronal plane at the level where the frontozygomatic suture was first observed to be the most prominent on each orbit. The surface area of each orbit was determined by manually tracing the orbital rim with the 'closed polygon' tool. This tool automatically calculated the surface area for each orbit (Fig. 8).

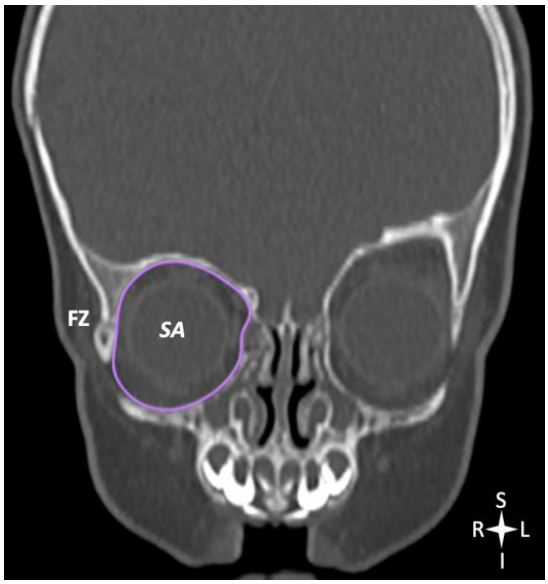

Figure 8: Segmentation of the orbital surface area (SA) in a patient with LUCS *(coronal view)*.

- Volume:

This measurement was taken on 2D axial slices. The interface between the inner bony walls and the soft tissue contents of each orbit was manually delineated on every slice of the CT images using the 'closed polygon' tool to determine the orbital volume. The bone-soft tissue interface was easily visible when the CT scan was adjusted into the bone window settings, the bone appeared white (high density) and the soft tissue contents appeared grey (medium density). Two areas of the orbit required particular attention: the anterior and posterior boundaries. The anterior boundary of the orbit was defined as the inner surface of the eyelid, this landmark was used to account for the spaces around the globe due to its variable location in the orbital cavity. Including the entire globe and protruding soft tissue in the volume calculation could be useful for evaluating cases in which external soft tissue volume is also important.[25,26] The posterior boundary was defined by a line connecting the lateral and medial walls of the optic foramen within the orbital cavity, thus excluding the optic canal from the volume calculations. The segmented orbital areas (ROIs) on each consecutive slice were selected, and the volume of each orbit was automatically calculated using the ROI volume tool (Fig. 9).

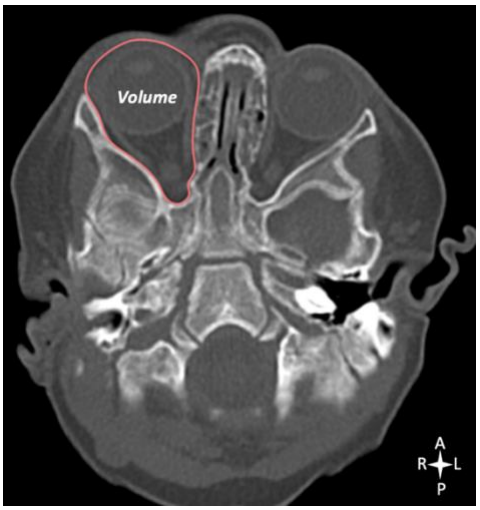

Figure 9: Segmentation technique used to outline the orbital cavity in a patient with LUCS *(axial view)*.

- Maximum vertical height between the supraorbital rims:

This measurement was taken in the coronal plane at the level where the frontozygomatic suture was first observed to be the most prominent on each orbit. Two horizontal lines were drawn, one from the highest point of the SOR on the ipsilateral side extending to the contralateral side (cranial line), and the other was drawn from the highest point of the SOR on the contralateral side

extending to the ipsilateral side (caudal line). The distance between the cranial and caudal lines calculated the maximum vertical height between the SORs.

The frontozygomatic suture that was first observed to be the most prominent on each orbit was not always on the same slice; therefore, one of the two horizontal lines was transcended onto the slice where the other horizontal line was placed. This was done to get both lines on the same slice so that the distance between these lines could be measured (Fig. 10).

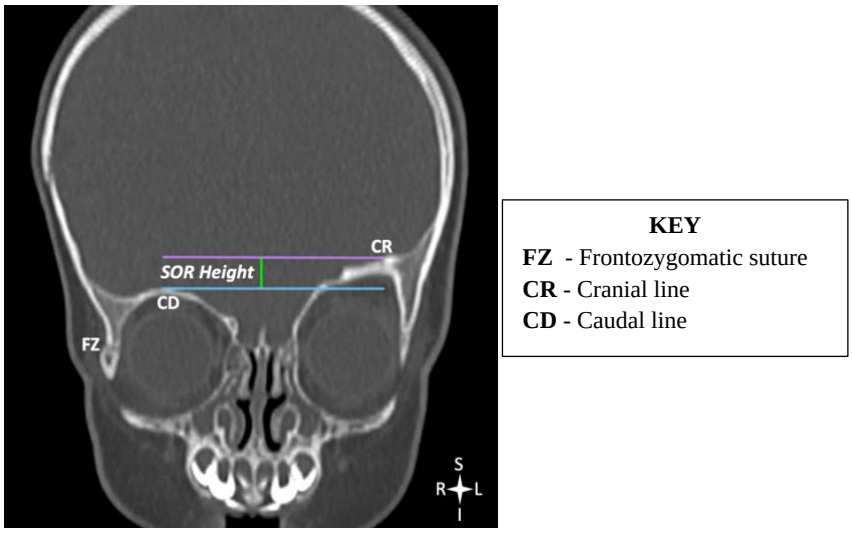

Figure 10: Maximum vertical height between the SORs (CR - CD) in a patient with LUCS *(coronal view)*.

2.3.8.3. Position of the ear

The measurements of the ear were conducted on a slice above and below the selected slice to ensure that the maximum diameter of the EAM was chosen. The maximum diameter of the EAM of the ipsilateral and contralateral ear was not always on the same slice; therefore, the midpoint of the EAM of one ear was transcended onto the slice where the midpoint of the EAM of the other ear was placed. This was done to get both the midpoints on the same slice so that the horizontal lines could be drawn, and the distances could be measured between the anterior and posterior lines as well as between the cranial and caudal lines.

The maximum AP distance and vertical height measurements of the ear were taken at the level where the maximum diameter of the EAM was observed on each ear (Fig. 11 and 12).

- Maximum AP distance:

The axial slice that portrayed the maximum diameter of the EAM on each ear was chosen and the midpoint of the EAM was used as a landmark. Two horizontal lines were drawn, one from the

midpoint of the EAM on the ipsilateral side extending to the contralateral side (anterior line), and the other was drawn from the midpoint EAM on the contralateral side extending to the ipsilateral side (posterior line). The distance between these anterior and posterior lines calculated the maximum AP distance between the ipsilateral and contralateral ear (Fig. 11).

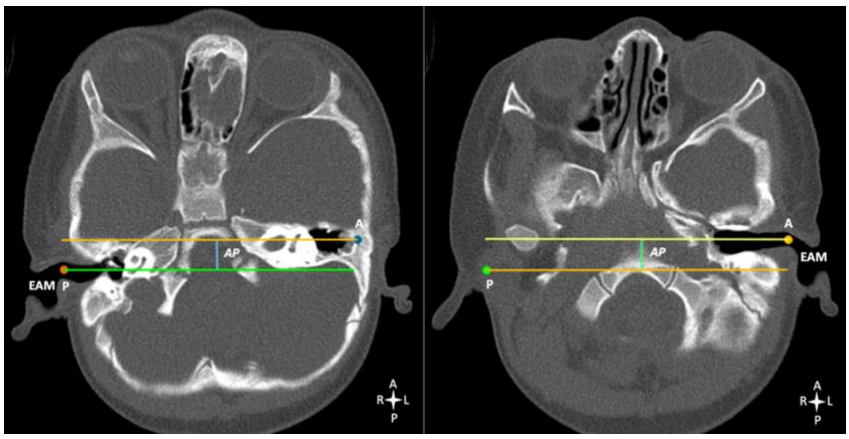

KEY
EAM - External auditory meatus
AP - Anteroposterior distance
A - Anterior line
P - Posterior line

Figure 11: Maximum AP distance between the ears (A - P) of a patient with LUCS *(axial view)*.

- Maximum vertical height:

The coronal slice that portrayed the maximum diameter of the EAM on each ear was chosen and the midpoint of the EAM was used as a landmark. Two horizontal lines were drawn, one from the midpoint of the EAM on the ipsilateral side extending to the contralateral side (caudal line), and the other was drawn from the midpoint EAM on the contralateral side extending to the ipsilateral side (cranial line). The distance between the cranial and caudal lines calculated the maximum vertical height between the ipsilateral and contralateral ear (Fig. 12).

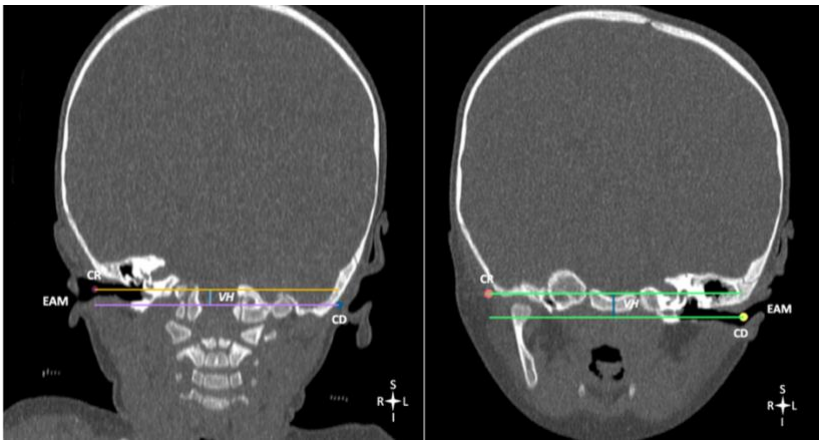

KEY
EAM - External auditory meatus
VH - Vertical height
CR - Cranial line
CD - Caudal line

Figure 12: Maximum vertical height between the ears (CR - CD) of a patient with LUCS *(coronal view)*.

2.3.9. Statistical analysis

Statistical data analysis was performed by using R Statistical Computing Software of the R Core Team, 2020, version 3.6.3. A p-value of less than 0.05 was considered statistically significant. The results were presented in the form of descriptive and inferential statistics. Multidimensional numerical variables were presented as parallel plots. Depending on the distribution of the differences in the before and after numerical values, the differences were assessed using either the paired t-test or Wilcoxon respectively. In addition, boxplots were used for the visual display of the descriptive patterns as well as a paired test. To determine the reliability of the morphometrical data, intra-observer and inter-observer reliability were calculated and represented as intraclass correlation coefficient (ICC) values. All statistical methods and analyses were conducted in consultation with a university statistician.

2.4. Results

2.4.1. Demographics and anatomical profile

The demographic information and anatomical profile for the study population are reported in Table 1. A total of 18 patients with non-syndromic ASP were included in this study, of which 7 (38.9%) were left-sided and 11 (61.1%) were right-sided. There were 8 (44.4%) males and 10 (55.6%) females. The mean age at the time of the CT scan was 14.7±16.7 months (range: 6 - 69 months). Patients were classified according to population groups as defined by Statistics South Africa[27] (Black, Coloured, Indian/Asian, and White). The patients in this study fit into those subgroups, with an exception of 1 who was classified as "other" in the hospital records. Among the 18 patients, 3 (16.7%) were Black, 2 (11.1%) were Coloured and 1 (5.6%) was other, with the majority being 6 (33.3%) Indian and 6 (33.3%) White. Substantial comparisons by race could not be made as the proportions of the race groups included in the patient cohort were skewed.

Table 1: Demographics and anatomical profile of patients with ASP

Overall (N=18)		
Age (Months)	Mean±SD	14.7±16.7
	Median(Q1-Q3)	8.00(6.00-13.0)
	Range	6.00-69.0
Sex	Female	10 (55.6%)
	Male	8 (44.4%)
Race	Black	3 (16.7%)
	Coloured	2 (11.1%)
	Indian	6 (33.3%)
	White	6 (33.3%)
	Other	1 (5.6%)
Laterality	LUCS	7 (38.9%)
	RUCS	11 (61.1%)

Note: SD = Standard Deviation,
ASP = Anterior synostotic plagiocephaly
LUCS = Left unilateral coronal synostosis
RUCS = Right unilateral coronal synostosis

2.4.2. Intra-observer reliability:

All measurements of the ACF, orbit and ear on the ipsilateral and contralateral sides yielded an ICC value of 1, indicating excellent reliability.

2.4.3. Inter-observer reliability:

All the measurements of the ACF, orbit and ear on the ipsilateral and contralateral sides revealed an ICC value of 1. This indicated excellent reliability.

2.4.4. Morphometry

It is important to note that for all parameters measured, the difference in the measurements between the ipsilateral and contralateral sides was calculated. This difference was expressed as a percentage of the contralateral side:

$$\% \text{ Difference} = [(\text{Ipsilateral}-\text{Contralateral})/(\text{Contralateral})]x100$$

When comparing the ipsilateral to the contralateral side, the increase or decrease in a specific parameter of the ACF, orbit or ear on the ipsilateral side are denoted with negative (-)and positive (+) signs respectively. However, for reporting purposes the (+) sign has not been shown, e.g. +2.3 reported as 2.3. In some instances, the absolute (i.e. that is the magnitude of the value irrespective of sign) measurements was considered.

The results of the investigated areas were as follows:
The comparisons were based on the paired test, although the group means were displayed.

2.4.5. Morphometry of the ACF

Width: A mean value of 42.8±4.87mm was reported on the ipsilateral side and 50.7±5.84mm on the contralateral side. This was statistically significant ($p<0.001$) (Fig. 13A). Despite the fact that the group means are stated, the comparisons were based on the paired test. The average percentage based on the paired differences was -15.3%±7.53% (range: -34.4% to -5.37%) between both sides (Table 2).

Length: The ipsilateral side had a mean length of 26.6±6.71mm, while the contralateral side had a mean length of 33.1±5.36mm. This resulted in a statistically significant difference ($p<0.001$), between both sides, an average percentage difference of -20.2%±9.91% (range: -39.6% to -1.59%) was determined (Fig. 13B) (Table 2).

Curvature: A mean of 61.1±9.81mm was recorded on the ipsilateral side, this was significantly ($p<0.001$) lower than the contralateral side, which had a mean of 79.4±9.65mm (Fig. 13C). The average percentage difference between the two sides was -23.1%±8.11% (ranging from -35.7% to -5.23%) (Table 2).

Angle: Mean values for the ipsilateral and contralateral sides were 49.9°±7.06° and 61.7°±7.02°, respectively; this was statistically significant ($p<0.001$) (Fig. 13D). An average percentage difference of -19.0%±7.90% (range: -34.7% to -1.87%) between the ipsilateral and contralateral sides was reported (Table 2).

Volume: The mean volume of the ACF on the ipsilateral side was 63.7±32.9cm^3, this was significantly ($p<0.001$) lower than the contralateral side (mean volume: 86.0±37.2cm^3) (Fig. 13E). As a result, the average percentage difference was -27.7%±11.4% (range: -46.5% to -9.17%) between both sides (Table 2).

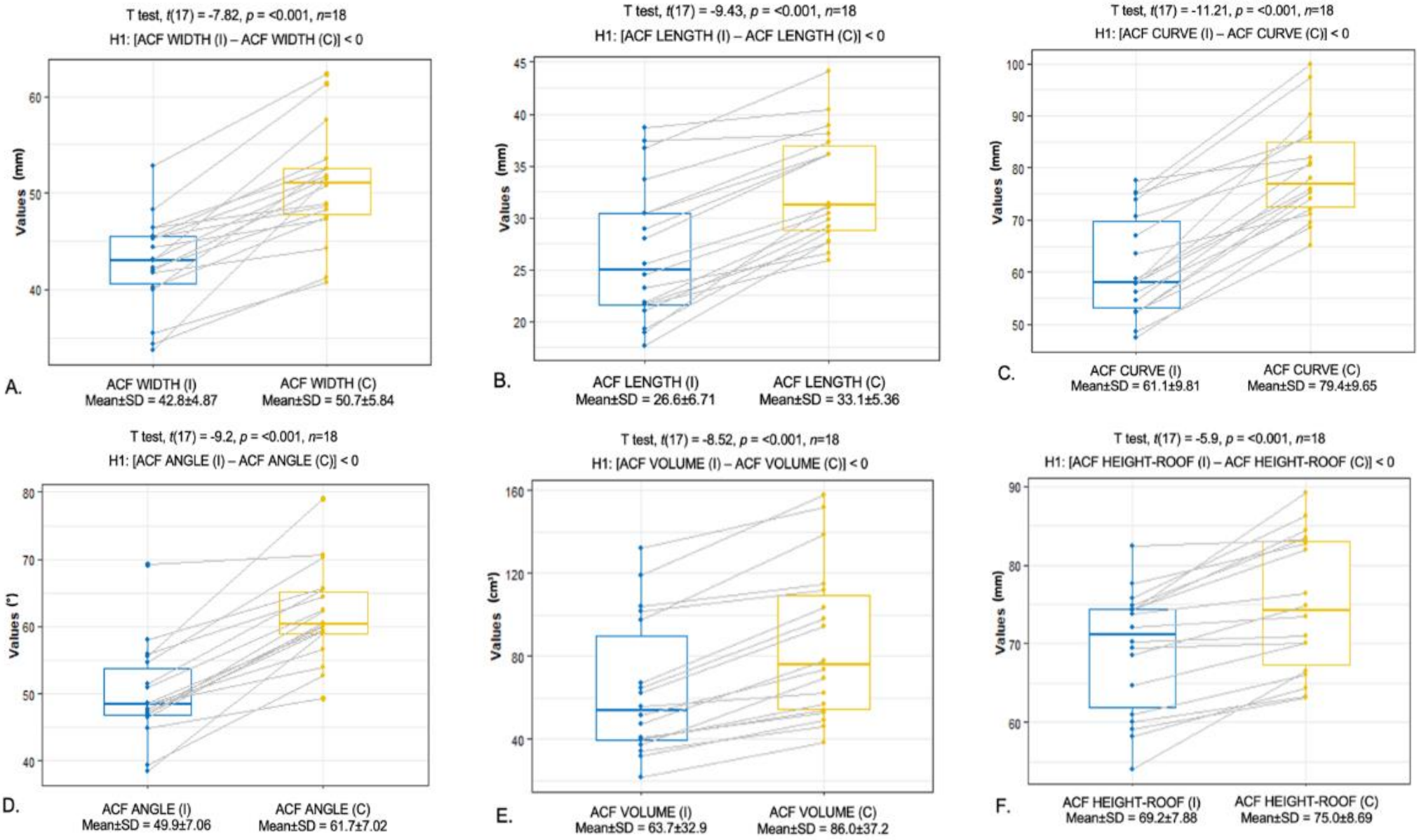
T test, t(17) = -7.82, p = <0.001, n=18
H1: [ACF WIDTH (I) – ACF WIDTH (C)] < 0
Values (mm)
A.
ACF WIDTH (I)
Mean±SD = 42.8±4.87
ACF WIDTH (C)
Mean±SD = 50.7±5.84
T test, t(17) = -9.43, p = <0.001, n=18
H1: [ACF LENGTH (I) – ACF LENGTH (C)] < 0
Values (mm)
B.
ACF LENGTH (I)
Mean±SD = 26.6±6.71
ACF LENGTH (C)
Mean±SD = 33.1±5.36
T test, t(17) = -11.21, p = <0.001, n=18
H1: [ACF CURVE (I) – ACF CURVE (C)] < 0
Values (mm)
C.
ACF CURVE (I)
Mean±SD = 61.1±9.81
ACF CURVE (C)
Mean±SD = 79.4±9.65
T test, t(17) = -9.2, p = <0.001, n=18
H1: [ACF ANGLE (I) – ACF ANGLE (C)] < 0
Values (°)
D.
ACF ANGLE (I)
Mean±SD = 49.9±7.06
ACF ANGLE (C)
Mean±SD = 61.7±7.02
T test, t(17) = -8.52, p = <0.001, n=18
H1: [ACF VOLUME (I) – ACF VOLUME (C)] < 0
Values (cm³)
E.
ACF VOLUME (I)
Mean±SD = 63.7±32.9
ACF VOLUME (C)
Mean±SD = 86.0±37.2
T test, t(17) = -5.9, p = <0.001, n=18
H1: [ACF HEIGHT-ROOF (I) – ACF HEIGHT-ROOF (C)] < 0
Values (mm)
F.
ACF HEIGHT-ROOF (I)
Mean±SD = 69.2±7.88
ACF HEIGHT-ROOF (C)
Mean±SD = 75.0±8.69

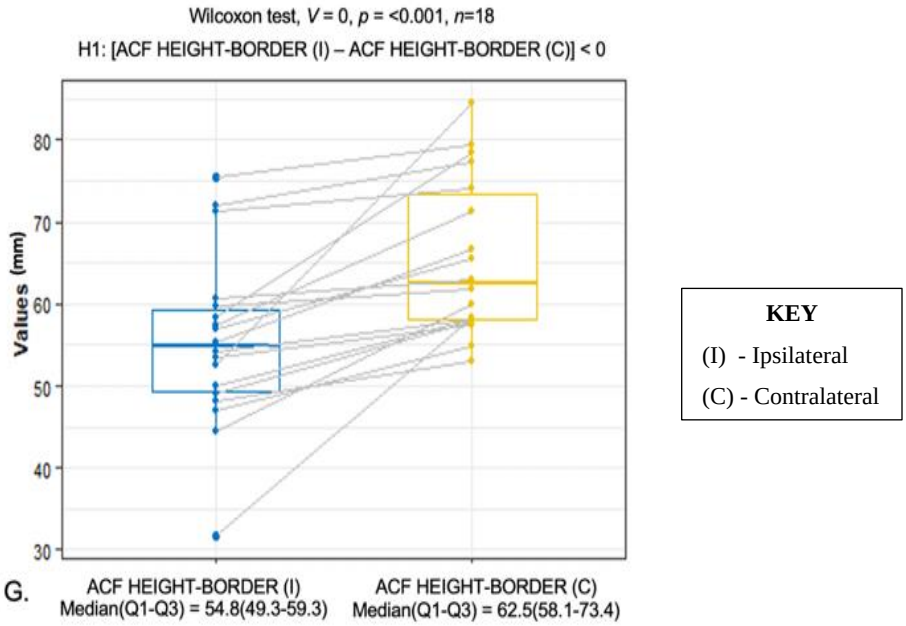

Figures 13A-G: Morphometric ACF parameters of ipsilateral *vs.* contralateral sides in ASP patients. **(A)** Width, **(B)** Length, **(C)** Curve, **(D)** Angle, **(E)** Volume, **(F)** Height-Roof, **(G)** Height-Border

Height-Roof (measured from the midpoint of the orbital roof): On the ipsilateral side, a mean value of 69.2±7.88mm was recorded, while on the contralateral side, a mean of 75.0±8.69mm was recorded (Fig. 13F). The average percentage difference between the two sides was -7.67%±5.20% (range: -18.8% to -0.738%) (Table 2).

Height-Border (measured from the superolateral border of the orbit): This measurement had a median(Q1-Q3) value of 54.8mm(49.3mm-59.3mm) on the ipsilateral side and 62.5mm(58.1mm -73.4mm) on the contralateral side (Fig. 13G). An average percentage difference of -13.5%(-18.8% to -6.65%) (range: -45.6% to -3.54%) was noted between both sides (Table 2).
ACF height between the ipsilateral and contralateral sides was statistically significant ($p<0.001$) in both methods (Table 2).

Overall, the ipsilateral side had significantly reduced mean or median values when compared to the contralateral side for all ACF parameters. The volume on the ipsilateral side decreased the most by -27.7%±11.4%, while the ACF height-roof decreased the least by -7.67%±5.20% (Table 2).

Table 2: Overall mean percentage differences for ACF parameters in patients with ASP (N=18)

ACF measurements	% diff. = Ipsilateral-Contralateral Mean±SD	(%) Range	p-value
Width	-15.3±7.53	-34.4 to -5.37	**<0.001**[a]
Length	-20.2±9.91	-39.6 to -1.59	**<0.001**[a]
Curve	-23.1±8.11	-35.7 to -5.23	**<0.001**[a]
Angle	-19.0±7.90	-34.7 to -1.87	**<0.001**[a]
Volume	-27.7±11.4	-46.5 to -9.17	**<0.001**[a]
Height-Roof	-7.67±5.20	-18.8 to -0.738	**<0.001**[a]
Height-Border	-13.5(-18.8 to -6.65)[#]	-45.6 to -3.54	**<0.001**[b]

Note: % diff. = Percentage difference, SD = Standard Deviation, ASP = Anterior synostotic plagiocephaly
[a]t-test, [b]Wilcoxon test
[#]Median(Q1-Q3) value is shown due to skewness in the data

2.4.6. Morphometry of the orbits

Length-SOR (in relation to the SOR): A mean length of 33.8±3.65mm was found and on the ipsilateral side as opposed to the contralateral side (38.0±3.99mm). A statistically significant difference was noted ($p<0.001$) (Fig. 14A). Despite the fact that the group means are stated, the comparisons were based on the paired test. The average percentage based on the paired differences was -10.8%±6.20% (range: -23.1% to -2.21%) between both sides (Table 3).

Length-IOR (in relation to the IOR): A mean length of 37.0±3.85mm was calculated on the ipsilateral side, this was significantly ($p<0.001$) higher than the contralateral side (33.7±3.38mm) (Fig. 14B). An average percentage difference of 9.56%±5.43% (range: 1.76% to 19.4%) between both sides was noted (Table 3).

Breadth: This measurement had a mean value of 24.7±3.10mm on the ipsilateral side and 26.7±2.64mm on the contralateral side. A statistically significant difference was noted ($p<0.001$) (Fig. 14C). The average percentage difference between the ipsilateral and contralateral sides was -7.55%±5.82% (range: -21.9% to -1.02%) (Table 3).

Height: The ipsilateral side had a mean height of 36.3±3.49mm, this was significantly greater ($p<0.001$) than the contralateral side (29.4±3.63mm) (Fig. 14D). The average percentage difference was 24.6%±13.5% (range: 6.80% to 55.4%) between both sides (Table 3).

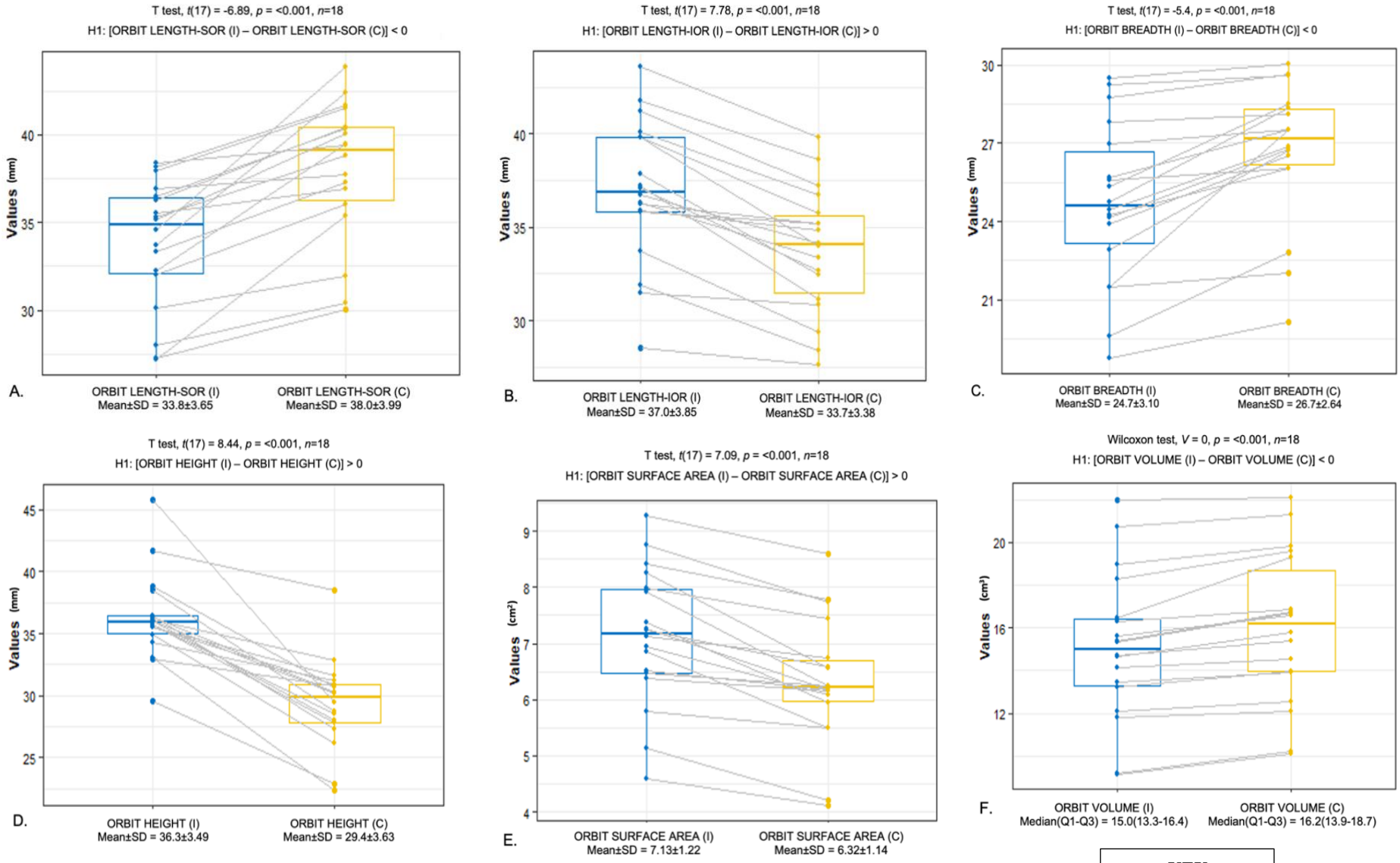

Figures 14A-F: Morphometric orbital parameters of ipsilateral *vs.* contralateral sides in ASP patients. **(A)** Length-SOR, **(B)** Length-IOR, **(C)** Breadth, **(D)** Height, **(E)** Surface area, **(F)** Volume

Surface area: The ipsilateral side had a mean value of 7.13±1.22cm^2, whereas the contralateral side reported a mean value of 6.32±1.14cm^2, this was statistically significant (p<0.001) (Fig. 14E). An average percentage difference of 13.2%±8.29% (range: 3.46% to 26.6%) was noted between both sides (Table 3).

Volume: A median(Q1-Q3) value of 15.0cm^3(13.3cm^3-16.4cm^3) was reported on the ipsilateral side and 16.2cm^3(13.9cm^3-18.7cm^3) on the contralateral side. This was statistically significant with a p-value of <0.001 (Fig. 14F). There was an average percentage difference of -4.94%(-7.83% to -3.38%) (range: -14.6% to -0.573%) between the ipsilateral and contralateral sides (Table 3).

Overall, the ipsilateral side had significantly lower mean or median values for orbital length-SOR, breadth, and volume parameters when compared to the contralateral side. Additionally, the ipsilateral side had significantly higher mean/median values for orbital length-IOR, height, and surface area parameters when compared to the contralateral side. The greatest decrease on the ipsilateral side was observed in the orbital length-SOR parameter (-10.8%±6.20%), whereas the greatest increase was observed in the orbital height parameter (24.6%±13.5%). Furthermore, when focussing on absolute average percentage differences orbital height had the greatest difference (24.6%±13.5%) whereas, orbital volume had the smallest difference [-4.94%(-7.83% to -3.38%)] (Table 3).

SOR maximum vertical height: The SOR on the ipsilateral side was more cranially positioned by a median value of 3.89mm(2.34mm-6.18mm) with a range of 1.39mm to 17.9mm (Table 4).

Table 3: Overall mean percentage differences for orbital parameters in patients with ASP (N=18)

Orbital measurements	% diff. = Ipsilateral-Contralateral Mean±SD	(%) Range	p-value
Length-SOR	-10.8±6.20	-23.1 to -2.21	**<0.001**[a]
Length-IOR	9.56±5.43	1.76 to 19.4	**<0.001**[a]
Breadth	-7.55±5.82	-21.9 to -1.02	**<0.001**[a]
Height	24.6±13.5	6.80 to 55.4	**<0.001**[a]
Surface area	13.2±8.29	3.46 to 26.6	**<0.001**[a]
Volume	-4.94(-7.83 to -3.38)[#]	-14.6 to -0.573	**<0.001**[b]

Note: % diff. = Percentage difference, SD = Standard Deviation, ASP = Anterior synostotic plagiocephaly, SOR = Supraorbital rim, IOR = Infraorbital rim

[a]t-test, [b]Wilcoxon test

[#]Median(Q1-Q3) value is shown due to skewness in the data

Table 4: Overall mean values for supraorbital rim and ear parameters in patients with ASP (N=18)

Measurements (mm)	Mean±SD (mm)	Range (mm)
SOR		
SOR max. vertical height	3.89(2.34-6.18)[#]	1.39 to 17.9
EAR		
Ear max. AP distance	9.33±2.85	3.98 to 14.6
Ear max. vertical height	5.87±3.68	1.05 to 14.0

Note: Max. = Maximum, SD = Standard Deviation, mm = millimeter
ASP = Anterior synostotic plagiocephaly, SOR = Supraorbital rim, AP = Anteroposterior
[#]Median(Q1-Q3) value is shown due to skewness in the data

2.4.7. Morphometry of the ears

Ear maximum AP distance: The ear on the ipsilateral side was more anteriorly positioned by a mean value of 9.33±2.85mm with a range of 3.98mm to 14.6mm (Table 4).

Ear maximum vertical height: The ear on the ipsilateral side was more caudally positioned by a mean value of 5.87±3.68mm (range:1.05mm to 14.0mm) (Table 4).

2.4.8. All parameters compared by age groups

The mean values for each parameter were compared between children in the ≤1 and >1-year-old age groups. There were statistically significant differences between these age groups for the following parameters: ACF angle (p=0.004), volume (p=0.020), and height-roof (p=0.027), as well as orbital breadth (p=0.006) and height (0.009). A trend was noticed for these significant parameters – the absolute average percentage differences were greater in the ≤1-year-old age group (Table 5).

Table 5: Mean values compared between children in the ≤1 and >1-year-old age groups (N=18)

Measurements (Mean±SD)	≤1yr (n=12)	>1yr (n=6)	p-value
ACF (% diff.)			
Width	-16.5±8.68	-12.8±4.05	0.341[a]
Length	-23.3±8.67	-14.0±9.97	0.057[a]
Curve	-25.3±6.36	-18.7±10.0	0.110[a]
Angle	-22.5±5.38	-11.9±7.70	**0.004[a]**
Volume	-32.0±9.70	-19.2±10.2	**0.020[a]**
Height-Roof	-9.53±4.86	-3.94±3.87	**0.027[a]**
Height-Border	-17.7±13.7	-10.2±5.20	0.221[a]
ORBIT (% diff.)			
Length-SOR	-9.98±5.91	-12.5±6.97	0.425[a]
Length-IOR	8.97±5.41	10.7±5.80	0.529[a]
Breadth	-10.0±5.49	-2.58±2.07	**0.006[a]**
Height	30.2±12.7	13.6±6.77	**0.009[a]**
Surface area	13.7±8.97	12.2±7.39	0.724[a]
Volume	-5.53±2.65	-6.12±4.95	0.743[a]
SOR (mm)			
SOR max. vertical height	5.81(3.05-8.70)[#]	2.37(2.34-3.31)[#]	0.147[b]
EAR (mm)			
Ear max. AP distance	9.71±3.05	8.57±2.48	0.438[a]
Ear max. vertical height	4.90±3.27	7.82±3.94	0.115[a]

Note: % diff. = Percentage difference, Max. = Maximum, SD = Standard Deviation, mm = millimeter, SOR = Supraorbital rim, IOR = Infraorbital rim, AP = Anteroposterior

[a]t-test, [b]Wilcoxon test

[#]Median(Q1-Q3) value is shown due to skewness in the data

2.4.9. All parameters compared by sex

The mean values for each parameter were compared between females and males. No statistically significant differences were found between sex for each parameter (Table 6).

Table 6: Mean values compared between females and males (N=18)

Measurements (Mean±SD)	Female (n=10)	Male (n=8)	p-value
ACF (% diff.)			
Width	-13.5±5.88	-17.4±9.16	0.291[a]
Length	-19.6±9.16	-21.0±11.4	0.777[a]
Curve	-21.2±6.99	-25.4±9.27	0.292[a]
Angle	-17.7±7.38	-20.5±8.76	0.481[a]
Volume	-24.3±11.5	-32.0±10.4	0.163[a]
Height-Roof	-7.38±3.37	-8.02±7.13	0.805[a]
Height-Border	-11.0(-14.4 to -5.46)[#]	20.4(-28.8 to -6.91)[#]	0.168[b]
ORBIT (% diff.)			
Length-SOR	-10.1±5.15	-11.8±7.57	0.576[a]
Length-IOR	9.03±5.42	10.2±5.75	0.653[a]
Breadth	-7.71±4.53	-7.36±7.47	0.904[a]
Height	20.1±8.85	30.2±16.7	0.117[a]
Surface area	10.9±7.55	16.1±8.75	0.197[a]
Volume	-6.04±4.23	-5.33±2.33	0.676[a]
SOR (mm)			
SOR max. vertical height	4.77±2.80	6.40±6.34	0.475[a]
EAR (mm)			
Ear max. AP distance	9.05±2.39	9.68±3.48	0.656[a]
Ear max. vertical height	5.78±4.38	5.99±2.85	0.908[a]

Note: % diff. = Percentage difference, Max. = Maximum, SD = Standard Deviation, mm = millimeter, SOR = Supraorbital rim, IOR = Infraorbital rim, AP = Anteroposterior

[a]t-test, [b]Wilcoxon test

[#]Median(Q1-Q3) value is shown due to skewness in the data

2.4.10. All parameters compared by laterality

The mean values for each parameter were compared between patients with LUCS and RUCS. No statistically significant differences were found between patients with LUCS and RUCS for each parameter (Table 7).

Table 7: Mean values compared between patients with LUCS and RUCS (N=18)

Measurements (Mean±SD)	LUCS (n=7)	RUCS (n=11)	p-value
ACF (% diff.)			
Width	-13.6±7.71	-16.3±7.59	0.468[a]
Length	-20.7±10.2	-19.9±10.2	0.884[a]
Curve	-21.2±9.50	-24.3±7.32	0.439[a]
Angle	-21.9±5.77	-17.1±8.74	0.222[a]
Volume	-25.3±12.7	-29.2±10.8	0.492[a]
Height-Roof	-7.94±3.90	-7.50±6.06	0.867[a]
Height-Border	-11.2±7.57	-17.7±13.8	0.269[a]
ORBIT (% diff.)			
Length-SOR	-11.4±7.95	-10.5±5.20	0.754[a]
Length-IOR	6.93±6.15	11.2±4.42	0.102[a]
Breadth	-8.37±4.08	-7.04±6.84	0.651[a]
Height	27.0±15.3	23.1±12.8	0.565[a]
Surface area	16.5±8.23	11.1±7.97	0.182[a]
Volume	-6.48±2.39	-5.25±4.01	0.477[a]
SOR (mm)			
SOR max. vertical height	4.16(2.37-8.28)[#]	3.61(2.21-5.81)[#]	0.587[b]
EAR (mm)			
Ear max. AP distance	9.54±2.28	9.20±3.27	0.811[a]
Ear max. vertical height	4.58±3.87	6.69±3.47	0.245[a]

Note: % diff. = Percentage difference, Max. = Maximum, SD = Standard Deviation, mm = millimeter, SOR = Supraorbital rim, IOR = Infraorbital rim, AP = Anteroposterior, LUCS = Left unilateral coronal synostosis, RUCS = Right unilateral coronal synostosis

[a]t-test, [b]Wilcoxon test

[#]Median(Q1-Q3) value is shown due to skewness in the data

2.4.11. All parameters compared across ACF inter-tangential angle groups

Using the ACF inter-tangential angle measurements obtained in this study, an attempt was made to grade the ASP patients according to severity. Due to the small sample size, only two inter-tangential angle groups (<65°and ≥65°) were possible. These two groups were insufficient to classify ASP patients according to severity.

The mean values for each parameter were compared between inter-tangential angle groups <65° and ≥65° (Table 8). No statistically significant differences were found between these groups for each parameter, however, there were a few intriguing trends that were noticed:

2.4.11.1. ACF

All ACF parameters had greater absolute average percentage differences in the ≥65° group (Table 8).

2.4.11.2. Orbit

The absolute average percentage differences in most of the orbital parameters (length-SOR, breadth, height, and surface area) were greater in the ≥65°group (Table 8).

2.4.11.3. Ear

The ≥65° group had higher mean values for the maximum AP distance and vertical height parameters of the ear (Table 8).

Table 8: Mean values compared across inter-tangential angle groups (N=18)

Measurements (Mean±SD)	<65° (n=6)	≥65° (n=12)	p-value
ACF (% diff.)			
Width	-13.6±6.55	-16.1±8.12	0.518[a]
Length	-13.9±8.84	-23.4±9.18	0.054[a]
Curve	-18.7±7.93	-25.3±7.56	0.104[a]
Angle	-16.7±9.83	-20.1±6.97	0.416[a]
Volume	-23.6±10.4	-29.7±11.7	0.299[a]
Height-Roof	-7.03±4.29	-7.99±5.75	0.725[a]
Height-Border	-12.7±9.30	-16.4±13.3	0.556[a]
ORBIT (% diff.)			
Length-SOR	-10.5±6.16	-11.0±6.40	0.872[a]
Length-IOR	10.6±6.53	9.06±5.04	0.594[a]
Breadth	-6.71±5.44	-7.97±6.19	0.678[a]
Height	21.5±17.2	26.2±11.8	0.508[a]
Surface area	10.6±8.08	14.5±8.43	0.369[a]
Volume	-6.47±4.25	-5.35±3.10	0.534[a]
SOR (mm)			
SOR max. vertical height	4.87(3.75-7.51)[#]	2.89(1.95-6.09)[#]	0.281[b]
EAR (mm)			
Ear max. AP distance	9.01±3.39	9.49±2.69	0.743[a]
Ear max. vertical height	5.07±2.39	6.27±4.21	0.532[a]

Note: % diff. = Percentage difference, Max. = Maximum, SD = Standard Deviation, mm = millimeter, SOR = Supraorbital rim, IOR = Infraorbital rim, AP = Anteroposterior

[a]t-test, [b]Wilcoxon test

[#]Median(Q1-Q3) value is shown due to skewness in the data

2.5. Discussion

ASP causes a twisting deformity that asymmetrically affects the majority of the craniofacial skeleton.[8] A successful repair of all aberrant aspects of ASP continues to remain a challenge for the craniofacial surgeon.[21] Although the phenotypical characteristics of ASP have been well documented, only a few studies have used a quantitative approach to analyse the impacted craniofacial features. The present study employed a novel method in association with anatomical landmarks to describe and analyse the morphometry of the ACF, orbit, and ear on the ipsilateral and contralateral sides of ASP patients, using CT scans. The rarity of ASP meant that only a few previous studies were available for discussion. This investigation reports on the position of the ear, as well as the statistically significant asymmetry in the ACF and orbital parameters in 18 non-syndromic ASP patients.

In the literature, there is a dichotomy of opinion regarding the descriptions of the ACF and orbital parameters that are mentioned in this study. Different authors used different methods and anatomical landmarks to define these parameters thus no direct comparisons could be made.

2.5.1. Morphometry of the ACF

Previous studies used anatomical landmarks that captured the length of the ACF diagonally, rather than using landmarks that provided a straight AP diameter to determine the true length of the ACF.[3,10,16] These studies reported that the length was significantly reduced on the ipsilateral side when compared to the contralateral side. This study observed a similar pattern and revealed a statistically significant difference, with an average difference of -20.2% between the ipsilateral and contralateral sides (Table 2). To measure the true length of the ACF, this study employed the most efficient method possible (Fig. 1). On the other hand, the angle of the ACF decreased significantly on the ipsilateral side as compared to the contralateral side by an average difference of -19.0% (Table 2). This significant trend was also reported in a number of studies.[3,10,16,17] Since growth perpendicular to the suture is inhibited, these results could be attributed to the ipsilateral flattening of the frontal bone, including the supraorbital rim. As a result, the ACF length on the ipsilateral side was shorter and the angle was more acute than on the contralateral side. The results of the lengths and angles of the ACF proved that there was asymmetry of the ACF with reduced growth on the ipsilateral side.

In comparison to the contralateral side, the ipsilateral side decreased significantly for the remaining ACF parameters. The average percentage differences calculated between the ipsilateral

and contralateral sides were as follows: height-roof (-7.67%), height-border (-13.5%), width (-15.3%), curvature (-23.1%), and volume (-27.7%) (Table 2). These parameters have not been documented in the literature previously. Furthermore, the results revealed that of all the significant ACF parameters, the volume was the most asymmetrical as it decreased the most and the height-roof dimension was the least asymmetrical as it decreased the least (Table 2). As described in the literature, in ASP patients on the ipsilateral side there is flattening of the frontal bone, a raised and flattened supraorbital rim, a superiorly displaced large sphenoid wing, and deviation of the ACF midline structures towards the ipsilateral side.[9-12,17] These anatomical variations affect the ACF length, angle, width, curvature, and height, resulting in a shorter, narrower, and shallower ACF on the ipsilateral side. All of these factors are thought to have affected the ACF volume, with the volume on the ipsilateral side being the most affected. Determination of the ACF volume in patients with ASP is crucial since they are at risk of increased intracranial pressure.[2] In terms of the ACF height, it was measured using two methods viz. (a) from the midpoint of the orbital roof to the inner table of the ACF, and (b) from the superolateral border of the orbit to the inner table of the ACF (Fig. 4). It is worth noting that the height-roof parameter, rather than height-border parameter, resulted in the smallest absolute average percentage difference – least asymmetrical. This could be attributable to the "harlequin" deformation on the ipsilateral orbit, which elevates the superolateral border of the orbit causing this region to be much closer to the inner table of the ACF.

2.5.2. Morphometry of the orbits

Previous studies observed side-to-side asymmetry in orbital volume, with the volume on the ipsilateral side being significantly lower than the volume on the contralateral side.[3,8,16,19,20] Different authors used their preferred orbital boundaries when segmenting the orbital cavity to calculate the volume.[3,16,19,20] In this study, the anterior boundary of the orbit was defined as the inner surface of the eyelid (Fig. 9). The trend discovered in this study was similar to the trend observed in the abovementioned studies: the volume of the ipsilateral orbit significantly decreased by an average difference of -4.94% when compared to the contralateral orbit (Table 3). Lo *et al.*[28] also noticed a similar pattern but reported no statistically significant association between orbital volume and the ipsilateral side.

Dvoracek *et al.*[8] also discussed orbital height and breadth, stating that the ipsilateral orbit is tall and narrow, whereas the contralateral orbit is shortened and widened. They discovered that the height on the ipsilateral orbit increased significantly by an average difference of 19.8% when compared to the height on the contralateral orbit, whereas the orbital breadth on the ipsilateral

orbit was reduced significantly by an average difference of -6.10% when compared to the breadth on the contralateral orbit. Their investigation and this study reported a similar pattern. A statistically significant difference was found between the two orbits in this study, with an average difference of 24.6% calculated for orbital height and an average difference of -7.55% calculated for orbital breadth (Table 3).

The remaining orbital parameters (surface area, length-SOR, and length-IOR) are novel and have not been discussed in previous studies, hence there was no data available for comparison. According to the results, the surface area on the ipsilateral orbit increased significantly as compared to the contralateral orbit, resulting in an average difference of 13.2% (Table 3). The length of the orbit was measured using two methods: (a) from the midpoint of the optic canal to the vertical line that marked the most anterior portion of the SOR, and (b) from the midpoint of the optic canal to the vertical line that marked the most anterior portion of the IOR (Fig. 6). When comparing the ipsilateral and contralateral sides, orbital length-SOR decreased significantly on the ipsilateral side by an average difference of -10.8%, whereas orbital length-IOR increased significantly on the ipsilateral side and reported an average difference of 9.56% (Table 3). This occurrence could be attributed to the ipsilateral supraorbital region being retracted, elevated, and displaced laterally or it could be related to the increased protrusion of the contralateral supraorbital region.[8] Concerning the protrusion of the ipsilateral IOR, this could be related to the 'C-shaped' malformation of the face in ASP patients.

When all orbital parameters were examined, the average percentage differences between the ipsilateral and contralateral sides for length-IOR, height, and surface area increased significantly on the ipsilateral side, whereas the length-SOR, breadth, and volume decreased significantly. Additionally, on the ipsilateral side, orbital length-SOR decreased the most, whereas orbital height increased the most. Interestingly, when the authors of this study focused on the absolute average percentage differences, the greatest difference (most asymmetrical) was found in the height, whilst the smallest difference (least asymmetrical) was observed in the volume (Table 3).

The results of the orbital parameters could be explained by the fact that the ipsilateral orbit displays the typical "harlequin" deformity, which is characterized by superior displacement of the greater sphenoid wing, a flattened and elevated supraorbital rim, and a shortened ACF on the ipsilateral side. Due to this, the ipsilateral orbit is more elongated, narrow, and shallow.

In the literature, there were no absolute measurements documented on the position of the SORs. Studies by Marsh *et al.*[17] and Mesa *et al.*[21] noted that the SOR of the ipsilateral orbit was higher than the SOR of the contralateral orbit. This study discovered a similar finding. When the maximum vertical height between the SORs was calculated, it was revealed that the ipsilateral SOR was on average 3.89mm more cranially positioned (Table 4). As previously stated, this occurrence may be related to the "harlequin" deformity on the ipsilateral orbit.

2.5.3. Morphometry of the ears

The position of the ear on the ipsilateral side as compared to the contralateral side is controversial with no consensus in the literature.[12,22,23] Most studies concur that the ear on the affected side is more anteriorly positioned.[12,22,23] The vertical positioning of the ear has varied reporting with some claiming the ear on the affected side to be cranially displaced and others that it is caudally located.[22,23] Previous studies have no clearly defined anatomical landmarks when locating the ear position. In addition, there are no absolute measurements documented to determine the ear position. In this study, we used the midpoint of the EAM as the best indicator of the position of the ear on both the ipsilateral and contralateral sides (Fig.11 and 12). This position on the ipsilateral side was compared to the contralateral side and the displacement was measured in both the anteroposterior (horizontal) and cranio-caudal (vertical) dimensions. It was found that the ipsilateral ear was displaced anteriorly by an average of 9.33mm and caudally by an average of 5.87mm (Table 4). This could be related to the forward deviation of the petrous part of the temporal bone or also due to the notable 'facial twist' (asymmetry) in ASP patients, which is defined as the deviation of the upper face towards the synostotic side and the deviation of the lower face away from the synostotic side.[10] The results obtained in this study for the ear are more accurate than what is mentioned in the literature since they based their conclusions on clinical assessment rather than employing a definable landmark and measuring the desired parameter.

2.5.4. Comparison of all parameters by age, sex, race & laterality

All parameters were evaluated between children in the ≤1 and >1-year-old age groups; it was found that for the ACF only the angle, volume, and height-roof were found to be statistically significant. Regarding the orbit, only the breadth and height resulted in statistically significant differences (Table 5). The absolute average percentage differences obtained between the ipsilateral and contralateral sides for these parameters were higher in the ≤1-year-old age group. This indicated that in the latter group, the significant parameters were more asymmetrical; this could be due to compensatory mechanisms that may be more evident after 1 year of age. No

statistically significant differences were found for the remaining parameters when analysed by age, sex, or laterality (Table 5, 6 and 7).

2.5.5. All parameters compared across ACF inter-tangential angle groups

This study attempted to propose a novel quantitative classification system for ASP patients based on severity by using the ACF inter-tangential angle measurements obtained in this study (Fig. 3). To the best of the authors' knowledge, the inter-tangential angle of the ACF appeared to be the most effective method for classifying ASP patients according to severity. Due to the small sample size, only two inter-tangential angle categories (<65° and ≥65°) were possible. These two categories were insufficient to propose a severity-based classification system for ASP patients. When the mean values for each parameter were compared between the inter-tangential angle groups, no statistically significant differences were found, however, there were a few interesting trends that highlighted the potential of the classification system. In the ≥65° group, all of the ACF, ear, and most orbital parameters (length-SOR, breadth, height, and surface area) were more asymmetrical, indicating that this group may be more severe than the <65° group (Table 8). It is envisaged that such a severity classification will assist surgeons to assess patients, plan the appropriate surgical procedure, and evaluate the postoperative outcomes. This classification system would be less time-consuming and more versatile than other classification systems that rely on physical examination.

The results confirmed that both the ACF and the orbit were significantly impacted in ASP, with the volume of the ACF being the most affected parameter. Previous studies were barely comparable due to different scan protocols, methods, and anatomical landmarks that were used to calculate the parameters of this current study. Furthermore, since some of the parameters were not mentioned in previous studies, there was no data available for comparison. No comparisons could be made between the races due to the small sample size (N=18). Additionally, it is acknowledged that there may be compensatory changes on the non-synostotic (contralateral) side of patients with unilateral anterior plagiocephaly and some authors may question the normality of this control. However, in unilateral anterior plagiocephaly finding an equivalent control to compare the morphometry is a challenge. If normal CT scans are used, the variability of age, sex, individual variations, and other factors would lead to many variables that would render the outcomes of this study less scientific. Whilst the authors of this study do concede that there are compensatory changes on the non-synostotic side of unilateral anterior plagiocephaly patients, the authors are of the opinion that comparison with the non-synostotic side is the most effective way to minimise the variables. Three-dimensional reconstructed CT scans provided the clearest

identification of all the hallmark characteristics of ASP. The measurements of the study may be beneficial to surgeons during corrective surgery by indicating the degree of the asymmetry on each side, making it easier to plan the technique and extent of surgical correction of the affected craniofacial structures. This study also provides an anatomical base in patients with ASP to be used as a potential reference to compare preoperative and postoperative results and assess the improvement of the deformity and monitor surgical outcomes.

2.6. Conclusion

This study reports anthropometric measurements of the ACF, orbit, and ear on the ipsilateral and contralateral sides in a select cohort of South African patients presenting with ASP, using preoperative CT scans. The results concluded that there was side-to-side asymmetry in the ACF, orbit, and ear. The volume was the most affected of all the significant ACF parameters. In terms of the orbit, the height was the most affected of all the significant parameters. Regarding the vertical and horizontal position of the ear, it was caudally and anteriorly displaced on the ipsilateral side when compared to the contralateral side. This study provided actual values to validate the hallmark characteristics of ASP, thereby contributing to the literature wherein current data is limited. These measurements may be beneficial to surgeons during corrective surgery by indicating the degree of the asymmetry on each side, making it easier to plan the technique and extent of surgical correction of the affected craniofacial structures. The results of this study have the potential to propose a grading system in ASP patients according to severity of the condition if the sample size is increased.

2.7. Declarations

2.7.1. Acknowledgments

The authors wish to acknowledge the financial assistance of the National Research Foundation (NRF) of South Africa towards this research (Grant Numbers: 123516). The opinions expressed and conclusions arrived at, are those of the authors and are not necessarily to be attributed to the NRF.

2.7.2. Author contributions

N Mohan: Project development, data collection, data analysis, manuscript writing and editing
R Harrichandparsad: Project development, data analysis, manuscript editing
L Lazarus: Project development, data analysis, manuscript editing

A Madaree: Project development, data analysis, manuscript editing (All authors provided intellectual input, contributed to manuscript revisions, and approved the final manuscript)

2.7.3. Conflict of Interest

The authors declare that they have no conflict of interest to report.

2.7.4. Ethical Approval

Institutional ethical clearance for this study was obtained from the Biomedical Research Ethics Committee of the University of KwaZulu-Natal (UKZN) (BREC/00002129/2020) and relevant authorities.

2.8. References

1. Kajdic N, Spazzapan P, Velnar T. Craniosynostosis - Recognition, clinical characteristics, and treatment. *Bosn J Basic Med Sci*. 2017;18(2):110-116.
2. Lee M, Hong H, Shim K. Quantitative Assessment of Shape Deformation of Regional Cranial Bone for Evaluation of Surgical Effect in Patients with Craniosynostosis. *Applied Sciences*. 2021;11(3):990.
3. Calandrelli R, Pilato F, Massimi L, *et al*. Quantitative analysis of cranial-orbital changes in infants with anterior synostotic plagiocephaly. *Child's Nervous System*. 2018;34(9):1725-1733.
4. Kronig S, Kronig O, Vrooman H, *et al*. Quantification of Severity of Unilateral Coronal Synostosis. *The Cleft Palate-Craniofacial Journal*. 2020;58(7):832-837.
5. Dias M, Samson T, Rizk E, *et al*. Identifying the Misshapen Head: Craniosynostosis and Related Disorders. *Pediatrics*. 2020;146(3).
6. Heuzé Y, Martínez-Abadías N, Stella J, *et al*. Unilateral and bilateral expression of a quantitative trait: asymmetry and symmetry in coronal craniosynostosis. *Journal of Experimental Zoology Part B: Molecular and Developmental Evolution*. 2012;318(2):109-122.

7. Moderie C, Govshievich A, Papay F, *et al*. Current Trends in Management of Nonsyndromic Unilateral Coronal Craniosynostosis: A Cross-sectional Survey. *Plastic and Reconstructive Surgery - Global Open*. 2019;7(5):e2229.
8. Dvoracek L, Bykowski M, Foglio A, *et al*. Objective Analysis of Fronto-Orbital Dysmorphology in Unilateral Coronal Craniosynostosis. *Journal of Craniofacial Surgery*. 2021;32(7):2266-2272.
9. Di Rocco C, Paternoster G, Caldarelli M, *et al*. Anterior plagiocephaly: epidemiology, clinical findings, diagnosis, and classification. A review. *Child's Nervous System*. 2012;28(9):1413-1422.
10. Captier G, Leboucq N, Bigorre M, *et al*. Plagiocephaly: morphometry of skull base asymmetry. *Surgical and Radiologic Anatomy*. 2003;25(3-4):226-233.
11. Raposo-do-Amaral C, Silva M, Menon D, *et al*. Anthropometric Study of Craniofacial Asymmetry in Unilateral Coronal Craniosynostosis. *Brazilian Journal of Plastic Surgery*. 2011;26(1):27-31.
12. Spazzapan P, Bošnjak R, Velnar T, *et al*. Anterior Plagiocephaly - A report of a case and operative technique. *Slovenian Medical Journal.* 2017;86(1-2).
13. Oh A, Wong J, Ohta E, *et al*. Facial Asymmetry in Unilateral Coronal Synostosis: Long-Term Results after Fronto-orbital Advancement. *Plast Reconstr Surg*. 2008;121(2):545-562.
14. Matushita H, Alonso N, Cardeal D, *et al*. Frontal–orbital advancement for the management of anterior plagiocephaly. *Child's Nervous System*. 2012;28(9):1423-1427.
15. Di Rocco C, Velardi F. Nosographic identification and classification of plagiocephaly. *Child's Nervous System*. 1988;4(1):9-15.
16. Calandrelli R, D'Apolito G, Massimi L, *et al*. Quantitative analysis of craniofacial dysmorphology in infants with anterior synostotic plagiocephaly. *Child's Nervous System*. 2016;32(12):2339-2349.
17. Marsh J, Gado M, Vannie M, *et al.* Osseous Anatomy of Unilateral Coronal Synostosis. *Cleft Palate Journal.* 1986;23:87-100.

18. Bentley R, Sgouros S, Natarajan K, *et al*. Changes in orbital volume during childhood in cases of craniosynostosis. *J Neurosurg*. 2002;96(4):747-754.
19. Beckett J, Persing J, Steinbacher D. Bilateral Orbital Dysmorphology in Unicoronal Synostosis. *Plast Reconstr Surg*. 2013;131(1):125-130.
20. Kronig S, Kronig O, Zurek M, *et al*. Orbital volume, ophthalmic sequelae and severity in unilateral coronal synostosis. *Child's Nervous System*. 2021;37(5):1687-1694.
21. Mesa J, Fang F, Muraszko K, *et al*. Reconstruction of unicoronal plagiocephaly with a hypercorrection surgical technique. *Neurosurg Focus*. 2011;31(2):e4.
22. Pelo S, Tamburrini G, Marianetti T, *et al*. Correlations between the abnormal development of the skull base and facial skeleton growth in anterior synostotic plagiocephaly: the predictive value of a classification based on CT scan examination. *Child's Nervous System*. 2011;27(9):1431-1443.
23. Bruneteau R, Mulliken J. Frontal Plagiocephaly: Synostotic, Compensational, or Deformational. *Plast Reconstr Surg*. 1992;89(1):21-31.
24. Otake S, Taoka T, Maeda M, *et al*. A guide to identification and selection of axial planes in magnetic resonance imaging of the brain. *Neuroradiol J*. 2018;31(4):336-344.
25. Ji Y, Qian Z, Dong Y, *et al*. Quantitative morphometry of the orbit in Chinese adults based on a three-dimensional reconstruction method. *J Anat*. 2010;217(5):501-506.
26. Shyu V, Hsu C, Chen C, *et al*. 3D-Assisted Quantitative Assessment of Orbital Volume Using an Open-Source Software Platform in a Taiwanese Population. *PLoS One*. 2015;10(3):e0119589.
27. Statistics South Africa. *Statistical Release P0340 Governance and Access to Justice. Pretoria: Statistics South Africa.* 2020. Accessed November 20, 2021. http://www.statssa.gov.za/publications/P0340/P03402019.pdf
28. Lo L, Marsh J, Kane A, *et al*. Orbital Dysmorphology in Unilateral Coronal Synostosis. *The Cleft Palate-Craniofacial Journal*. 1996;33(3):190-197.

CHAPTER 3: SYNTHESIS

3.1. Synthesis

This present retrospective chart study investigated the degree of asymmetry on the synostotic (ipsilateral) side and non-synostotic (contralateral) side of the craniofacial features that are involved in anterior synostotic plagiocephaly (ASP). Due to the paucity of literature pertaining to the morphometric analysis of these craniofacial features, this study aimed to evaluate and compare the morphometry of the anterior cranial fossa (ACF), orbit, and ear on the ipsilateral and contralateral sides in a select South African population of patients diagnosed with ASP using preoperative computed tomography (CT) scans. If ASP is not treated, it can lead to increased intracranial pressure, as well as serious cosmetic and socio-psychological repercussions (Moderie *et al.*, 2019). Knowledge of the morphometric data of these features may simplify the procedure for the surgeons to correct the affected structures because it indicates the extent of the asymmetry on each side. This will aid in efficient planning of the technique and extent of surgical correction of the affected structures. A total of 18 patients, 8 males (44.4%) and 10 females (55.6%) with non-syndromic ASP were recorded, consistent with the literature that ASP has a female predominance of 60 to 75% of cases occurring in females (Spazzapan *et al.*, 2017, Dias *et al.*, 2020). Previous studies have found that the right side is more commonly affected, this study also found that 61.1% of patients had right coronal suture involvement and 38.9% had left-sided involvement (Di Rocco *et al.*, 2012; Heuzé *et al.*, 2012).

A few prior studies have quantified the asymmetry of some of the ACF and orbital parameters stated in this study. Different authors have used different methods and anatomical landmarks to define these parameters in the literature. As a result, no direct comparisons could be made.

3.1.1. Anterior cranial fossa

The following ACF parameters of this study have yet to be reported in the literature: height, width, length of curvature, and volume. Only the length and angle of the ACF were documented in the literature. This study reported significant side-to-side asymmetry of the ACF. When compared to the contralateral side, all the ACF parameters were significantly decreased on the ipsilateral side. In terms of ACF length, this study noted a similar pattern as the previous studies, with the length being significantly shorter on the ipsilateral side than the contralateral side (Captier *et al.*, 2003; Calandrelli *et al.*, 2016 and Calandrelli *et al.*, 2018). The studies conducted by Marsh *et al.* (1986), Captier *et al.* (2003), Calandrelli *et al.* (2016) and Calandrelli *et al.* (2018) reported that the

ipsilateral angle was significantly smaller as opposed to the contralateral angle, this trend was also noticed in this study. After evaluating all of the parameters, it was discovered that the ACF volume decreased the most by -27.7% (range: -46.5% to -9.17%), making it the most asymmetrical parameter, while the ACF height-roof (measured from the midpoint of the orbital roof) decreased the least by -7.67% (range: -18.8% to -0.738%), making it the least asymmetrical (Page 57: Chapter 2, Table 2). These findings could be characterized by the skull compensating for its inability to expand perpendicular to the affected suture by growing more parallel to the unaffected sutures, resulting in limited growth on one side and compensatory growth on the other side of the skull (Van Veelen-Vincent *et al.*, 2010). This has an impact on all aspects of the ACF, eventually resulting in a short, narrow, and shallow ACF, with the volume being the most impacted.

3.1.2. Orbits

The orbital length and surface area parameters of this study have yet to be documented. In the literature, only orbital breadth, height, and volume were reported. This study found significant side-to-side asymmetry of the orbit. Two methods were used to determine the length of the orbit (Page 47: Chapter 2, Fig. 1F), orbital length (in relation to the SOR) significantly decreased on the ipsilateral side, while orbital length (in relation to the IOR) significantly increased on the ipsilateral side when compared to the contralateral side. This could be due to the retraction of the ipsilateral SOR and the formation of a 'facial twist' in ASP patients. In terms of the orbital surface area, on the ipsilateral orbit, the surface area also increased significantly. Furthermore, this study reported that the height of the orbit increased significantly, whereas the breadth decreased significantly on the ipsilateral side when compared to the contralateral side. Orbital height and breadth, discussed by Dvoracek *et al.* (2021), reported a similar trend as this study, adding that the ipsilateral orbit was high and narrow, whereas the contralateral orbit was short and wide. The orbital volume was determined by manually delineating the interface between the inner bony walls and the soft tissue contents of each orbit on every slice of the CT images, with the anterior boundary of the orbit defined by the inner surface of the eyelid and the posterior boundary defined by a line connecting the lateral and medial walls of the optic foramen within the orbital cavity (Page 49: Chapter 2, Fig.1I). Previous authors segmented the orbit using their preferred orbital boundaries. These authors reported that the volume of the ipsilateral orbit was significantly decreased when compared to the contralateral orbit (Bentley *et al.*, 2002; Beckett *et al.*, 2013; Calandrelli *et al.*, 2018, Dvoracek *et al.*, 2021, and Kronig *et al.*, 2021). This study noted a similar pattern. After analysing all the orbital parameters, it was discovered that orbital height increased the most by 24.6% (range: 6.80% to 55.4%), making it the most asymmetrical parameter, while

orbital volume decreased the least by -4.94% (range: -14.6% to -0.573%) making it the least asymmetrical (Page 59: Chapter 2, Table 3). Lastly, there are no measurements of the position of the SOR in the literature, however, Marsh *et al.* (1986) and Mesa *et al.* (2011) found that the SOR of the ipsilateral orbit was higher than the SOR of the contralateral orbit. A similar finding was reported in this study. The ipsilateral SOR was displaced cranially by an average of 3.89mm, ranging from 1.39mm to 17.9mm (Page 60: Chapter 2, Table 4). The larger wing of the sphenoid bone becomes steeply angled in an upward fashion leading to the "harlequin" deformity of the ipsilateral orbit. As a result, the ipsilateral orbit becomes elongated, thin, and shallow, with the orbital height parameter being the most affected.

3.1.3. Position of ears

To determine the position of the ears, this study measured the maximum anteroposterior (horizontal) diameter and vertical height (cranio-caudal), these were compared between the ipsilateral and contralateral ears. This study used the midpoint of the external auditory meatus (EAM) as a landmark as it was considered as the best indication of ear position on both the ipsilateral and contralateral sides in this investigation (Page 51: Chapter 2, Fig.1K and L). The ipsilateral ear was found to be anteriorly displaced by an average of 9.33mm, ranging from 3.98mm to 14.6mm, and caudally displaced by an average of 5.87mm, ranging from 1.05mm to 14.0mm (Page 60: Chapter 2, Table 4). This result could be associated with the notable 'facial twist' or 'C'-shaped malformation (asymmetry) in ASP patients. When determining the ear position in previous investigations, there were no clearly defined anatomical landmarks. Furthermore, no absolute measurements for determining the ear location have been documented. In the literature, there is no consensus on the position of the ear on the ipsilateral side vs the contralateral side. The ear on the ipsilateral side was more anteriorly positioned, according to most research (Bruneteau and Mulliken *et al.*, 1992; Pelo *et al.*, 2011; Spazzapan *et al.*, 2017). There was varied reporting with regards to the vertical location of the ear, with some reporting that the ear on the ipsilateral side was cranially displaced and others asserting that it was caudally positioned (Bruneteau and Mulliken *et al.*, 1992; Pelo *et al.*, 2011).

3.1.4. Comparisons according to age, sex, race and laterality

Only the age variable indicated statistically significant differences. The angle, volume, and height-roof parameters were significant in the ACF, while only the breadth and height parameters were significant in the orbit (Page 61: Chapter 2, Table 5). These significant parameters were

more asymmetrical in the ≤1-year-olds rather than the >1-year-olds. This could be due to the compensatory mechanisms that become more apparent after the first year of life.

3.1.5. All parameters compared across ACF inter-tangential angle groups

Using the ACF inter-tangential angle measurements, this study attempted to provide a novel quantitative classification system for ASP patients based on severity. Only two inter-tangential angle groups (<65° and ≥65°) were achievable given the limited sample size. These two groups were insufficient to establish a severity-based classification system. No statistically significant differences were found when all the parameters were compared between these two groups, however, trends were noticed in that all the ACF, ear, and most of the orbital parameters (length-SOR, breadth, height, and surface area) were more asymmetrical in the ≥65° group (Page 65: Chapter 2, Table 8). The authors' primary focus was on the findings of the ACF because it is the most influenced structure in ASP. Whilst there were no statistically significant differences in the ACF related to the inter-tangential angle, the trend observed highlighted the potential of this attempted classification system. An increase in sample size will most likely culminate in a graded plagiocephaly classification system. Such a severity classification is envisaged to aid surgeons in assessing patients, planning the appropriate surgical treatment, and evaluating the postoperative outcomes.

3.2. Limitations of the study

This study investigated the degree of asymmetry in the craniofacial features on either side of the skull and face in ASP patients. Data was acquired from the Inkosi Albert Luthuli Central Hospital (IALCH), which is a regional public hospital and is the only Craniofacial Unit in KwaZulu-Natal. Since the patient cohort was limited to this province, this may affect the generalization of the results. The sample size was limited, not only because the data was obtained from a single craniofacial centre, but also due to the low prevalence of the condition of 1 per 10 000 live births (Dias *et al.*, 2020). A total of 29 cases of ASP were acquired in this study, however, 11 of them were eliminated because they were either syndromic or had multiple-suture synostosis, and thus did not meet the inclusion criteria. Due to the sample size being relatively small, it did not have enough power to detect smaller effect sizes, hence this study could not propose a severity-based classification system, and substantial comparisons by race could not be made as the proportions of the race groups included in the patient cohort was skewed.

3.3. Recommendations for future research

If the sample size is increased, more than two inter-tangential angle groups would be achieved, and grading ASP patients according to severity would be possible. If a robust severity-based classification system is devised it will advantageous as it will assist surgeons with diagnosis and selection of the most appropriate type and timing of surgical intervention, it could also be used to assess other population groups internationally. This novel classification system would also be less time-consuming and more versatile than other classification systems that rely on physical examination. Substantial comparisons between race groups could also be made with an increased sample size. This study can be used as a reference for future research by comparing preoperative and postoperative data to monitor surgical outcomes and assess the improvement of the deformity. Long-term follow-up of these patients and a larger sample size would provide more information on how craniofacial asymmetry changes with age and growth, as well as the need for any surgical revision in adulthood.

3.4. Conclusion

ASP results in morphological alterations to the skull and face, making it challenging for a surgeon to successfully correct the craniofacial skeleton to a normal appearance. Using preoperative CT images, this novel study aimed to report anthropometric measurements of the ACF, orbit, and ear on the ipsilateral and contralateral sides in a select cohort of South African patients with ASP. The findings revealed that the ACF, orbit, and ear had side-to-side asymmetry. The volume of the ACF was affected the most and in terms of the orbit, the height was most affected. This study augments the existing literature on ASP by providing actual values to validate the hallmark characteristics of ASP that have not been previously recorded. The morphometric data could help surgeons attain normality of the affected craniofacial structure by giving them an indication of the magnitude of the asymmetry on the ipsilateral side compared to the contralateral side; it will make it easier to plan the surgical technique and extent of the correction. The results of this study have the potential to propose a grading system in ASP patients according to severity of the condition if the sample size is increased.

3.5. References

1. Beckett, J., Persing, J. and Steinbacher, D. (2013). Bilateral Orbital Dysmorphology in Unicoronal Synostosis. *Plastic and Reconstructive Surgery*, 131(1), pp.125-130.
2. Bentley, R., Sgouros, S., Natarajan, K., Dover, M. and Hockley, A. (2002). Changes in orbital volume during childhood in cases of craniosynostosis. *Journal of Neurosurgery*, 96(4), pp.747-754.
3. Bruneteau, R. and Mulliken, J. (1992). Frontal Plagiocephaly: Synostotic, Compensational, or Deformational. *Plastic and Reconstructive Surgery*, 89(1), pp.21-31.
4. Calandrelli, R., D'Apolito, G., Massimi, L., Gaudino, S., Visconti, E., Pelo, S., Di Rocco, C. and Colosimo, C. (2016). Quantitative analysis of craniofacial dysmorphology in infants with anterior synostotic plagiocephaly. *Child's Nervous System*, 32(12), pp.2339-2349.
5. Calandrelli, R., Pilato, F., Massimi, L., Panfili, M., Di Rocco, C. and Colosimo, C. (2018). Quantitative analysis of cranial-orbital changes in infants with anterior synostotic plagiocephaly. *Child's Nervous System*, 34(9), pp.1725-1733.
6. Captier, G., Leboucq, N., Bigorre, M., Canovas, F., Bonnel, F., Bonnafé, A. and Montoya, P. (2003). Plagiocephaly: morphometry of skull base asymmetry. *Surgical and Radiologic Anatomy*, 25(3-4), pp.226-233.
7. Di Rocco, C., Paternoster, G., Caldarelli, M., Massimi, L. and Tamburrini, G. (2012). Anterior plagiocephaly: epidemiology, clinical findings, diagnosis, and classification. A review. *Child's Nervous System*, 28(9), pp.1413-1422.
8. Dias, M., Samson, T., Rizk, E., Governale, L. and Richtsmeier, J. (2020). Identifying the Misshapen Head: Craniosynostosis and Related Disorders. *Pediatrics*, 146(3).
9. Dvoracek, L., Bykowski, M., Foglio, A., Ayyash, A., Pfaff, M., Losee, J. and Goldstein, J. (2021). Objective Analysis of Fronto-Orbital Dysmorphology in Unilateral Coronal Craniosynostosis. *Journal of Craniofacial Surgery*, 32(7), pp.2266-2272.
10. Heuzé, Y., Martínez-Abadías, N., Stella, J., Senders, C., Boyadjiev, S., Lo, L. and Richtsmeier, J. (2012). Unilateral and bilateral expression of a quantitative trait: asymmetry and symmetry in coronal craniosynostosis. *Journal of Experimental Zoology Part B: Molecular and Developmental Evolution*, 318(2), pp.109-122.
11. Kronig, S., Kronig, O., Zurek, M. and Van Adrichem, L. (2021). Orbital volume, ophthalmic sequelae and severity in unilateral coronal synostosis. *Child's Nervous System*, 37(5), pp.1687-1694.
12. Marsh, J., Gado, M., Vannier, M. and Stevens, W. (1986). Osseous Anatomy of Unilateral Coronal Synostosis. *Cleft Palate Journal*, 23, pp.87-100.

13. Mesa, J., Fang, F., Muraszko, K. and Buchman, S. (2011). Reconstruction of unicoronal plagiocephaly with a hypercorrection surgical technique. *Neurosurgical Focus*, 31(2), p.e.4.
14. Moderie, C., Govshievich, A., Papay, F., Fearon, J., Gosain, A. and Doumit, G. (2019). Current Trends in Management of Nonsyndromic Unilateral Coronal Craniosynostosis: A Cross-sectional Survey. *Plastic and Reconstructive Surgery - Global Open*, 7(5), p.e2229.
15. Pelo, S., Tamburrini, G., Marianetti, T., Saponaro, G., Moro, A., Gasparini, G. and Di Rocco, C. (2011). Correlations between the abnormal development of the skull base and facial skeleton growth in anterior synostotic plagiocephaly: the predictive value of a classification based on CT scan examination. *Child's Nervous System*, 27(9), pp.1431-1443.
16. Spazzapan, P., Bošnjak, R., Velnar, T. and Cassisi, A. (2017). Anterior Plagiocephaly - A report of a case and operative technique. *Slovenian Medical Journal*, 86(1-2).
17. Van Veelen-Vincent, M., Mathijssen, I., Arnaud, E., Renier, D. and Di Rocco, F. (2010). Craniosynostosis. *Neurosurgery*, pp.501-528.

APPENDIX A:
JOURNAL SUBMISSION

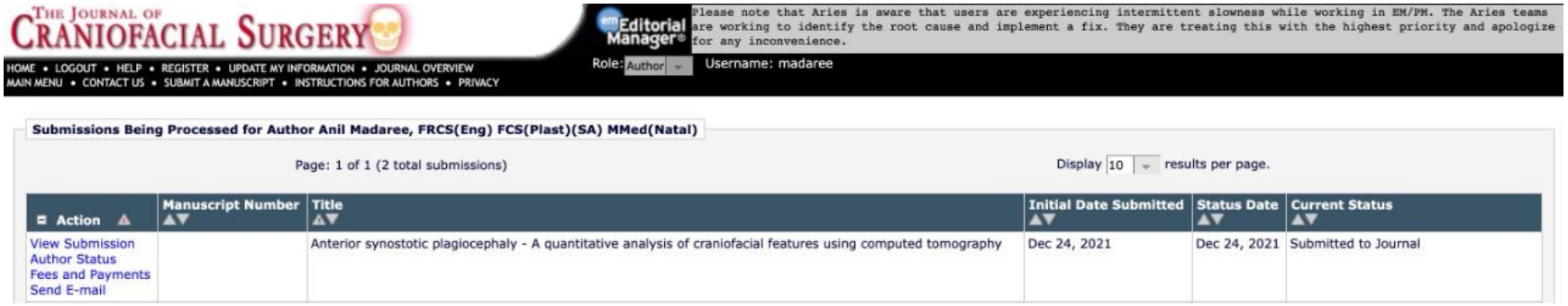

THE JOURNAL OF CRANIOFACIAL SURGERY

Editorial Manager

Please note that Aries is aware that users are experiencing intermittent slowness while working in EM/PM. The Aries teams are working to identify the root cause and implement a fix. They are treating this with the highest priority and apologize for any inconvenience.

HOME • LOGOUT • HELP • REGISTER • UPDATE MY INFORMATION • JOURNAL OVERVIEW
MAIN MENU • CONTACT US • SUBMIT A MANUSCRIPT • INSTRUCTIONS FOR AUTHORS • PRIVACY

Role: Author Username: madaree

Submissions Being Processed for Author Anil Madaree, FRCS(Eng) FCS(Plast)(SA) MMed(Natal)

Page: 1 of 1 (2 total submissions) Display 10 results per page.

Action	Manuscript Number	Title	Initial Date Submitted	Status Date	Current Status
View Submission Author Status Fees and Payments Send E-mail		Anterior synostotic plagiocephaly - A quantitative analysis of craniofacial features using computed tomography	Dec 24, 2021	Dec 24, 2021	Submitted to Journal

APPENDIX B:
FULL ETHICAL APPROVAL

UNIVERSITY OF KWAZULU-NATAL
INYUVESI YAKWAZULU-NATALI

18 March 2021

Miss Nivana Mohan (216017401)
School of Lab Med & Medical Sc
Westville

Dear Miss Mohan,

Protocol reference number: BREC/00002129/2020
Project title: Anterior Synostotic Plagiocephaly - A Quantitative Analysis of Craniofacial Changes using Computed Tomographic Review
Degree Purposes: MMedSci

EXPEDITED APPLICATION: APPROVAL LETTER

A sub-committee of the Biomedical Research Ethics Committee has considered and noted your application.

The conditions have been met and the study is given full ethics approval and may begin as from 18 March 2021. Please ensure that outstanding site permissions are obtained and forwarded to BREC for approval before commencing research at a site.

This approval is subject to national and UKZN lockdown regulations, see (http://research.ukzn.ac.za/Libraries/BREC/BREC_Lockdown_Level_1_Guidelines.sflb.ashx). Based on feedback from some sites, we urge PIs to show sensitivity and exercise appropriate consideration at sites where personnel and service users appear stressed or overloaded.

This approval is valid for one year from 18 March 2021. To ensure uninterrupted approval of this study beyond the approval expiry date, an application for recertification must be submitted to BREC on the appropriate BREC form 2-3 months before the expiry date.

Any amendments to this study, unless urgently required to ensure safety of participants, must be approved by BREC prior to implementation.

Your acceptance of this approval denotes your compliance with South African National Research Ethics Guidelines (2015), South African National Good Clinical Practice Guidelines (2006) (if applicable) and with UKZN BREC ethics requirements as contained in the UKZN BREC Terms of Reference and Standard Operating Procedures, all available at http://research.ukzn.ac.za/Research-Ethics/Biomedical-Research-Ethics.aspx.

BREC is registered with the South African National Health Research Ethics Council (REC-290408-009). BREC has US Office for Human Research Protections (OHRP) Federal-wide Assurance (FWA 678).

The sub-committee's decision will be noted by a full Committee at its next meeting taking place on 13 April 2021.

Yours sincerely,

[redacted]

Prof D Wassenaar
Chair: Biomedical Research Ethics Committee

Biomedical Research Ethics Committee
Chair: Professor D R Wassenaar
UKZN Research Ethics Office Westville Campus, Govan Mbeki Building
Postal Address: Private Bag X54001, Durban 4000
Email: BREC@ukzn.ac.za
Website: http://research.ukzn.ac.za/Research-Ethics/Biomedical-Research-Ethics.aspx

APPENDIX C:
UKZN GATEKEEPER PERMISSION

UNIVERSITY OF KWAZULU-NATAL
INYUVESI YAKWAZULU-NATALI

14 December 2020

To whom it may concern

This letter serves to inform that the School of Laboratory Medicine and Medical Sciences grants **N Mohan (student number: 216017401)** permission to conduct the study referenced **BREC/00002129/2020** titled: Anterior Synostotic Plagiocephaly: A Quantitative Analysis of Craniofacial Changes using Computed Tomographic Review. This permission is only valid for the time period stipulated in the BREC application.

Sincerely

[redacted]

Dr A Khathi

Academic Leader Human Body Form and Function Theme

Room E3-408
Department of Human Physiology
School of Laboratory Medicine and Medical Sciences
College of Health Sciences
University of KwaZulu Natal
Tel: 0312607585
Fax: 0312607132

APPENDIX D:
IALCH GATEKEEPER PERMISSION

health
Department:
Health
PROVINCE OF KWAZULU-NATAL

DIRECTORATE:

[redacted]
Physical Address: 800 Bellair Road, Mayville, 4058
Postal Address: Private Bag X08i Mayville, 4058
Tel: 0312401059 Fax 031240105 Email: ursulanun@ ialch.cp.za
WWW. kznhealth.gqltzq

[redacted] Medical M ag rl !
Office
ALCH

Reverence:BREC/000
Enquiries: Medical Management

15 December 2020

Ms N Mohan (216017401)
School of Laboratory Medicine & Medical Science Westville

Dear Ms Mohan

RE: PERMISSION TO CONDUCT RESEARCH AT IALCH

I have pleasure in informing you that permission has been granted to you by the Medical Manager to conduct research on: Anterior Svnostotic Plagiocephalv- A Quantitative Analysis of Craniofacial Changes using Computed Tomographic Review.

Kindly take note of the following information before you continue:

1 . Please ensure that you adhere to all the policies, procedures, protocols and guidelines of the Department of Health with regards to this research.
2. This research will only commence once this office has received confirmation from the Provincial Health Research Committee in the KZN Department of I-lealth.
3. Kindly ensure that this office is informed before you commence your research.
4. The hospital will not provide any resources for this research.
5. You will be expected to provide feedback once your research is complete to the Medical Manager.

Yours faithfully
[redacted]
Dr A Har ichandparsad
Clinical Care Manager

health
Department:
Health
PROVINCE OF KWAZULU-NATAL
KWAZULU-NATAL
Fighting Disease, Fightjng Pove!ty, Giving Hope

DIRECTORATE:

Physical Address: BOO Bellair Roadi Mayville. 4058
Postal Address: Private Bag xoa, Mayville. 4058
Tell 0312401059 Fax: 0312401050 Email: ursulanun@ ialch.coza
wwwkznhealthqov„za

office o/ The I Managbr
IALCH

15 December 2020

Ms N Mohan (216017401)
School of Laboratory Medicine & Medical Science Westville

Dear Ms Mohan

Re: Approved Research: Ref No: BREC/00002129/2020: Anterior Svnostotic Plagiocephalv — A Ouantitative Analysis of Craniofacial Changes using Computed Tomographic Review

As per the policy of the Provincial Health Research Committee (PHRC), you are hereby granted permission to conduct the above mentioned research once all relevant documentation has been submitted to PHRC inclusive of Full Ethical Approval.

Kindly note the following.

1 . The research should adhere to all policies, procedures, protocols and guidelines of the KwaZulu-Natal Department or Health.
2. Research will only commence once the PHRC has granted approval to the researcher.
-3. The researcher must ensure that the Medical Manager is informed before the commencement of the research by means of the approval letter by the chairperson of the PHRC.
4. The Medical Manager expects to be provided feedback on the findings of the research.
5. Kindly submit your research to:

The Secretariat
Health Research & Knowledge Management
330 Langaliballe Street, Pietermaritzburg, 3200
Private Bag X9501 , Pietermaritzburg, 3201
Tel: 033395-3123, Fax 033394-3782
Email: hrkm@kznhealth.gov.za

Yours faithfully

[redacted]

Dr A Harri handparsad
Clinical Care Manager

APPENDIX E:
DOH PERMISSION

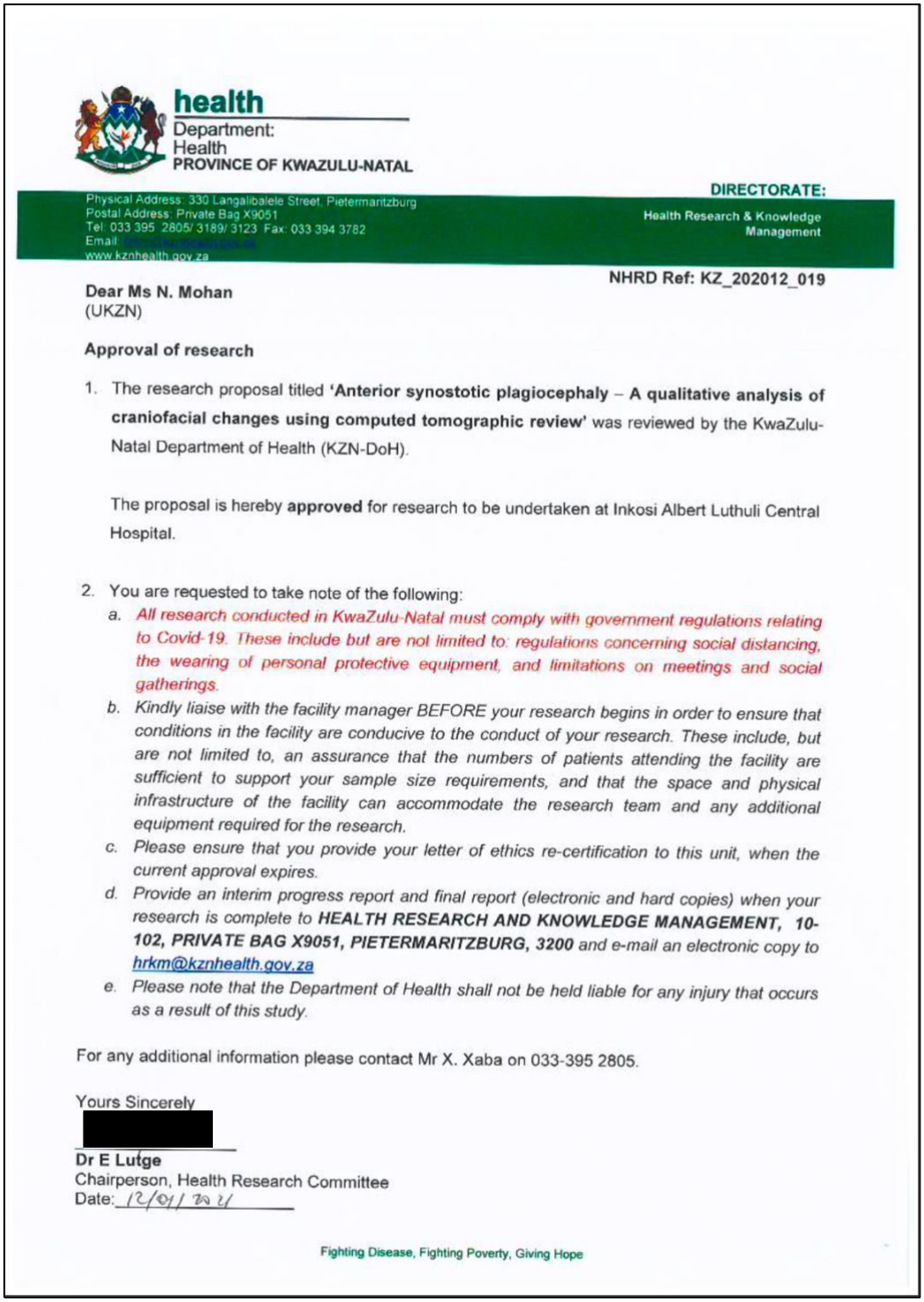

health
Department:
Health
PROVINCE OF KWAZULU-NATAL

Physical Address: 330 Langalibalele Street, Pietermaritzburg
Postal Address: Private Bag X9051
Tel: 033 395 2805/ 3189/ 3123 Fax: 033 394 3782
Email:
www.kznhealth.gov.za

DIRECTORATE:
Health Research & Knowledge Management

NHRD Ref: KZ_202012_019

Dear Ms N. Mohan
(UKZN)

Approval of research

1. The research proposal titled **'Anterior synostotic plagiocephaly – A qualitative analysis of craniofacial changes using computed tomographic review'** was reviewed by the KwaZulu-Natal Department of Health (KZN-DoH).

   The proposal is hereby **approved** for research to be undertaken at Inkosi Albert Luthuli Central Hospital.

2. You are requested to take note of the following:
   a. *All research conducted in KwaZulu-Natal must comply with government regulations relating to Covid-19. These include but are not limited to: regulations concerning social distancing, the wearing of personal protective equipment, and limitations on meetings and social gatherings.*
   b. *Kindly liaise with the facility manager BEFORE your research begins in order to ensure that conditions in the facility are conducive to the conduct of your research. These include, but are not limited to, an assurance that the numbers of patients attending the facility are sufficient to support your sample size requirements, and that the space and physical infrastructure of the facility can accommodate the research team and any additional equipment required for the research.*
   c. *Please ensure that you provide your letter of ethics re-certification to this unit, when the current approval expires.*
   d. *Provide an interim progress report and final report (electronic and hard copies) when your research is complete to* ***HEALTH RESEARCH AND KNOWLEDGE MANAGEMENT, 10-102, PRIVATE BAG X9051, PIETERMARITZBURG, 3200*** *and e-mail an electronic copy to* hrkm@kznhealth.gov.za
   e. *Please note that the Department of Health shall not be held liable for any injury that occurs as a result of this study.*

For any additional information please contact Mr X. Xaba on 033-395 2805.

Yours Sincerely

[redacted]

Dr E Lutge
Chairperson, Health Research Committee
Date: 12/01/2021

Fighting Disease, Fighting Poverty, Giving Hope

APPENDIX F: GRAPH 1

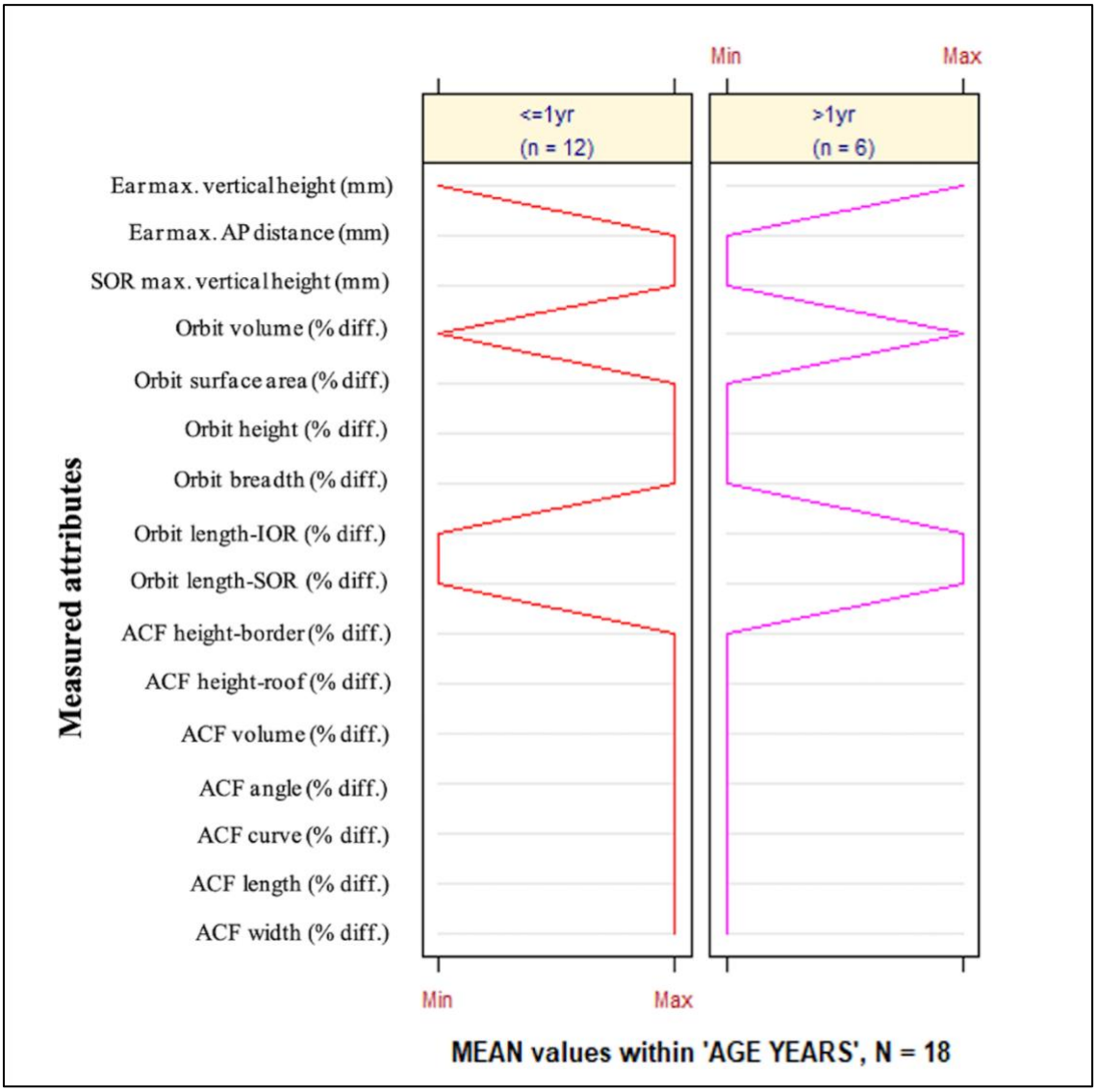

APPENDIX G: GRAPH 2

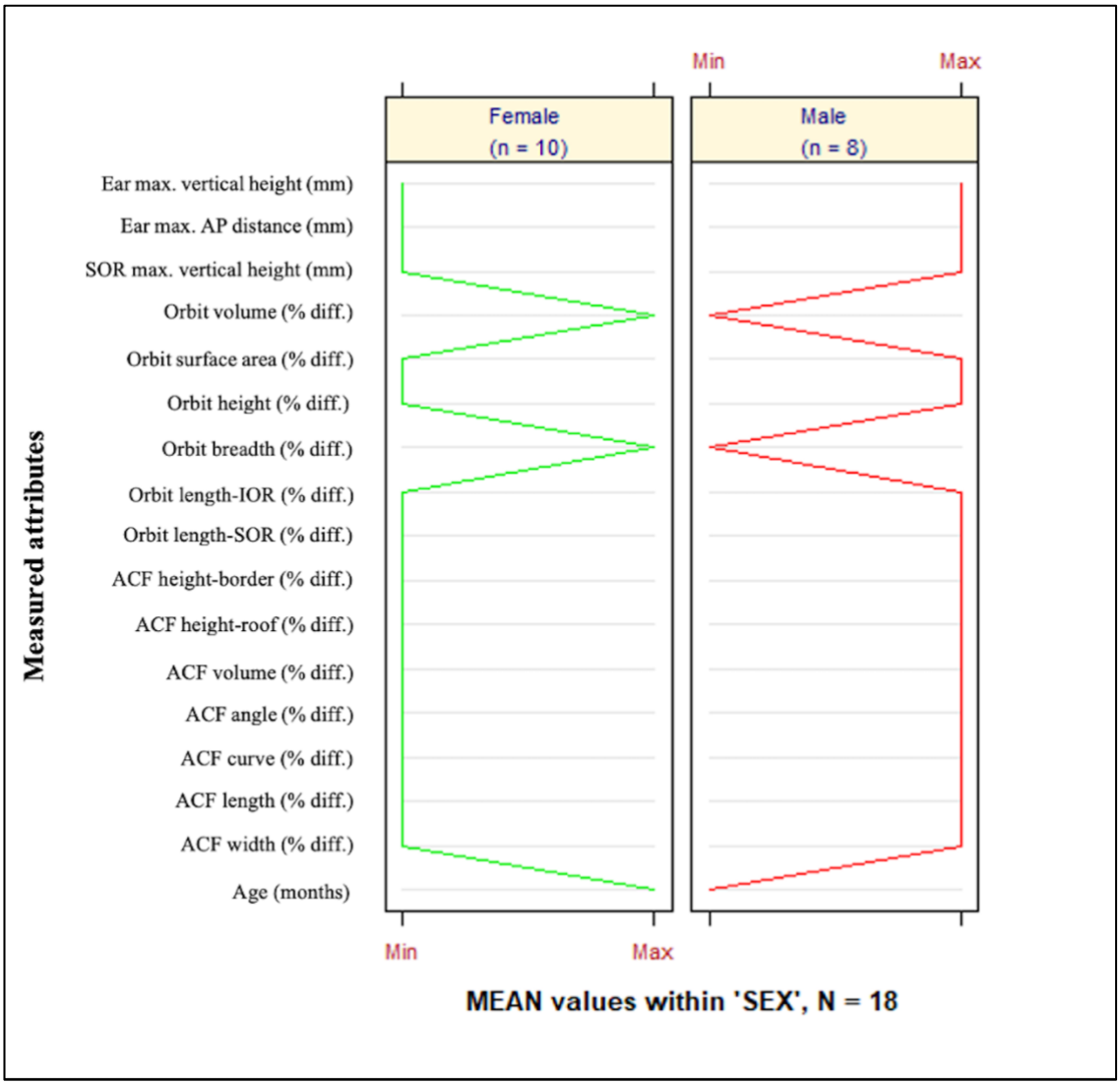

APPENDIX H: GRAPH 3

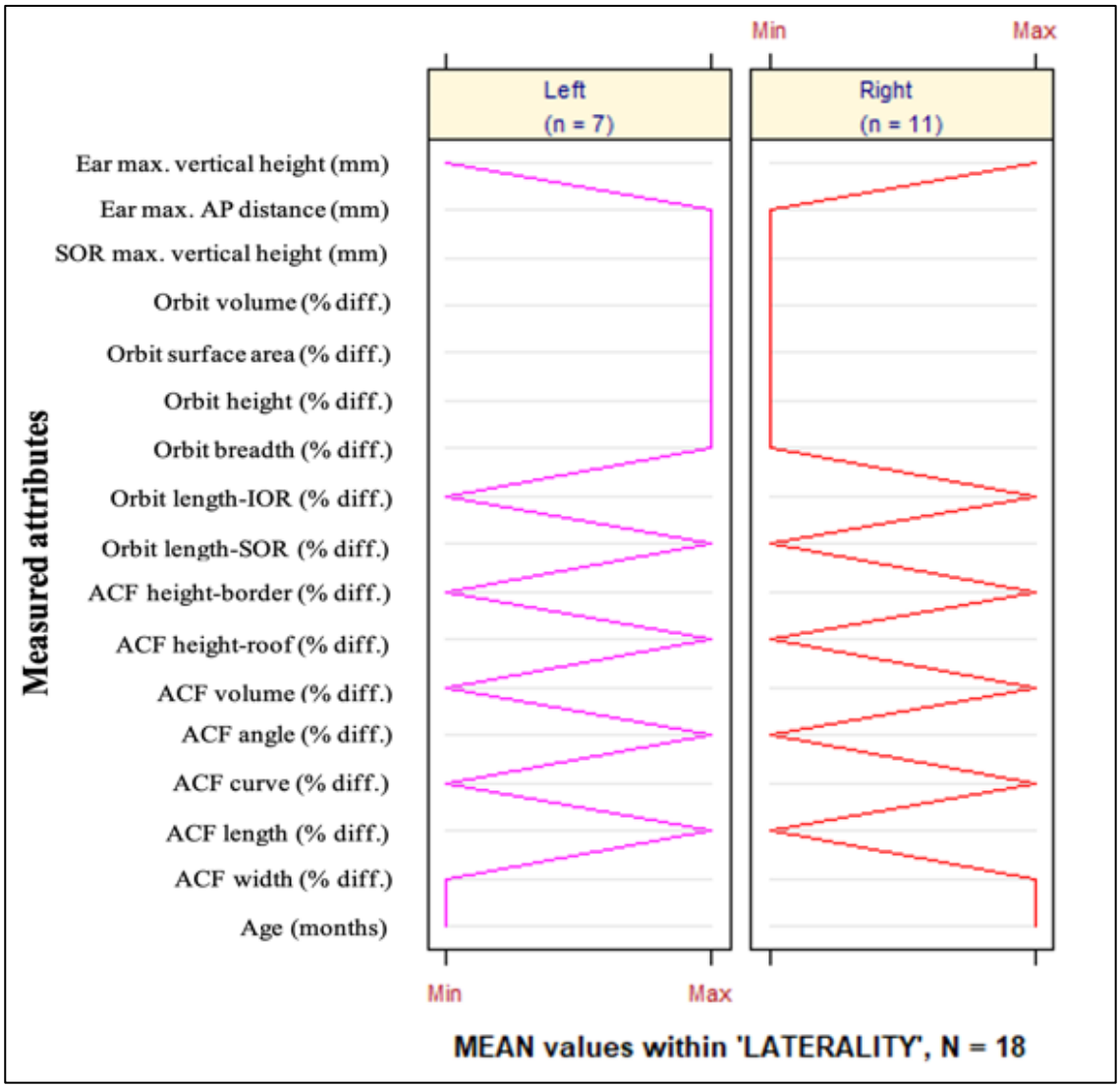

APPENDIX I: GRAPH 4

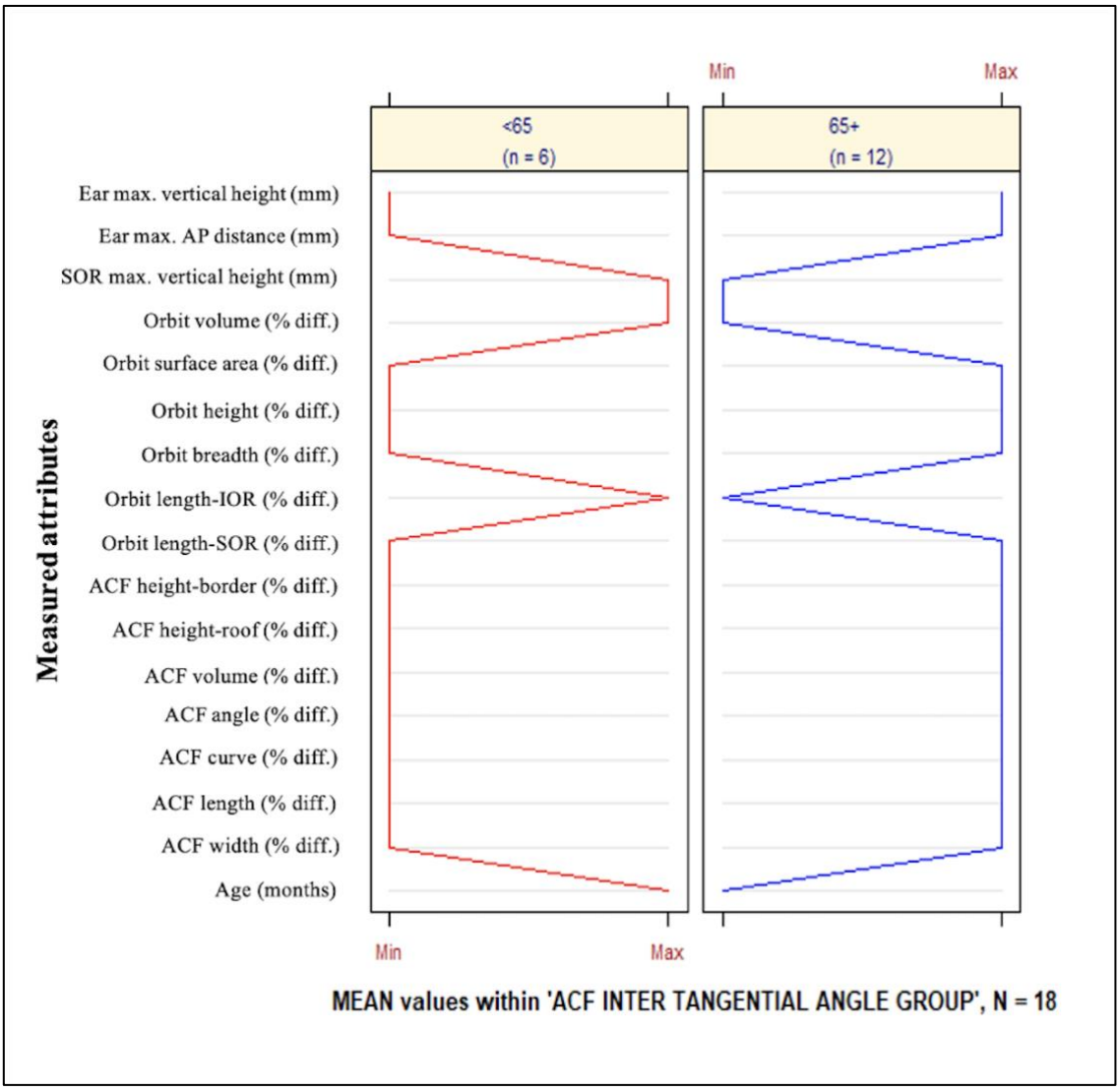

APPENDIX J: DATA SHEET SAMPLE 1

CT NO.	AGE (MONTHS)	SEX	RACE	LATERALITY	ANTERIOR CRANIAL FOSSA			
					WIDTH		LENGTH	
					IPSILATERAL SIDE	CONTRALATERAL SIDE	IPSILATERAL SIDE	CONTRALATERAL SIDE

(Data available on request)

APPENDIX K: DATA SHEET SAMPLE 2

CT NO.	AGE (MONTHS)	SEX	RACE	LATERALITY	ANTERIOR CRANIAL FOSSA: ANGLE		
					IPSILATERAL SIDE	CONTRALATERAL SIDE	INTER-TANGENTIAL ANGLE

(Data available on request)

APPENDIX L: DATA SHEET SAMPLE 3

CT NO.	AGE (MONTHS)	SEX	RACE	LATERALITY	ANTERIOR CRANIAL FOSSA: LENGTH OF CURVE	
					IPSILATERAL SIDE	CONTRALATERAL SIDE

(Data available on request)

APPENDIX M: DATA SHEET SAMPLE 4

CT NO.	AGE (MONTHS)	SEX	RACE	LATERALITY	ANTERIOR CRANIAL FOSSA: VOLUME		
					IPSILATERAL SIDE	CONTRALATERAL SIDE	SEGMENTAL DIFFICIENCY

(Data available on request)

APPENDIX N: DATA SHEET SAMPLE 5

CT NO.	AGE (MONTHS)	SEX	RACE	LATERALITY	ANTERIOR CRANIAL FOSSA			
					HEIGHT (ORBITAL ROOF)		HEIGHT (SUPERO-LATERAL BORDER OF ORBIT)	
					IPSILATERAL SIDE	CONTRALATERAL SIDE	IPSILATERAL SIDE	CONTRALATERAL SIDE

(Data available on request)

APPENDIX O: DATA SHEET SAMPLE 6

CT NO.	AGE (MONTHS)	SEX	RACE	LATERALITY	ORBIT - LENGTH			
					SUPRAORBITAL RELATION		INFRAORBITAL RELATION	
					IPSILATERAL SIDE	CONTRALATERAL SIDE	IPSILATERAL SIDE	CONTRALATERAL SIDE

(Data available on request)

APPENDIX P: DATA SHEET SAMPLE 7

CT NO.	AGE (MONTHS)	SEX	RACE	LATERALITY	ORBIT				
					BREADTH		HEIGHT		SUPRAORBOTAL RIM DIFFERENCE
					IPSILATERAL SIDE	CONTRALATERAL SIDE	IPSILATERAL SIDE	CONTRALATERAL SIDE	

(Data available on request)

APPENDIX Q: DATA SHEET SAMPLE 8

CT NO.	AGE (MONTHS)	SEX	RACE	LATERALITY	ORBIT			
					SURFACE AREA		VOLUME	
					IPSILATERAL SIDE	CONTRALATERAL SIDE	IPSILATERAL SIDE	CONTRALATERAL SIDE

(Data available on request)

APPENDIX R: DATA SHEET SAMPLE 9

CT NO.	AGE (MONTHS)	SEX	RACE	LATERALITY	PLACEMENT OF THE EAR	
					MAXIMUM ANTERO-POSTERIOR DIAMETER	DIFFERENCE IN MAXIMUM VERTICAL HEIGHT

(Data available on request)

APPENDIX S: TURNITIN REPORT

Masters Thesis (Nivana Mohan)

ORIGINALITY REPORT

8%	5%	6%	0%
SIMILARITY INDEX	INTERNET SOURCES	PUBLICATIONS	STUDENT PAPERS

PRIMARY SOURCES

1	livrepository.liverpool.ac.uk Internet Source	1%
2	"Textbook of Pediatric Neurosurgery", Springer Science and Business Media LLC, 2020 Publication	1%
3	Rosalinda Calandrelli, Fabio Pilato, Luca Massimi, Marco Panfili, Concezio Di Rocco, Cesare Colosimo. "Quantitative analysis of cranial-orbital changes in infants with anterior synostotic plagiocephaly", Child's Nervous System, 2018 Publication	1%
4	www.ncbi.nlm.nih.gov Internet Source	1%
5	www.drderderian.com Internet Source	1%
6	G. Captier, N. Leboucq, M. Bigorre, F. Canovas, F. Bonnel, A. Bonnaf, P. Montoya. "Plagiocephaly: morphometry of skull base	<1%